University of Strathclyde
Institute of Pharmacy and Biomedical Sciences

Evaluation of PAMAM dendrimers as delivery vehicles for platinum based anticancer drugs

By

Gordon Kirkpatrick

A thesis presented in fulfilment of the requirements for the degree of Doctor of Philosophy

2012

Declaration

This thesis is the result of the author's original research. It has been composed by the author and has not been previously submitted for examination which has led to the award of a degree.

Signed: Date:

Acknowledgements

First and foremost I would like to thank my family for their support during the last twelve years I've spent finding new ways to prolong my student status. There is no doubt in my mind that I wouldn't be at this stage without them.

Leanne, who has suffered more than anyone else throughout this whole process, I can honestly say thanks for pushing and the many blunt words. It took a few years but I've finally caught up.

Thanks also to my supervisor Dr Nial Wheate for allowing me to come on this challenging project and for the support and guidance throughout the last three years. The invaluable life lessons and numerous 'one time in the military' stories are things I'll always remember.

Similar praise also goes to my other supervisor Dr Oliver Sutcliffe for numerous discussions over the way of things, geeky interests and occasionally science.

I couldn't ask for a better research group to work with: the effervescent Dr Sarah Brown, efficient Dr Katherine Trotter, impassioned Shonagh Walker, rambunctious Gemma Craig and diligent Rabbab Oun. Here's to tea at half past 10.

David Stirling of the University of the West of Scotland for the ICP-AES analysis, Jane Plumb of the Beatson Institute for Cancer Research for carrying out the *in vivo* and *in vitro* analysis and Denise Gilmour for the ICP-MS analysis

I was lucky enough to have an office full of friends so here's to Sabin, Jessica, Giacomo, Michelle, Jen Law, Nabila and Mohammed. Special mention to Jen Mains, there is no one better to be stuck in a corner with.
To all above and all missed out.....Thank you.

Publications

G.J. Kirkpatrick, et al., Evaluation of anionic half generation 3.5–6.5 poly(amidoamine) dendrimers as delivery vehicles for the active component of the anticancer drug cisplatin, J. Inorg. Biochem. 2011, **105**, 1115-1122.

Conference Proceedings

Gordon J. Kirkpatrick, Oliver B. Sutcliffe, David J. Flint and Nial J. Wheate, PAMAM dendrimers as delivery vehicles for platinum anticancer drugs, Journal of Biological Inorganic Chemistry, 2009, 14, S125. DOI: 10.1007/s00775-009-0538-0

Project Funding

This project was funded through a grant awarded by Medical Research Scotland, grant number 271 FRG titled Folic acid directed delivery of platinum (II)-based anticancer drugs using PAMAM dendrimers. This award was made to Dr Nial Wheate, Dr Oliver Sutcliffe and Professor David Flint and totalled £145,332. The scholarship awarded to Gordon Kirkpatrick was provided by the Scottish Funding Council.

Contents

Abstract

Four carboxylate terminated half generation polyamdioamine (PAMAM) dendrimers (G3.5- G6.5) were conjugated with the active components of cisplatin, $\{Pt(NH_3)_2\}^{2+}$, or oxaliplatin, $\{Pt(R,R\text{-dach})\}^{2+}$, to form dendrimer platinate complexes.

The platinum content of the cisplatin containing complexes was measured using inductively coupled plasma atomic emission spectroscopy. The number of cisplatin molecules was found to increase with increasing dendrimer size, 22 – 94, however the assumed bidentate binding mode allows for a total of 32 – 256 cisplatin moieties per dendrimer. Whilst the number of cisplatin moieties increases with dendrimer size, a decrease in the binding efficiency is also observed with dendrimer size, 68 – 37% (G3.5-6.5). This decrease is probably due to the close proximity of surface groups of larger dendrimers, i.e. more branched, increasing the difficulty in deprotonating the carboxylic acids to obtain the carboxylate required for coupling.

The release of the platinum from the dendrimers, in the active form, was evaluated using ^{1}H NMR or inductively coupled plasma mass spectroscopy (ICP-MS). An increase in the number of active cisplatin molecules released is observed with larger dendrimers, four from the G3.5 dendrimer to 59 from the G6.5 dendrimer, with the release efficiency increasing from 18 – 63%. Diffusion ordered spectroscopy NMR was also used to determine the size of the dendrimer platinate complexes. The free dendrimers increased from 2.72 to 5.93 nm, cisplatin dendrimer platinates from 1.66 to 4.01 nm and oxaliplatin dendrimer platinates from 4.03 to 14.51.

The dendrimer platinates and free dendrimers were tested *in vitro* against the A2780 and A2780cis cancer cell lines and their activity compared to cisplatin. In all cases the dendrimer platinates showed reduced activity when compared to cisplatin whilst the free dendrimer showed no activity *in vitro*, $IC_{50} > 100$ mM. The *in vivo* activity of the G6.5

dendrimer platinate was tested in nude mice bearing A2780 xenografts and compared to cisplatin using a single dose of equivalent concentration and the G6.5 dendrimer platinate was shown to have a similar activity *in vivo* as cisplatin after 6 days.

Similar dendrimer-platinate complexes were formed with the active component of oxaliplatin, $\{Pt(R,R\text{-dach})\}^{2+}$. The dendrimer-platinates were found to contain 12-63 platinum molecules per dendrimer, a reduction on the number observed for the complexes formed with the active component of cisplatin. The size of the oxaliplatin dendrimer-platinates was also determined to be greater than the cisplatin equivalent, most likely as a result of aggregation due to the hydrophobic nature of the dach ligand. The number of platinum groups released from the dendrimer is also lower than the equivalent cisplatin complexes with only 2-43 platinum moieties being released. The platinum was shown to be released from the dendrimer in an initial burst release within the first 2 hours, accounting for 85% of the releasable platinum. The $\{Pt(R,R\text{-dach})\}^{2+}$ dendrimer-platinates were shown to be more cytotoxic *in vitro* than the free $\{Pt(R,R\text{-dach})\}^{2+}$ complex.

In a further study a folic acid targeting group was also attached to the dendrimers to allow active targeting of cancer cells through the folate receptor. Folic acid was conjugated to 1,6-diamminohexane via an amide coupling reaction. The linker was then attached to the dendrimer through a further amide coupling reaction prior to the addition of the platinum complexes. The resulting complexes were found to contain 3-8 folate targeting groups depending on dendrimer size. The targeted cisplatin dendrimer-platinates were shown to be more cytotoxic than the non-targeted complexes however the opposite was observed for the $\{Pt(R,R\text{-dach})\}^{2+}$ dendrimer-platinates. The uptake of platinum by the cells increased for the folate targeted cisplatin dendrimer-platinates but decreased for the $\{Pt(R,R\text{-dach})\}^{2+}$ dendrimer-platinates.

Abbreviations

1D-DOSY	One dimensional diffusion ordered spectroscopy
56MESS	[(5,6-dimethyl-1,10-phenanthroline)(1*S*,2*S*-diaminocyclohexane) platinum(II)]$^{2+}$
A	Adenine
A2780	Human ovarian cancer cell line
A2780cis/cp	Human ovarian cancer cell line, cisplatin resistant
B16F10	Murine melanoma cells
C	Cytosine
CB[*n*]	Cucurbit[*n*]uril
DACH	1*R*,2*R*-diaminocyclohexane
DSC	Differential scanning calorimetry
EPR	Enhanced permeation and retention
FDA	Food and Drug Administration
G	Guanine
G3.5	3.5 generation PAMAM dendrimer, carboxylate-terminated
G4.5	4.5 generation PAMAM dendrimer, carboxylate-terminated
G5.5	5.5 generation PAMAM dendrimer, carboxylate-terminated
G6.5	6.5 generation PAMAM dendrimer, carboxylate-terminated
G4	Fourth generation PAMAM dendrimer, amine terminated
HPMA	Hydroxypropyl methacrylate
ICP-AES	Inductively coupled plasma atomic emission spectrometry
ICP-MS	Inductively couple plasma mass spectroscopy
ICP-OES	Inductively coupled plasma optical emission spectroscopy
kDa	Kilo Daltons
L1210	Mouse lymphocytic lukemia cells
MMR	Mismatch repair enzyme

MTT	(3-(4,5-dimethylthiazol-2yl)-2,5-diphenyltetrazolium bromide.
NMR	Nuclear magnetic resonance
NOSEY	Nuclear overhauser enhancement spectroscopy
PAMAM	Polyamidoamine
Phen	Phenanthroline
PPI	Poly(propylene) imine
T	Thymine
T3P	Propane phosphonic acid anhydride
TEA	Triethylamine
TGA	Thermogravimetric analysis
TMS	3-(trimethylsilyl)-1-propane sulfonic acid
WST-1	(4-(3-(4-iodophenyl)-2-(4-nitrophenyl)-2H-tetrazol-3-ium-5-yl)benzene-1,3-disulfonate)

Part 1: Passive tumour targeting

Chapter 1: Introduction

1.1 Cancer

Cancer is one of the largest causes of death worldwide. One in three people will develop cancer during their lifetimes, with one in four deaths in the United States being attributed to cancer.[1] There are a number of different routes through which cancer can develop, including: cell mutations, i.e. chromosomal and nucleotide sequence abnormalities; or exposure to chemical carcinogens including nicotine; and physical agents such as ultra violet light.[2, 3] The development of cancer within the body is a multistep process during which cells acquire abnormal proliferation and invasive behaviour.[2] The first stage in tumour development is the mutation of DNA which is not corrected or sufficiently corrected.[3] This is followed by the uncontrolled growth and proliferation of the mutated cells and finally by metastasis, where the cells invade surrounding tissues and other areas through the circulatory system.[3] The mechanisms that facilitate these steps provide a number of potential targets, including DNA, for the development of anticancer drugs.

1.2 Platinum anticancer drugs

A wide range of drugs are available for use in treatment regimes including platinum based anticancer drugs.[2] In the 1960s Rosenberg, interested in the effect of electromagnetic fields on the cell division of *E. Coli* observed that the bacteria grew as very long filaments over 300 times the length of the normal short rods.[4] The reason for this change was shown to be due to the electrolytic degradation products from the platinum electrodes. Chemical analysis identified these active compounds as *cis*-$[PtCl_2(NH_3)_2]$ (cisplatin, Figure 1) and a platinum(IV) analogue, *cis*-$[PtCl_4(NH_3)_2]$.[4] After recognising the antitumour potential of cisplatin the same group performed further tests against a number of bacteria and subsequently Sarcoma 180 and Leukemia L1210 cancer bearing mice to show marked tumour regression.[5]

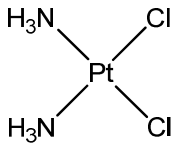

Figure 1.1 The structure of cisplatin.

Since the original observation by Rosenberg, platinum based drugs have become an important class of agents in the treatment of a number of cancers including: testicular, ovarian, bladder, head and neck; and small-cell or non-small-cell lung cancers.[6, 7] Currently there are approximately 130 drugs approved by the Food and Drug Administration (FDA, USA) for use in cancer treatment, including the platinum-based drugs cisplatin, carboplatin and oxaliplatin.[8]

1.2.1 Action of cisplatin

The transporters controlling copper influx into the cell have been shown to be important in the uptake of cisplatin. Of particular importance is CTR1, a membrane spanning P-type ATPase specialised for copper; as knock-out of the CTR1 in some studies led to reduced uptake of cisplatin.[9] Low intracellular chloride concentrations are important in the formation of the active mono- and diaquo-cisplatin complexes. The active form of cisplatin is formed by intracellular aquation through displacement of the chlorido leaving groups by water molecules, Scheme 1.1.[4, 7] The aquated electrophilic platinum complex can then react with nucleophilic cellular targets. The cytotoxic effect of cisplatin is achieved through binding to the N7-site of purine bases, Figure 1.2, in DNA to form intrastrand and interstrand cross-links and DNA-protein cross-links.[7, 10] The most abundant of the cross-links formed with cisplatin are the intrastrand cross-links between adjacent bases 1,2-d(GpG) or 1,2-d(ApG) which account for 65% and 25%, respectively, of the total adducts formed by cisplatin.[11] The key cellular event in the mechanism of cisplatin is apoptosis.[4, 7]

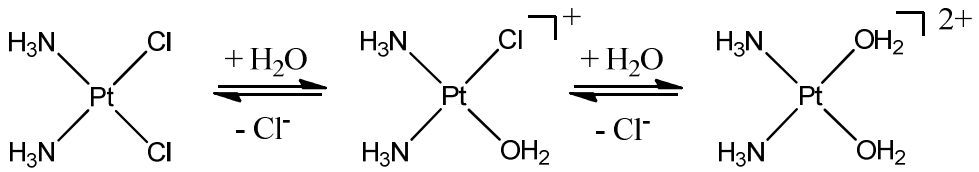

Scheme 1.1 The formation of the mono- (middle) and di-aquated (right) forms of cisplatin.

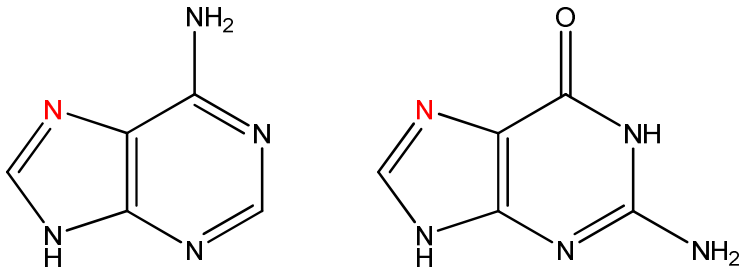

Figure 1.2 The purine bases of DNA adenine (left) and guanine (right); the N7 site is shown in red.

Apoptosis is a process of programmed cell death that controls the development and homeostasis of multicellular organisms through the elimination of aged, damaged or mutated cells.[7] The process that leads to the initiation of apoptosis after treatment with cisplatin is not clearly understood, however, the suppressor p53 protein is believed to play an important role.[7] The protein p53 is responsible for the regulation of cell growth by initiation and prevention of programmed cell death.[12]

Although cisplatin is commonly used for the treatment of a range of cancers there are a number of detrimental aspects to its use. Side effects can arise during treatment with cisplatin and include: severe nephrotoxicity, nausea and chronic neurotoxicity.[4-6] The clinical use of cisplatin is also limited due to resistance.[13] Some tumour cells are naturally resistant to cisplatin, thus restricting its use, and in other cases resistance can develop through a number of mechanisms including: reduced drug uptake, enhanced drug efflux, increased cellular detoxification due to increased thiol-containing species

such as glutathione and/or metallothioneins, enhanced tolerance of platinum-DNA adducts and increased repair of platinum-DNA damage.[7, 13, 14]

The development and approval of cisplatin as a cancer therapeutic led to increased interest in the synthesis and biological testing of many cisplatin analogues as well as studies into elements close to platinum in the periodic table such as palladium and gold.[4] Substantial research has been undertaken towards making cisplatin based chemotherapy safer for patients by reducing the toxicity as well as designing complexes that are able to overcome cisplatin resistance.[4, 7] This research lead to the development of the second and third generation drugs carboplatin and oxaliplatin.

1.2.2 Carboplatin

Carboplatin, *cis*-diammine-[1,1-cyclobutanedicarboxylato]platinum(II), (Figure 1.3) was jointly developed by Johnson Matthey and the Institute of Cancer Research (London), and was approved for clinical use in the 1980s.[4] The rationale that led to the discovery of carboplatin was that a more stable leaving group than chlorido may lower the toxicity of the drug without affecting the efficacy.[4]

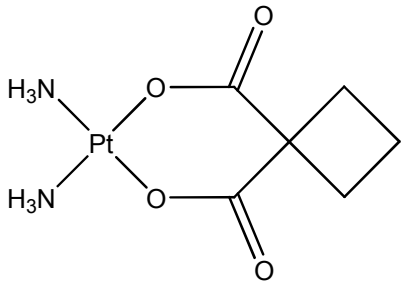

Figure 1.3 The structure of carboplatin.

Cisplatin was modified from the classical PtA_2X_2 structure to incorporate a tightly bound chelated cyclobutanedicarboxylate ring in place of the two anionic leaving groups.[15] In the formation of the active carboplatin complex the mono-aquated complex of carboplatin has been shown to form at a slower rate than the corresponding cisplatin complex.[15] The second aquation reaction, the displacement of the monodentate ligand to

form the diaquo active complex occurs much more rapidly.[15] When this compound was tested it was found to have a similar mechanism of action as cisplatin; induction of apoptosis.[15]

Carboplatin, when compared to cisplatin, is devoid of nephrotoxicity, less toxic to the gastrointestinal tract and less neurotoxic.[4, 5, 15] During treatment it can be given at much higher doses than cisplatin but is still limited due to myelosuppression, where reduced bone marrow activity leads to fewer red and white blood cells and platelets.[4, 5, 10] Although the mechanism of action of both cisplatin and carboplatin is essentially the same, much higher concentrations of carboplatin (20-40 fold) are required to achieve the same level of activity. The mechanisms of resistance to carboplatin are the same as those of cisplatin and carboplatin is still only active towards the same range of tumours as cisplatin.[4, 5]

1.2.3 Oxaliplatin

The resistance of some tumours towards both cisplatin and carboplatin increased the need for a drug that could circumvent the resistance. To achieve this goal a different structural modification of the classical cisplatin structure was undertaken to produce oxaliplatin, Figure 1.4. The structure of oxaliplatin contains two chelating groups around the platinum(II) centre, 1*R*,2*R*-diaminocyclohexane (DACH) as the carrier ligand and oxalate as the leaving group.[15]

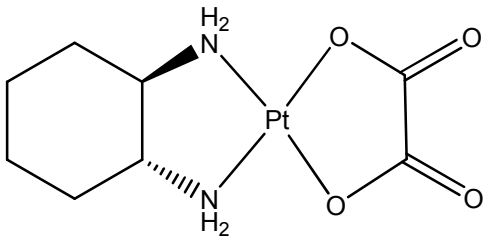

Figure 1.4 The structure of oxaliplatin.

The mechanism of action of oxaliplatin is similar to that of cisplatin and carboplatin and the intrastrand adducts are found at similar sites in DNA.[10] There are some structural differences in the 1,2-intrastrand DNA cross-links, and the number of adducts formed by oxaliplatin is lower than that of cisplatin, although a comparable level of cytotoxicity is achieved.[4, 16, 17] The DNA adducts formed by oxaliplatin are much more bulky and hydrophobic than those formed with cisplatin or carboplatin and as a result oxaliplatin is more effective at inhibiting DNA synthesis.[16] The DACH ligand projects into the major groove of DNA and prevents, through steric hindrance, the damage recognition proteins such as the mismatch repair (MMR) enzyme from binding. This effect provides oxaliplatin cytotoxicity in some tumours that are resistant to cisplatin.[5, 16]

Clinical trials of oxaliplatin carried out in France showed activity in patients with colon cancer, previously acknowledged as being insensitive to cisplatin and carboplatin.[5] As well as colorectal cancer, oxaliplatin has also been found to be active in 5-fluorouracil refractory tumours, platinum resistant ovarian cancer, non-small cell lung cancers and non-Hodgkin's lymphomas.[16] There are also a number of other advantages provided by oxaliplatin, including: increased water solubility and much lower toxicity in comparison to cisplatin.[4, 5] Even with these advantages the use of oxaliplatin is limited due to its neurological toxicity and severe adverse effects due to increased intracellular accumulation in normal cells during the course of treatment.[5]

Although the platinum based drugs show good activity at the tumour site the number of severe side effects that arise during treatment can limit their use.[18] There are also a number of other issues that arise due to the size of the drug, including: unfavourable pharmacokinetics (i.e. their short circulation time in the blood); their lack of specificity for tumours; they are evenly distributed throughout the body and damage all rapidly dividing cells.[19] It is possible to overcome these problems using a drug targeting strategy.[18, 19]

1.3 Drug delivery vehicles

The original concept of drug targeting was developed over a century ago by Paul Ehrlich who proposed a "magic bullet complex" that contained two different components, the first to recognise and bind to the target and another to provide the desired therapeutic action.[19] Since the development of the original hypothesis the model has been expanded to a five component model consisting of: (i) a water soluble carrier; (ii) a targeting moiety; (iii) a spacer region; (iv) an inert carrier polymer and (v) the drug.[20] Through this method of drug targeting it is possible to design systems that increase the circulation time of the drug by increasing the overall size of the complex as well as increasing the specificity of the drug by exploiting the enhanced permeation and retention (EPR) effects that occur in tumour vasculature.[19]

The EPR effect arises due to differences between the blood vessels surrounding the tumours and those of normal tissues, Figure 1.5.[21] The blood vessels in tumours are irregular in shape, dilated, leaky or defective and the endothelial cells in the vessels are poorly aligned.[22] The defects within the vasculature results in blood plasma components such as macromolecules, nano- and lipid particles, entering the tumour tissue more effectively.[22] The increased permeability of tumours allows the passage of larger molecules into the cells than would normally occur.[18] This enhanced permeability can therefore be exploited by macromolecular drugs and macromolecular pro-drugs as these would pass through into the tumour, but not into healthy tissue, thus increasing the selectivity of these drugs.[19] The EPR effect also allows drugs to accumulate in the tumour site due to poor lymphatic drainage.[18]

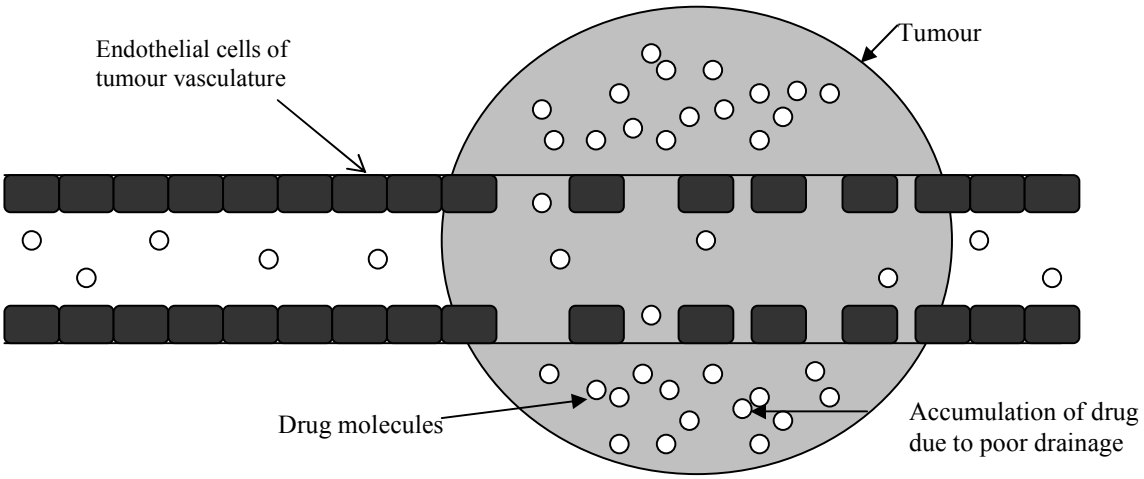

Figure 1.5 The enhanced permeation and retention effect in tumour vasculature.

There are a number of different types of drug delivery vehicles that can be used to target selectively the tumour sites: cucurbiturils, cyclodextrins, calixarenes, carbon nanotubes, liposomes/niosomes and dendrimers.

1.3.1 Cucurbit[*n*]urils

Cucurbit[*n*]urils (CB[*n*]s) are macropolycyclic compounds comprised of *n* subunits and are synthesised by the condensation of glycoluril and formaldehyde in acidic media to form a distinctive pumpkin-like shaped compound, Figure 1.6.[23-26] Cucurbit[6]uril (CB[6]) was originally synthesised in 1905, first characterised in 1981, and was, until the discovery of CB[5], CB[7] , CB[8] and the isolation of free CB[10] after the year 2000, the main focus of attention towards using cucurbit[*n*]urils in host-guest chemistry.[23, 26, 27]

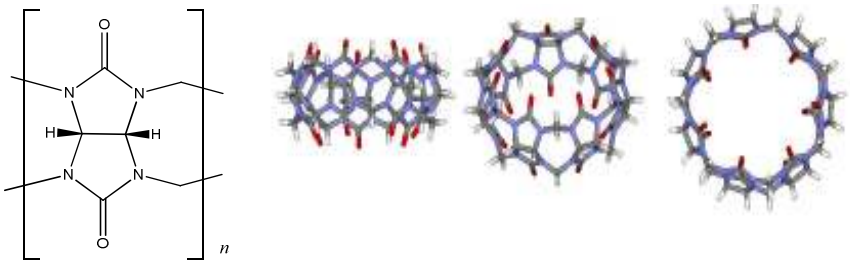

Figure 1.6 The chemical structure of cucurbit[*n*]uril, *n* = 5,6,7,8 or 10, and the three-dimensional structure of cucurbit[*7*]uril.

Cucurbit[*n*]urils have two symmetrical hydrophilic carbonyl lined portals and the diameter of the CB[5]-CB[8] portals range from ~2.4 to ~6.9 Å.[23, 25] The internal cavities of the CB[*n*]s also range from ~4.4 to ~8.8 Å.[23, 25] The cavities of the CB[*n*]s can be used to fully or partially encapsulate smaller molecules including the platinum anticancer drugs cisplatin and oxaliplatin.[25, 28] The encapsulated platinum complexes are stabilised through ion-dipole and dipole-dipole interactions at the portals and hydrophobic interactions within the cavity.[25, 29]

The size of the portals and cavities dictate which of the cucurbit[*n*]urils can be used as hosts for molecules of different sizes.[23, 29] The portal of CB[5] is too small to permit a coordinated platinum and the cavity of CB[10] is too large to hold strongly a platinum complex when dissolved at biological concentrations.[25] Cisplatin is neutral and is held within the cavity of CB[7] but the aquated hydrolysis product binds to the portal of CB[7]. In contrast carboplatin does not interact with CB[7] and oxaliplatin is partially encapsulated, Figure 1.7.[23, 25, 28]

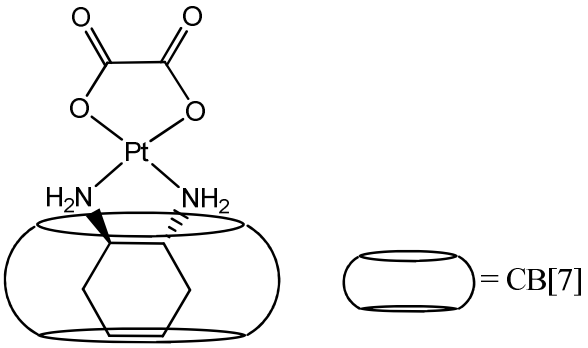

Figure 1.7 A schematic diagram showing oxaliplatin partially encapsulated by CB[7].

The ability of CB[*n*]s to encapsulate molecules in this way provides a number of benefits in the delivery of the platinum drugs. The encapsulated drugs are protected from degradation, through hydrolysis or attack from glutathiones and metallothioneins.[25, 28] The effect of CB[*n*] encapsulation on drug cytotoxicity has not been fully elucidated. For some drugs the activity is increased, for others it remains the same and in some cases the activity is decreased.[25]

Previous efforts into the development of CB[*n*]s as macromolecular drug delivery vehicle have been carried out using partially encapsulated platinum based DNA intercalators.[30, 31] Cytotoxicity studies carried out in the L1210 murine leukaemia cell line of both free and CB[6] encapsulated DNA intercalators showed comparable IC_{50} values between the free and encapsulated forms, Table 1.1.[30] The same group demonstrated the ability to tune the cytotoxicity of the encapsulated intercalating complex through use of different sized cucurbit[*n*]urils.[31] The reported cytotoxicity results of three encapsulated DNA intercalators of the type [Pt(5-Cl-phen)(ancillary ligand)]$^{2+}$ in the L1210 cell line showed differing effects depending on the size of the cucurbit[*n*]uril used, Table 1.2.[30] These results support the potential for use of cucurbit[*n*]urils as drug delivery vehicles.

Table 1.1 The IC_{50} values for the series of free and CB[6] encapsulated platinum(II) DNA intercalators in the L1210 murine leukaemia cell line.

Complex	IC_{50} (μM)	
	Free complex	**CB[6] encapsulated**
Cisplatin	1	n/a
56MESS[30]	0.0092 ± 0.0008	0.011 ± 0.004
5MESS[30]	0.033 ± 0.014	0.038 ± 0.02
47MESS[30]	0.13 ± 0.001	0.17 ± 0.01
5CLSS[30]	0.13 ± 0.003	0.05 ± 0.008
PHENSS[30]	0.25 ± 0.02	0.41 ± 0.01
3478MESS[30]	0.87 ± 0.03	0.60 ± 0.05

Table 1.2 The IC_{50} values for the series of free and CB[6,7,8] encapsulated platinum(II) DNA intercalators in the L1210 murine leukaemia cell line.

Complex	IC_{50} (μM)			
	Free	**CB[6]**	**CB[7]**	**CB[8]**
5CLEN[31]	13.5 ± 1.77	>50	13.5 ± 0.06	27.5 ± 3.2
5CLRR[31]	1.53 ± 0.29	2.96 ± 0.66	>50	3.4 ± 0.32
5CLSS[31]	0.13 ± 0.003	0.05 ± 0.008	>50	0.57 ± 0.08

Before cucurbit[*n*]urils can be employed as drug delivery vehicles their low solubility and resistance towards functionalisation must be addressed.[23, 25-27] Increased solubility can be achieved through (i) synthesis of cucurbit[*n*]urils with cyclohexanoglycoluril and formaldehyde or (ii) introduction of polar groups into the structure.[23, 26] Whilst encapsulation with CB[*n*]s can prevent the intracellular degradation of platinum drugs,

they will not increase their selectivity for tumours.[25] Selectivity can be increased by the introduction of a targeting group at the surface of the CB[*n*], however, this is made difficult due to the resistance of the CB[*n*]s towards functionalisation.[26]

1.3.2 Cyclodextrins

Cyclodextrins are cyclic (α-1-4) oligosaccharides of α-D-glucopyranose containing a hydrophobic central cavity and a hydrophilic surface, Figure 1.8.[32] The rigidity of the bonds connecting the glucopyranose units prevents free rotation and as a result the cyclodextrins are cone shaped.[33] The most common cyclodextrins are those with six, seven or eight glucopyranose units and these are designated α-cyclodextrin, β-cyclodextrin and γ-cyclodextrin, respectively, Figure 1.8.[32-35] Smaller cyclodextrins are thought not to exist due to steric factors, however, larger cyclodextrins with up to 13 glucopyranose units have been reported.[32]

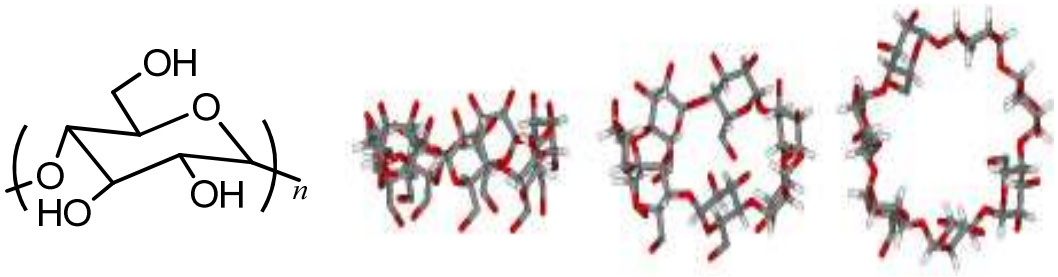

Figure 1.8 The general structure and three-dimensional shape of cyclodextrins, n = 4-13.

Cyclodextrins can act as a drug delivery vehicles in a similar manner to cucurbit[*n*]urils as drug molecules can be held inside the central cavity of the cyclodextrin.[36] The cavity is lined with the skeletal carbon and oxygen atoms of the glucose residues creating a lipophilic microenvironment.[32] During the formation of cyclodextrin-drug complexes no covalent bonds are broken or formed and the drugs quickly dissociate in aqueous solution.[32] As well as encapsulation of the drug, cyclodextrins can provide a number of

additional benefits including: (i) increased solubility; (ii) increased dissolution rate; (iii) prevention of degradation in the gastrointestinal tract; (iv) increased shelf life; (v) alteration of membrane fluidity to lower barrier function and (vi) competitive inclusion complexation with other biological components such as bile acids (to aid release of the encapsulated drug).[37, 38]

Cyclodextrins also have a number of issues relating to their use in pharmaceutical applications. The nephrotoxicity of the parent α- and β-cyclodextrins is problematic; however this can be overcome by the use of modified cyclodextrins.[35, 38, 39] The cyclodextrins are also degraded by α-amylases present in both human saliva and the pancreas, via cleavage of the α-1,4 glycosidic bonds.[39] Modification of cyclodextrin hydroxyl groups can be used to lower the rate of enzyme degradation by reducing the affinity of the cyclodextrins for the enzyme or lowering the intrinsic reactivity of the enzymes.[39]

1.3.3 Calix[*n*]arenes

Calix[*n*]arenes are cyclic oligomers of repeating phenolic units joined together via methylene bridges. They are synthesised through the base catalysed condensation of *p*-alkylphenols with formaldehyde in a simple one pot synthesis.[40-42] Calix[*n*]arenes adopt a bowl shaped conformation made up of 4-20 monomer units with the major calix[*n*]arenes having four, six and eight monomer units, Figure 1.9.[40, 41, 43] Due to the shape of the calix[*n*]arenes, an inner cavity forms with the phenolic hydroxyl groups on the lower (smaller) rim and the *p*-substituents on the upper rim.[44]

Figure 1.9 The general structure and three-dimensional structure of the calix[*n*]arenes, *n* = 4-20.

This cavity makes the calix[*n*]arenes potentially useful as drug delivery vehicles as they can be used to host small molecules or ions. The size of the cavity determines the size of the molecules and ions that can be bound.[41, 43] The potential of calix[*n*]arenes as delivery vehicles has been shown through their encapsulation of platinum(II)-based DNA intercalators and a dinuclear platinum(II) complex.[40] As potential hosts for drugs calix[*n*]arenes have a number of other advantages that make them attractive as delivery vehicles including: (i) simple one pot synthesis, (ii) ease of modification at the upper and lower rims and (iii) tunable molecular shapes and conformations.[42]

As promising as the calix[*n*]arenes are they do have issues surrounding their use, primarily the lack of solubility of unmodified calix[*n*]arenes.[40, 43] In order to improve their solubility calix[*n*]arenes are often modified to *p*-sulphanatocalix[*n*]arenes as these derivatives provide the highest possible aqueous solubility, Figure 1.10.[40]

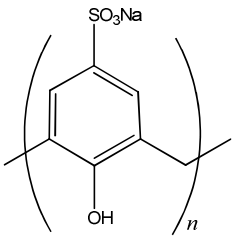

Figure 1.10 The general stucutre of *p*-sulfonatocalix[*n*]arenes, *n* = 4-20.

1.3.4 Carbon Nanotubes

Carbon nanotubes can be categorised by their structure into two main types: single walled carbon nanotubes and multiwalled carbon nanotubes, Figure 1.11.[45] Single walled carbon nanotubes consist of a single layer of graphene, with surface area ~ 2600 m^2/g rolled into a cylindrical tube and the multiwalled nanotubes are made up of several layers of concentric cylinders with a space of ~0.34 nm between each layer.[45, 46] Single walled nanohorns, a subtype of the single walled carbon nanotubes, have diameters that

range from 2-5 nm, with typical lengths of 40-50 nm and amass to form a spherical aggregate of diameter 80-100 nm, the tips of which are closed off by a cone shaped cap (horn).[47, 48]

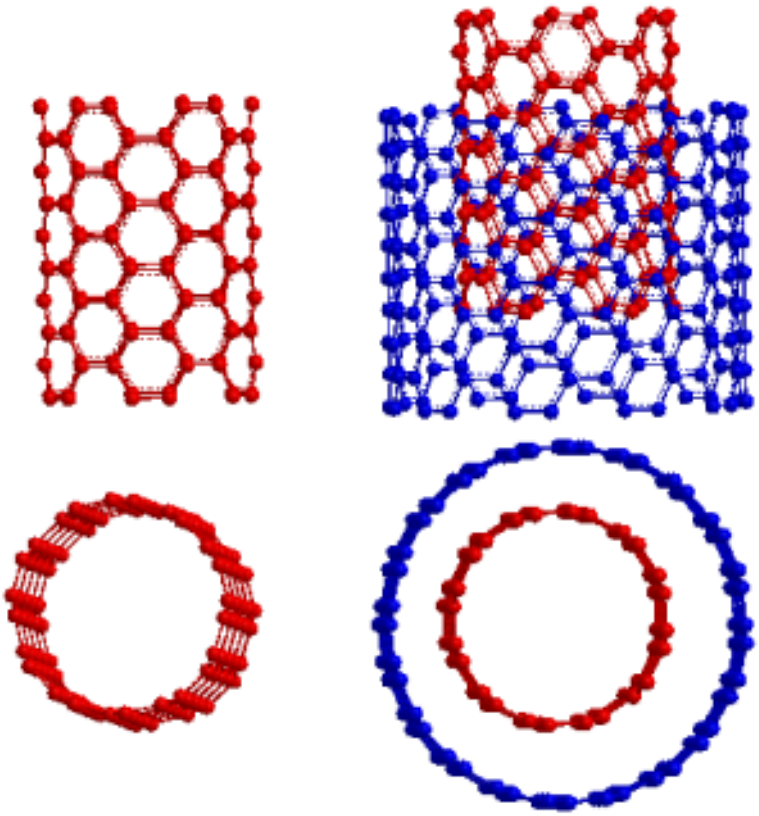

Figure 1.11 A graphical representation of a single walled carbon nanotube (left) and multi-walled carbon nanotube (right).

As drug delivery vehicles carbon nanotubes and nanohorns are unique. They can be used to encapsulate drugs and small molecules inside the tube and/or adsorbed onto the surface of the tubes.[45, 47, 49] Studies with cisplatin absorbed onto the wall of a single walled carbon nanohorn have shown that the release of the drug can be controlled and the amount of the drug that accumulates in tumour cells increases compared to the drug on its own.[45, 47, 49] There have also been studies with platinum(IV) anticancer agents

attached to single walled carbon nanotubes as a means to circumvent cisplatin resistance.[50] The carbon nanotubes are also attractive as delivery vehicles as they easily move through cell membranes, via endocytosis (*i.e.* the nanotubes are entrapped within an intracellular vesicle formed by invagination of the plasma membrane and membrane fusion).[51]

The use of carbon nanotubes is limited due to concerns over their biocompatibility.[51] Studies have also shown that water-soluble functionalised carbon nanotubes are rapidly cleared from blood.[51] The large size distribution of the nanotubes affects biodistribution of attached drugs and this limits their use in drug delivery.[51]

1.3.5 Liposomes and niosomes

Liposomes are artificial spherical phospholipid-based vesicles that consist of a lipid bilayer similar to a cell membrane, Figure 1.12, and niosomes are non-ionic surfactant vesicles.[52-54] The lipid bilayer of liposomes consists of amphiphiles that have hydrophilic heads and hydrophobic tails that orientate themselves in aqueous solvents to form a sphere with a hydrophobic outer layer and inner core.[55] The physical properties of niosomes are similar to liposomes.[53, 54] The inner core of liposomes and niosomes can be used for encapsulation of other materials, including drugs, with the diameter of the core determining the size of the material permitted.

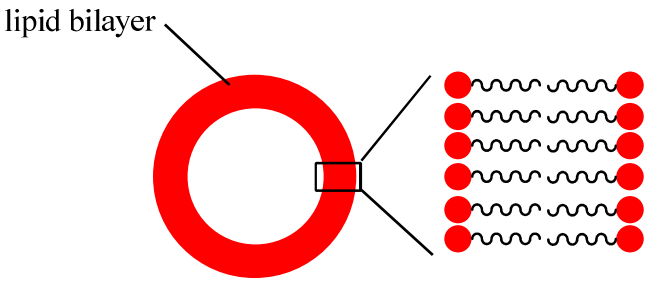

Figure 1.12 A representation of a liposome and the phospholipid bilayer.

The core can be used to encapsulate both hydrophilic and hydrophobic drugs, the later being made possible because dissolved hydrophobic solutes cannot pass through the lipid bilayer. Controlled release can be achieved from the central core of liposomes and niosomes through a number of mechanisms including: (i) pH dependent neutralisation of charged functional groups present in the membrane; (ii) pH dependent hydrolysis of non-charged cleavable components integrated into the membrane; (iii) thiolysis of membrane lipids containing disulfide bonds and (iv) through use of thermo-sensitive liposomes that can exploit transition temperatures between 41-43 ^{o}C.[51] Previous studies have shown favourable results in the delivery of a number of different types of drugs including antibiotics and platinum anticancer drugs.[56, 57]

Cytotoxicity studies involving the platinum drugs prompted interest in the development of new liposome encapsulated platinum drugs. There is currently one liposomal platinum drug in preclinical trials, Aroplatin^{TM}, which originally contained encapsulated cisplatin, Figure 1.13. [58-62] Initial success in phase II trials of Aroplatin led to development of further trials, however, by the initiation of these trials it was clear that Aroplatin would deliver no additional benefit compared to the current treatment regime.[58] Aroplatin has since been reformulated, to replace the cisplatin with an oxaliplatin-like platinum complex to increase the safety and pharmacokinetic profile. This new formulation is currently in phase I trials (Figure 1.14).

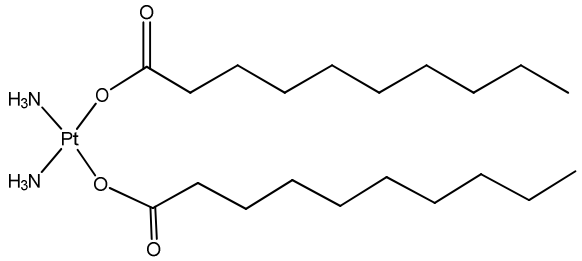

Figure 1.13 The original structure of Aroplatin

.

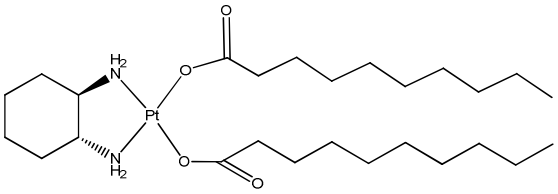

Figure 1.14 The reformulated structure of Aroplatin with the inclusion of the DACH-containing platinum complex.

There are, however, a number of detrimental aspects to be considered with the use of liposomes. Liposomes are phagocytozed by macrophages in the liver and rapidly removed from circulation.[55, 63] Other potential difficulties are the possible interaction of liposomes with macromolecules and cell surfaces.[55] Sterically stabilised, or stealth, liposomes stay in circulation for longer and can accumulate, via the EPR effect.[63]

1.3.6 Dendrimers

Dendrimers are spherical hyperbranched structures that have a precisely controlled size, shape and end-group functionality.[64, 65] There are a number of different types of dendrimer including the polypropylene imine, PPI, dendrimer with a 1,*N*-diaminoalkane core and the polyamido amine, PAMAM, dendrimer with an ammonia or 1,*N*-diaminoalkane core, Figure 1.15.[66] The dendritic structure is made up of layers between each cascade called generations with the core of the dendrimer often referred to as generation zero.[64]

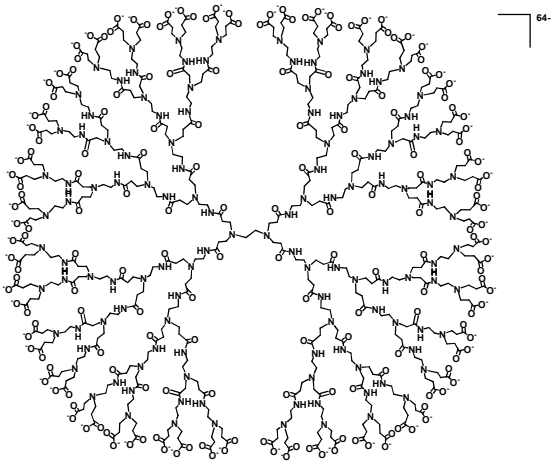

Figure 1.15 A generation 3.5 PAMAM dendrimer.

The generations are often defined by the number of cascade points between the core and the surface, *i.e.* a generation 3 (G3) dendrimer will have three cascade points between the core and surface.[64, 67] The surface of full generation PPI and PAMAM dendrimers are covered with amine groups, but PAMAM dendrimers can also have half generations with terminating carboxylate groups.[64, 66] The amine groups on the surface can become protonated resulting in a polycationic charge on the dendrimer, the half generation PAMAM dendrimers have a polyanionic charge.[66,67] The increasing number of functional groups can be used to increase the available drug payload when used as drug delivery vehicles.

There are a number of different routes available for the synthesis of dendrimers including: divergent, convergent, combined convergent-divergent routes and click chemistry.[67, 68]

The divergent route used by both by Tomalia and Newkome in the original syntheses of dendrimers, reacts a multifunctional initiator core with a monomer unit and builds the dendrimer from the core in a stepwise repetitive reaction sequence, Figure 1.16.[67-70] The first class of dendrimers synthesised through this route was the polyamidoamine

(PAMAM), prepared by coupling *N*-(2-aminoethyl)acrylamide monomers to an ammonia core.[71]

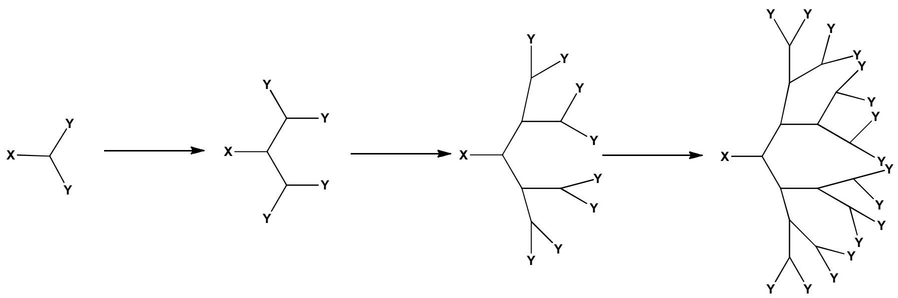

Figure 1.16 A schematic representation of the divergent synthesis route as described by Tomalia and Newkome, X is the initiator core and Y is the monomer unit.

In order to achieve the synthesis of the desired structure Tomalia employed exhaustive Michael addition reactions followed by exhaustive amidation reactions.[69] The problems associated with this synthetic strategy are: possible side reactions that yield incomplete or imperfect dendrimers, an exponentially increasing number of reactions with each stage of dendrimer growth requiring a large excess of reagents and difficulty maintaining structural uniformity and purification of the final products, with column chromatography required to obtain the desired final product.[71, 72] Synthesis of higher generation dendrimers through this route is also difficult due to increasing steric hindrance with larger dendrimers.[72]

Frechet and co-workers carried out the divergent synthesis of aliphatic ester dendrimers by anhydride coupling.[71, 72] This modification allowed for a reduction in the number of purification steps required and overall simplification of the purification process to simple extraction and precipitation.[71, 72] The highest generation dendrimer synthesised through this route was a G6 and this was obtained in both high purity and yield as well as good polydispersity, poly dispersity index (PDI) ~ 1.03.[72]

Maraval *et al* also described a modified divergent route to the synthesis of dendrimers.[73] This route reduced the number of reactions required to complete the synthesis by

reacting two monomer units CA_2 and DB_2 with an A_3 or B_3 core depending on the first monomer unit being used, without the use of activating agents.[73] This method greatly reduced the amount of solvents required and no activating agents are required to initiate the reaction.[73] The dendrimers obtained through this sequence of reactions can also be reacted with other monomer units such as the CA_5 leading to a rapid increase in the number of end groups available for subsequent modification.[73] A G4 dendrimer synthesised from the DB_2 and A_3 reaction was subsequently reacted with a CA_5 monomer increasing the total number of end groups from 48 to 250 in one step.[73]

The convergent approach to the synthesis of dendrimers was originally described by Hawker and Frechet.[71, 74, 75] In contrast to the divergent, the convergent route makes use of the symmetrical nature of these structures to begin the synthesis at what will become the periphery of the dendrimer, Figure 1.17.[74, 75] The individual branches are synthesised first and then attached a functionalised core in order to obtain the dendrimer structure.[67, 68, 75] The starting material in the synthesis will contain the functional groups that eventually become the surface groups of the dendrimer as well as a functional group that will be used to continue the growth of the branch.[74, 75] The starting material is condensed with a monomer unit containing at least two coupling sites and a protected functional group.[74, 75] Following the coupling reaction the functional group is activated and the branches are grown by an iterative process until the required length is achieved.[74, 75] When the desired branch length is achieved the functional group at the focal point of the branch is coupled to a polyfunctional core to give the completed dendrimer structure e.g. direct coupling of the starting material to the core would produce a G1 dendrimer.[74, 75]

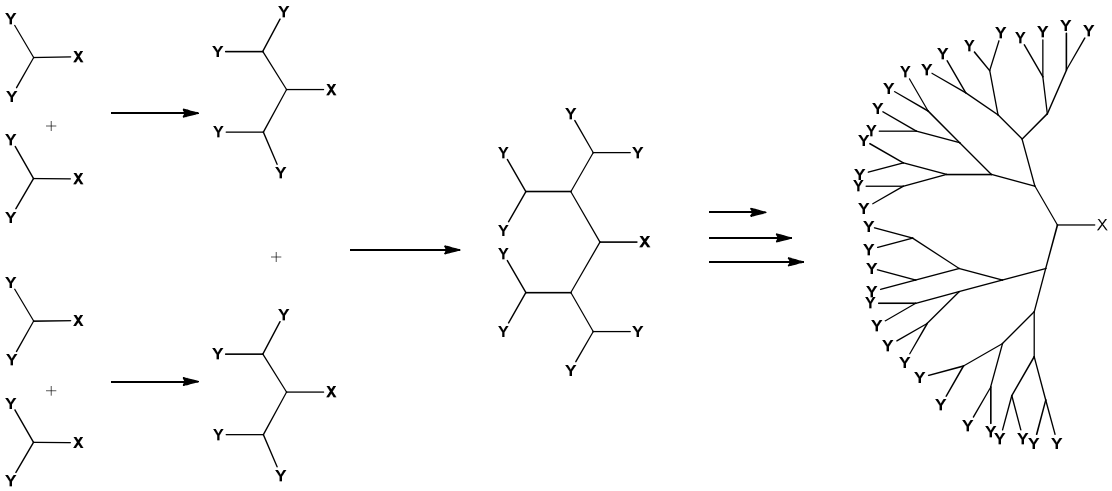

Figure 1.17 A schematic representation of the convergent approach as described by Hawker and Frechet.

The immediate benefit of this route is the reduction in the number of reaction steps required to construct the dendrimer as this allows greater synthetic control.[74] The purification of the final dendrimer is also much easier as the reaction byproducts are substantially different from the desired product and the large excess of reagents is no longer required.[71, 74, 75] Monodispersity can also be improved through the convergent route as there are fewer nonideal growth events.[71, 75] The polydispersity index of the original polyether dendrimer synthesised in this manner was between 1.01-1.02. The yield of larger dendrimers synthesised throught he convergent route drops off quickly, 84% for G4 compared to 51% for G6.[71, 74, 75] This reduction in yield is a result of steric crowding around the focal point of the branches lowering the reactivity of the branches towards the functionalised core.[71, 74, 75] This problem and the increasing difficulty in chromatographic analysis of the larger dendrimers again led to the development of a double-staged route to the synthesis of higher generation dendrimers.[71]

The double-stage approach synthesis of dendrimers is achieved through the use of monomers containing functional groups at either end of their structure in order to build

both the branches of the dendrimer and a multifunctional 'hypercore', a smaller generation dendrimer, and couple them together to make the completed dendrimer.[71, 76] The construction of hypercores using flexible structures creates space between the branches and can be used to overcome the steric hindrance observed in conventional convergent synthesis.[71, 76] The double-stage synthesis differs from the convergent route described above as the larger dendritic branches are no longer coupled to directly to the central core of the structure but are coupled to a smaller completed dendrimer.[76]

Kawaguchi *et al.* first described a double exponential technique that combined convergent-divergent routes.[77] In this route the branches are built in a divergent fashion then coupled to a multifunctional core as in the convergent route.[77] The monomer units, G1 branches, used to build the branches contain two or more functional groups as the surface groups or for continuing branch growth and another as the focal point.[77] These groups are orthogonally protected to allow the selective deprotection of the appropriate functional groups required to progress the construction of the dendrimer.[77] The first stage of the reaction is to deprotect the surface groups on one monomer unit and the focal point on another.[77] These are then reacted together in the ratio of 1:X (X being the number of surface functional groups in the monomer) to form the second generation branch.[77] The fourth generation dendrimer branch is made in a divergent process by selectively deprotecting the surface groups of the G2 dendron and the focal point of the monomer unit and combining these in the required ratio.[77] Subsequent generations are also synthesised through the same sequence of reactions.[77] When the required branch length has been achieved the completed dendrimer is obtained by deprotecting the functional group at the core of the structure and coupling this to a functionalised core as in the conventional convergent route.[77]

This method can be used to quickly assemble larger dendrimers but it is also subject to the same disadvantages that occur in both the convergent and divergent routes.[71, 77] The number of deprotection and activation steps increases exponentially with each generation and highly efficient reaction schemes are therefore required.[71, 77] The size of

the dendrimer also doubles with each successive generation and only a small number of generations can be synthesised before significant steric hindrance is encountered.[71, 77]

Click chemistry is the term frequently used to refer to a number of extremely versatile reactions.[78] There are a number of criteria that must be met in order for the reaction to be classified as click chemistry including: the reaction must be highly selective and give near 100% yields, can be carried out in a number of different solvents irrespective of protic/aproptic or polar/nonpolar character and proceed at various types of interfaces such as solid/solid, solid/liquid and liquid/liquid interfaces.[78, 79] The other criteria that make click reactions attractive as potential synthetic routes is the need for only stoichiometric amounts of starting material, the virtual absence of reaction by-products, the ability to carry out reactions at room temperature and the ease of extraction and purification.[78, 79]

The copper(I) click reaction was discovered independently by Meldal and Sharpless and is similar to classical Huisgen cycloaddition.[80] In the classical reaction the product obtained is a mixture of 1,4- and 1,5-disubstituted triazole regioisomers, however, the copper(I) catalysed click reaction leads to the selective formation of the 1,4-disubstituted 1,2,3-triazole heterocycles and at a faster rate even at room temperature.[71, 78-81] Copper(I) click chemistry has been shown to be applicable in divergent synthesis of dendrimers. Wooley *et al* used the 1,3-dipolar cycloaddition reaction to obtain dendrimers with alkyne and azide terminal groups with triazole linkages between generations.[82] The high selectivity of the copper click reaction means that it is highly compatible with almost all the functional group types present in biomacromolecules such as proteins, polysaccharides and DNA/RNA.[80] The limitation of these reactions is the toxicity of the copper if it is difficult to remove from the final polymer.[80]

Diels Alder (DA) reactions are another type of click chemistry that has been successfully used to synthesise dendrimers. As early as 1997 work was under way involving the construction of dendritic materials using DA chemistry and Mullen *et al* used DA

cycloaddition between tetraphenylcycopentadieone and mono-, di-, and tetra-, and hexaphenylacetylene.[79] The dendritic complexes that were syntheised by this group were quite different from those obtained through the methods described above and the reaction carried out to obtain the structures proved to be irreversible due to the lose of carbon monoxide and synchronous armonatization.[79] Diels Alder chemistry can be used to construct the dendrimers through both the convergent and divergent routes.

Dendrimers can be used to encapsulate drugs in their interior or to conjugate with the drug to form macromolecular prodrugs.[67] As the size of the dendrimer increases there is an exponential increase in the number of functional end groups.[83] The larger the number of end groups the greater the number of sites available for conjugation with drugs.[83] The increase in size of the dendrimer also increases the efficiency of drug encapsulation.[83] Dendrimers often adopt a globular shape with a hydrophobic interior which provides a lipophilic environment for encapsulation of drugs (in particular those which have low water solubility).[84] The outer layer of some dendrimers are hydrophilic which increases their circulation in the body and in turn increases the circulation of the drugs contained within.[84] Dendrimers can be readily functionalised at the peripheral groups, core and along their branches which allows for the inclusion of targeting moieties, solubilising agents and the attachment of drugs directly to the dendrimer.[85, 86]

Dendrimers have previously been used in order to improve the uptake and efficacy of the platinum anticancer drugs. A study by Duncan *et al*. with a 3.5 generation PAMAM dendrimer and cisplatin has shown that the dendrimer-cisplatin conjugate is 10 times more water soluble than cisplatin alone.[87] They have also shown that the platinum drug loading of dendrimers is higher than that of other polymers such as HPMA and linear polyamidoamine, having carrying capacities of 20-25 wt%, 3-8 wt% and 5-10 wt%, respectively.[87] The dendrimer-platinate complex also accumulates selectively in s.c.B16F10 tumour tissue due to the EPR effect and the concentration of platinum delivered to the tumour is also much higher.[87] Haxton *et al.* have also shown that a hyperbranched polyglycerol dendrimer (with carboxylic acid end groups) and an

aliphatic polyester dendrimer (with hydroxyl end groups) bind strongly to cisplatin to form particularly stable complexes that allow for controlled drug release.[88]

1.4 Aims

The platinum anticancer drugs are effective at treating tumours, however, they are limited due to their lack of specificity for the cancer cells as well as the resistance. The large number of surface groups, high monodispersity and low cytotoxicity of dendrimers are properties that make them good candidates as drug delivery vehicles for platinum anticancer drugs. The PAMAM dendrimers have been sporadically investigated with platinum drugs, either as a delivery vehicle or as a ligand of the drug itself. There have, however, been no systematic studies carried to determine the effect of the dendrimer generation and platinum drug on the properties of the drug delivery system. The aim of this work is to:

- carry a comparative study of the G3.5-6.5 PAMAM dendrimers with both cisplatin and oxaliplatin moieties as these represent the classical platinum complex and the complex which has shown to overcome the resistance to the platinum complexes.
- Exmine the size of the free dendrimer and dendrimer palatinate complexes in order to determine what effect the loading of the platinum complexes has on the size of the overall complexes.
- Quantify the platinum drugs loaded on the dendrimer. In addition the number released will also be quantified and correlations made between the dendrimer generation and the load/release capability.
- Examine the DNA binding capability of the dendrimer platinates to ensure they retain the ability to form platinum DNA adducts after conjugation to the dendrimer.
- Analyse the free dendrimer and dendrimer-platinate complexes for both *in vitro* and *in vivo* cytotoxicity.

1.5 References

1. Jemal, A.; Siegel, R.; Ward, E.; Hao, Y.; Xu, J.; Murray, T.; Thun, M. J. Cancer Statistics 2008. *CA Cancer J. Clin.* **2008,** 58, 71-96.

2. Bignold, L. P. *Cancer: Cell Structures, Carcinogens and Genomic Instability*. Birkhauser: Basel, 2005.

3. Neuberger, A.; Tatum, E. L. *Carcinogenesis as a Biological Problem*. North-Holland: Oxford, 1974; Vol. 34.

4. Kelland, L. The resurgence of platinum-based cancer therapy. *Nat. Rev. Cancer* **2007,** 7, 573-584.

5. Wong, E.; Giandomenico, C. M. Current status of platinum-based antitumor drugs. *Chem. Rev.* **1999,** 99, 2451-2466.

6. Nishiyama, N.; Okazaki, S.; Cabral, H.; Miyamoto, M.; Kato, Y.; Sugiyama, Y.; Nishio, K.; Matsumura, Y.; Kataoka, K. Novel Cisplatin-Incorporated Polymeric Micelles Can Eradicate Solid Tumors in Mice. *Cancer Res.* **2003,** 63, 8977-8983.

7. Dietrich, A.; Mueller, T.; Paschke, R.; Kalinowski, B.; Behlendorf, T.; Reipsch, F.; Fruehauf, A.; Schmoll, H.-J.; Kloft, C.; Voight, W. 2-(4-(tetrahydro-2H-pyran-2-yloxy)-undecyl)-propane-1,3-diamminedichloroplatinum(II): A Novel Platinum Compound that Overcomes Cisplatin Resistance and Induces Apoptosis Mechanisms Different from that of Cisplatin. *J. Med. Chem.* **2008,** 51, 5413-5422.

8. Wheate, N. J.; Brodie, C. R.; Collins, J. G.; Kemp, S.; Aldrich-Wright, J. R. DNA intercalators in cancer therapy: Inorganic and organic drugs and their spectroscopic tools of analysis. *Mini Rev. Med. Chem.* **2007,** 7, 627-648.

9. Heffeter, P.; Jungwirth, U.; Jakupec, M.; Hartinger, C.; Galanski, M.; Elbling, L.; Micksche, M.; Keppler, B.; Berger, W. Resistance against novel anticancer metal compounds: Differences and similarities. *Drug Resist. Update.* **2008,** 11, 1-16.

10. Desoize, B.; Madoulet, C. Particular aspects of platinum compounds used at present in cancer treatment. *Crit. Rev. Oncol. Hemat.* **2002,** 42, 317-325.

11. Crul, M.; van Waardenburg, R. C. A. M.; Beijnen, J. H.; Schellens, J. H. M. DNA-based drug interactions of cisplatin. *Cancer Treat. Rev.* **2002,** 28, 291-303.

12. Fojta, M.; Pivonkova, H.; Brazdova, M.; Kovarova, L.; Palecek, E.; Pospisilova, S.; Vojtesek, B.; Kasparkova, J.; Brabec, V. Recognition of DNA modified by antitumour cisplatin by "latent" and "active" protein p53. *Biochem. Pharmacol.* **2003,** 65, 1305-1316.

13. Kartalou, M.; Essigmann, J. M. Mechanisms of resistance to cisplatin. *Mutat. Res.* **2001,** 478, 23-43.

14. Kemp, S.; Wheate, N. J.; Pisani, M. P.; Aldrich-Wright, J. R. Degradation of fully coordinated platinum(II)-based DNA intercalators by reduced *L*-glutathione. *J. Med. Chem.* **2008,** 51, 2787-2794.

15. Pucci, D.; Bellusci, A.; Bernardini, S.; Bloise, R.; Crispini, A.; Federici, G.; Liguori, P.; Lucas, M. F.; Russo, N.; Valentini, A. Bioactive fragments synergically involved in design of new generation Pt(II) and Pd(II)-based anticancer compounds. *Dalton Trans.* **2008**, 5897-5904.

16. Misset, J. L.; Bleiberg, H.; Sutherland, W.; Bekradda, M.; Cvitkovic, E. Oxaliplatin clinical activity: a review. *Crit. Rev. Oncol. Hemat.* **2000,** 35, 75-93.

17. Faivre, S.; Chan, D.; Salinas, R.; Woynarowska, B.; Woynarowski, J. M. DNA strand breaks and apoptosis induced by oxaliplatin in cancer cells. *Biochem. Pharmacol.* **2003,** 66, 225-237.

18. Jun, Y. J.; Kim, J. I.; Jun, M. J.; Sohn, Y. S. Selective tumor targeting by enhanced permeability and retention effect. Synthesis and antitumor activity of polyphosphazene-platinum(II) conjugates. *J. Inorg. Biochem.* **2005,** 99, 1593-1601.

19. Torchilin, V. P. Drug targeting. *Eur. J. Pharma. Sci.* **2000,** 11, S81-S91.

20. Soyez, H.; Schacht, E.; Vanderkerken, S. The crucial role of spacer groups in macromolecular prodrug design. *Adv. Drug Deliver. Rev.* **1996,** 21, 81-106.

21. Tanaka, T.; Shiramoto, S.; Miyashita, M.; Fujishima, Y.; Kaneo, Y. Tumor targeting based on the effect of enhanced permeability and retention (EPR) and the mechanism of receptor-mediated endocytosis (RME). *Int. J. Pharm.* **2004,** 277, 39-61.

22. Lyer, A. K.; Khaled, G.; Fang, J.; Maeda, H. Exploiting the enhanced permeability and retention effect for tumour targeting. *Drug Discov. Today* **2006,** 11, 812-818.

23. Lee, J. W.; Samal, S.; Selvapalam, N.; Kim, H.-J.; Kim, K. Cucurbituril Homologues and Derivatives: New Opportunities in Supramolecular Chemistry. *Acc. Chem. Res.* **2003,** 36, 621-630.

24. Kim, J.; Jung, I.-S.; Kim, S.-Y.; Lee, E.; Kang, J.-K.; Sakamoto, S.; Yamaguchi, K.; Kim, K. New Cucurbituril Homologues: Synthesis, Isolation, Characterisation, and X-ray Crystal Structures of Cucurbit[*n*]uril (*n* = 5, 7, and 8). *J. Am. Chem. Soc.* **2000,** 122, 540-541.

25. Wheate, N. J. Improving platinum(II)-based anticancer drug delivery using cucurbit[*n*]urils. *J. Inorg. Biochem.* **2008,** 102, 2060-2066.

26. Kim, K.; Selvapalam, N.; Ko, Y. H.; Park, K. M.; Kim, D.; Kim, J. Functionalized cucurbiturils and their applications. *Chem. Soc. Rev.* **2007,** 36, 267-279.

27. Kim, K.; Selvapalam, N.; Oh, D. H. Cucurbiturils - a new family of host molecules. *J. Incl. Phenom. Macro.* **2004,** 50, 31-36.

28. Jeon, Y. J.; Kim, S.-Y.; Ko, Y. H.; Sakamoto, S.; Yamaguchi, K.; Kim, K. Novel molecular drug carrier: Encapsulation of oxaliplatin in cucurbit[7]uril and its effects on stability and reactivity of the drug. *Org. Biomol. Chem.* **2005,** 3, 2122-2125.

29. Marquez, C.; Hudgins, R. R.; Nau, W. M. Mechanism of host-guest complexation by cucurbituril. *J. Am. Chem. Soc.* **2004,** 126, 5806-5816.

30. Wheate, N. J.; Taleb, R. I.; Krause-Heuer, A. M.; Cook, R. L.; Wang, S.; Higgins, V. J.; Aldrich-Wright, J. R. Novel platinum(II)-based anticancer complexes and molecular hosts as their drug delivery vehicles. *Dalton Trans.* **2007**, 5055-5064.

31. Kemp, S.; Wheate, N. J.; Wang, S.; Collins, J. G.; Ralph, S. F.; Day, A. I.; Higgins, V. J.; Aldrich-Wright, J. R. Encapsulation of platinum(II)-based DNA intercalators within cucurbit[6,7,8]urils. *J. Biol. Inorg. Chem.* **2007,** 12, 969-979.

32. Loftsson, T.; Brewster, M. E. Pharmaceutical Applications of Cyclodextrins. 1. Drug Solubilization and Stabilization. *J. Pharma. Sci* **1996,** 85, 1017-1025.

33. Hapiot, F.; Tilloy, S.; Monflier, E. Cyclodextrins as supramolecular hosts for organometallic complexes. *Chem. Rev.* **2006,** 106, 767-781.

34. Rajewski, R. A.; Stella, V. J. Pharmaceutical Applications of Cyclodextrins. 2. In vivo drug delivery. *J. Pharm. Sci.* **1996,** 85, 1142-1169.

35. Stella, V. J.; Rajewski, R. A. Cyclodextrins: Their future in drug formulation and delivery. *Pharmaceutical Res.* **1997,** 14, 556-567.

36. Oda, Y.; Yanagisawa, H.; Maruyama, M.; Hattori, K.; Yamanoi, T. Design, synthesis and evaluation of D-galactose-b-cyclodextrin conjugates as drug-carrying molecules. *Bioorg. Med. Chem.* **2008,** 16, 8830-8840.

37. Uekama, K.; Hirayama, F.; Arima, H. Recent aspect of cyclodextrin-based drug delivery system. *J. Incl. Phenom. Macro.* **2006,** 56, 3-8.

38. Cucinotta, V.; Mangano, A.; Nobile, G.; Santoro, A. M.; Vecchio, G. New platinum(II) complexes of b-cyclodextrin diamine derivatives and their antitumor activity. *J. Inorg. Biochem.* **1993,** 52, 183-190.

39. Irie, T.; Uekama, K. Pharmaceutical Applications of Cyclodextrins. III. Toxicological Issues and Safety Evaluation. *J. Pharma. Sci* **1997,** 86, 147-162.

40. Krause-Heuer, A. M.; Wheate, N. J.; Tilby, M. J.; Pearson, D.; Ottley, C. J.; Aldrich-Wright, J. R. Substituted beta-cyclodextrin and calix[4]arene as encapsulatory vehicles for platinum(II)-based DNA intercalators. *Inorg. Chem.* **2008,** 47, 6880-6888.

41. Martino, M.; Neri, P. Chemistry of calix[7]arenes. *Mini Rev. Org. Chem.* **2004,** 1, 219-231.

42. Lo, H.-S.; Yip, S.-K.; Zhu, N.; Yam, V. W.-W. The first example of Pt---Pt interacion in platinum(II) complexes beaing bulky tri-*tert*-butyl-2,2' :6',2''-terpyridine pendants *via* conformational control of the calix[4]arene moiety *Dalton Trans.* **2007**, 4386-4389.

43. Gaeta, C.; Caruso, T.; Mincolelli, M.; Troisi, F.; Vasca, E.; Neri, P. *p*-sulfonatocalix[7]arene: synthesis, protolysis, and binding ability. *Tetrahedron* **2008,** 64, 5370-5378.

44. Kon, N.; Iki, N.; Miyano, S. Inclusion behavior of water-soluble thiacalix- and cali[4]arenes towards substituted benzenes in aqueous solution. *Org. Biomol. Chem.* **2003,** 1, 751-755.

45. Prato, M.; Kostarelos, K.; Bianco, A. Functionalized Carbon Nanotubes in Drug Sesign and Discovery. *Accounts Chem. Res.* **2008,** 41, 60-68.

46. Liu, Z.; Sun, X.; Nakayama-Ratchford, N.; Dai, H. Supramolecular chemistry on water-soluble carbon nanotubes for drug loading and delivery. *ACS Nano* **2007,** 1, 50-56.

47. Ajima, K.; Maigne, A.; Yudasaka, M.; Iijima, S. Optimum hole-opening condition for cisplatin incorporation in single-wall carbon nanohorns and its release. *J. Phys. Chem. B* **2006,** 110, 19097-19099.

48. Matsumura, S.; Ajima, K.; Yudasaka, M.; Iijima, S.; Shiba, K. Dispersion of Cisplatin-Loaded Carbon Nanohorns with a Conjugate Comprised of an Artifical Peptide Aptamer and Polyethylene Glycol. *Mol. Pharmaceut.* **2007,** 4, 723-729.

49. Ajima, K.; Murakami, T.; Mizoguchi, Y.; Tsuchida, K.; Ichihashi, T.; Iijima, S.; Yudasaka, M. Enhancement of *In Vivo* Anticancer Effects of Cisplatin by Incorporation Inside Single-Wall Carbon Nanohorns. *ACS NANO* **2008,** 2, 2057-2064.

50. Feazell, R. P.; Nakayama-Ratchford, N.; Dai, H.; Lippard, S. J. Soluble single-walled carbon nanotubes as longboat delivery systems for platinum(IV) anticancer drug design. *J. Am. Chem. Soc.* **2007,** 129.

51. Son, S. J.; Bai, X.; Lee, S. B. Inorganic hollow nanoparticles and nanotubes in nanomedicine: Part 1. Drug/gene delivery applications. *Drug Discov. Today* **2007,** 12, 650-656.

52. Patrick, G. L. *An Introduction to Medicinal Chemistry*. Second ed.; Oxford University Press: Oxford, 2001; p 123-152.

53. Choi, M. J.; Maibach, H. I. Liposomes and Niosomes as Topical Drug Delivery Systems. *Skin Pharmacol Physiol* **2005,** 18, 209-219.

54. Fang, J.-Y.; Hong, C.-T.; Chiu, W.-T.; Wang, Y.-y. Effect of liposomes and niosomes on skin permeation of enoxacin. *Int. J. Pharm.* **2001,** 219, 61-72.

55. Felnerova, D.; Viret, J.-F.; Gluck, R.; Moser, C. Liposomes and virosomes as delivery systems for antigens, nucleic acids and drugs. *Curr. Opin. Biotech.* **2004,** 15, 518-529.

56. Pinto-Alphandary, H.; Andremont, A.; Couvreur, P. Target delivery of antibiotics using liposomes and nanoparticles: research and applications. *Int. J. Antimicrob. Ag.* **2000,** 13, 155-168.

57. Junior, A. D. C.; Vieira, F. P.; De Melo, V. J.; Lopes, M. T. P.; Silveira, J. N.; Ramaldes, G. A.; Garnier-Suillerot, A.; Pereira-Maia, E. C.; De Oliveira, M. C. Preparation and cytotoxicity of cisplatin-containing liposomes. *Braz. J. Med. Biol. Res.* **2007,** 40, 1149-1157.

58. Dragovich, T.; Mendelson, D.; Kurtin, S.; Richardson, K.; Von Hoff, D.; Hoos, A. A Phase 2 trial of the liposomal DACH platinum L-NDDP in patients with therapy-refractory advanced colorectal cancer. *Cancer Chemother. Pharmacol.* **2006,** 58, 759-764.

59. Lu, C.; Perez-Soler, R.; Piperdi, B.; Walsh, G. L.; Swisher, S. G.; Smythe, W. R.; Shin, H. J.; Ro, J. Y.; Feng, L.; Truong, M.; Yalamanchili, A.; Lopez-Berestein, G.; Hong, W. K.; Khokhar, A. R.; Shin, D. M. Phase II study of a liposome-entrapped cisplatin analog (L-NDDP) administered intrapleurally and pathologic response rates in patients with malignant pleural mesothelioma. *J. Clin. Oncol.* **2005,** 23, 3495-3501.

60. Sood, P.; Thurmond, K. B.; Jacob, J. E.; Waller, L. K.; Silva, G. O.; Stewart, D. R.; Nowotnik, D. P. Synthesis and characterization of AP5346, a novel polymer-linked diaminocyclohexane platinum chemotherapeutic agent. *Bioconjugate Chem.* **2006,** 17, 1270-1279.

61. Rice, J. R.; Gerberich, J. L.; Nowotnik, D. P.; Howell, S. B. Preclinical efficacy and pharmokinetics of AP5346, a novel diaminocyclohexane-platinum tumor-targeting drug delivery system. *Clin. Cancer Res.* **2006,** 12, 2248-2254.

62. Campone, M.; Rademaker-Lakhai, J. M.; Bennouna, J.; Howell, S. B.; Nowotnik, D. P.; Beijnen, J. H.; Schellens, J. H. M. Phase I and pharmacokinetic trial of AP5346, a

DACH-platinum-polymer conjugate, administered weekly for three out of every 4 weeks to advanced solid tumor patients. *Cancer Chemother. Pharmacol.* **2007,** 60, 523-533.

63. Petrak, K. Essential properties of drug-targeting delivery systems. *DDT* **2005,** 10, 1667-1673.

64. Boas, U.; Heegaard, P. M. H. Dendrimers in drug research. *Chem. Soc. Rev.* **2004,** 33, 43-63.

65. Howell, B. A.; Fan, D.; Rakesh, L. Thermal decomposition of a generation 4.5 PAMAM dendrimer platinum drug conjugate. *J. Therm. Anal. Calor.* **2006,** 85, 17-20.

66. Pisani, M. J.; Wheate, N., J.; Keene, F. R.; Aldrich-Wright, J. R.; Collins, J. Anionic PAMAM dendrimers as drug delivery vehicles for transition metal based anticancer drugs. *J. Inorg. Biochem.* **2008**.

67. Wolinsky, J. B.; Grinstaff, M. W. Therapeutic and diagnostic applications of dendrimers for cancer treatment. *Adv. Drug Del. Rev.* **2008,** 60, 1037-1055.

68. Najlah, M.; D'Emanuele, A. Crossing cellular barriers using dendrimer nanotechnologies. *Curr. Opin. Pharmacol.* **2006,** 6, 522-527.

69. Tomalia, D. A.; Baker, H.; Dewald, J.; Hall, M.; Kallos, G.; Martin, S.; Roeck, J.; Ryder, J.; Smith, P. A New Class of Polymers: Starburst-Dendritic Macromolecules. *Polymer J.* **1985,** 17, 117-132.

70. Newkome, G. R.; Yao, Z.-q.; Baker, G. R.; Gupta, V. K. Cascade Molecules: A New Approach to Micelles A [27]-Arborol. *J. Org. Chem.* **1985,** 50, 2004-2006.

71. Medina, S. H.; El-Sayed, M. E. H. Dendrimers as Carriers for Delivery of Chemotherapeutic Agents. *Chem. Rev.* **2009,** 109, 3141-3157.

72. Ihre, H.; De Jesus, P.; Frechet, J. M. J. Fast and Convenient Divergent Synthesis of Aliphatic Ester Dendrimers by Anhydride Coupling. *J. Am. Chem. Soc.* **2001,** 123, 5908-5917.

73. Maraval, V.; Pyzowski, J.; Caminade, A.-M.; Majoral, J.-P. "Lego" Chemistry for the Straightforward Synthesis of Dendrimers. *J. Org. Chem.* **2003,** 68, 6043-6046.

74. Hawker, C. J.; Frechet, J. M. J. Preparation of Polymers with Controlled Molecular Architecture. A New Convergent Approach to Dendritic Macromolecules. *J. Am. Chem. Soc.* **1990,** 112, 7638-7647.

75. Hawker, C. J.; Frechet, J. M. J. Control of Surface Functionality in the Synthesis of Dendritic Macromolecules Using the Convergent-Growth approach. *Macromolecules* **1990,** 23, 4726-4729.

76. Wooley, K. L.; Hawker, C. J.; Frechet, J. M. J. Hyperbranched Macromolecules via a Novel Double-Stage Convergent Growth Approach. *J. Am. Chem. Soc.* **1991,** 113, 4252-4261.

77. Kawaguchi, T.; Walker, K. L.; Wilkins, C. L.; Moore, J. S. Double Exponential Dendrimer Growth. *J. Am. Chem. Soc.* **1995,** 117, 2159-2165.

78. Carlmark, A.; Hawker, C.; Hult, A.; Malkoch, M. New methodologies in the construction of dendritic materials. *Chem. Soc. Rev.* **2009,** 38, 352-362.

79. Franc, G.; Kakkar, A. K. Diels-Alder "Click" Chemistry in Designing Dendritic Macromolecules. *Chem. Eur. J.* **2009,** 15, 5630-5639.

80. van Dijk, M.; Rijkers, D. T. S.; Liskam, R. M. J.; van Nostrum, C. F.; Hennink, W. E. Synthesis and Applications of Biomedical and Pharmaceutical Polymers via Click Chemistry Methodologies. *Bioconjugate Chem.* **2009,** 20, 2001-2016.

81. Antoni, P.; Nystrom, D.; Hawker, C. J.; Hult, A.; Malkoch, M. A chemoselective approach for the accelerated synthesis of well-defined dendritic architectures. *Chem. Commun.* **2007**, 2249-2251.

82. Joralemon, M. J.; O'Reilly, R. K.; Matson, J. B.; Nugent, A. K.; Hawker, C. J.; Wooley, K. L. Dendrimers Clicked Together Divergently. *Macromolecules* **2005,** 38, 5436-5443.

83. Agarwal, A.; Asthana, A.; Umesh, G.; Jain, N. K. Tumour and dendrimers: a review on drug delivery aspects. *J. Pharm. Pharmacol.* **2008,** 60, 671-688.

84. Fernandez, L.; Gonzalez, M.; Cerecetto, H.; Santo, M.; Silber, J. J. Solubilzation and release properties of dendrimers. Evaluation as prospective drug delviery systems. *Supramol. Chem.* **2006,** 18, 633-643.

85. Ravoo, B. J. Nanofabrication with metal containing dendrimers. *Dalton Trans.* **2008**, 1533-1537.

86. Lee, C. C.; Gillies, E. R.; Fox, M. E.; Guillaudeu, S. J.; Fréchet, J. M. J.; Dy, E. E.; Szoka, F. C. A single dose of doxorubicin-functionalised bow-tie dendrimer cures mice bearing C-26 colon carcinomas. *Proc. Natl. Acad. Sci. U.S.A* **2006,** 103, 16649-16654.

87. Malik, N.; Evagorou, E. G.; Duncan, R. Dendrimer-platinate: a novel approach to cancer chemotherapy. *Anti-Cancer Drug.* **1999,** 10, 767-776.

88. Haxton, K. J.; Burt, H. M. Hyperbranched polymers for controlled release of cisplatin. *Dalton Trans.* **2008**, 5872-5875.

Chapter 2:Cisplatin-PAMAM dendrimer-platinates

2.1 INTRODUCTION

As stated at the end of chapter 1, examination of dendrimers as delivery vehicles for several different types of platinum drugs and complexes has been sporadic.[1-8] These dendrimers have included PAMAM, polyglycerol,[8] poly(propyleneimine)[9], and thiol-yne derived[7] dendrimers with the active components of both cisplatin[3] and oxaliplatin[2] and a novel DNA intercalating platinum complex.[1] In some cases the platinum drugs are attached non-reversibly to the dendrimer through coordination to the amine groups, but in most cases the drugs are attached either by electrostatic attraction[1] or through reversible but direct coordination of the platinum atom to the terminal carboxylate groups.[2,3] In one case, a G1 poly(propyleneimine) dendrimer was used as the central bridging ligand in a tetranuclear platinum complex, instead of as a drug delivery vehicle.[9] Whilst the resultant complex was able to bind guanosine, it demonstrated little cytotoxicity.

In this chapter a systematic study of four anionic half-generation PAMAM dendrimers (G3.5-6.5) bound to the active component of cisplatin (*cis*-$[Pt(NH_3)_2]^{2+}$) has been completed to better evaluate this family of dendrimers as delivery vehicles for platinum drugs. The dendrimer-platinate complexes were characterised by one dimensional and diffusion ^{1}H NMR, inductively coupled plasma atomic emission spectrometry (ICP-AES) and drug release monitored using guanosine binding experiments. Finally, *in vitro* cytotoxicity was determined using the A2780, A2780cis and A2780cp ovarian cancer cell lines and *in vivo* cytotoxicity in a A2780 tumour xenograft.

2.2 RESULTS and DISCUSSION

2.2.1 Cisplatin hydrolysis

In order to attach the active component of cisplatin to the dendrimers cisplatin needs to be aquated so that it can form reversible coordinate bonds to the dendrimer carboxylate groups, Figure 2.1. Cisplatin can either be mono-aquated and form a single bond with

the dendrimer or bis-aquated and form two bonds. It was hypothesised that the use of bis-aquated cisplatin would increase the probability of platinum binding to the dendrimer and result in maximum drug loading.

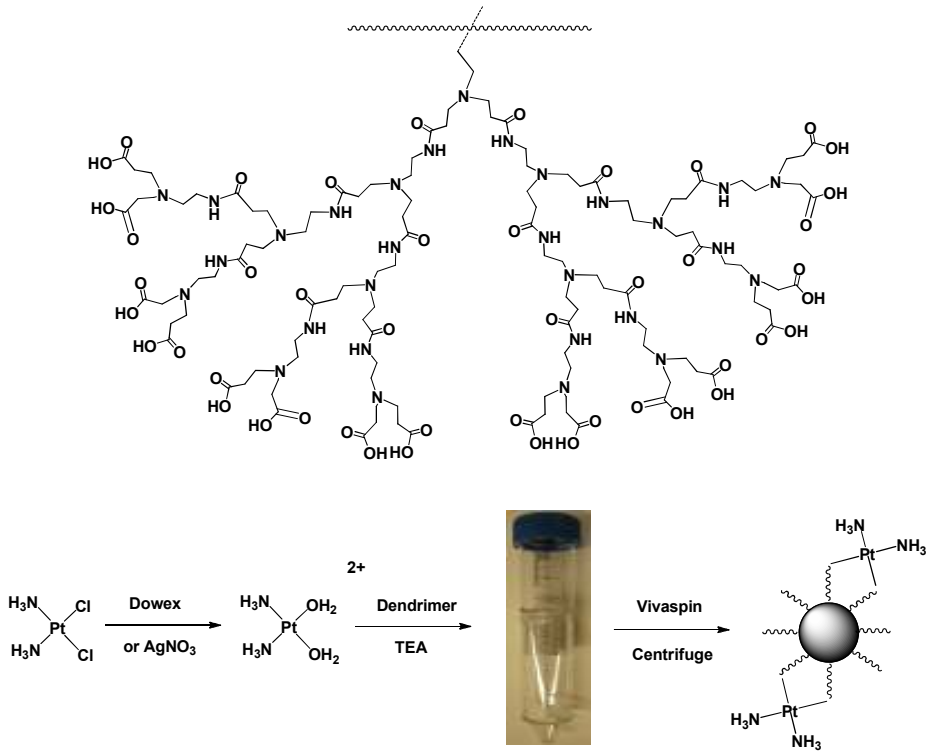

Figure 2.1. The chemical structure of a generation 2.5 PAMAM dendrimer showing one hemisphere of the polymer (Top), aquation and subsequent attachment of the active component of cisplatin to the dendrimers (bottom).

Aquation of platinum drugs is usually achieved using $AgNO_3$, which reacts with the chlorido ligands to form AgCl as an insoluble white precipitate.[10] Whilst this method has been used for many years it is not ideal as the reaction must be done in the absence of light to ensure that the silver does not undergo redox reduction, which can degrade the platinum complex. The AgCl can also form a very fine precipitate which can be difficult to remove, and finally, as a precious metal, the use of silver greatly adds to the cost of

drug production when manufactured on an industrial scale. As such, a more efficient and cheaper method for the aquation of platinum drugs was sought.

Dowex® is a common laboratory stationary phase used in chromatography for separating compounds based on charge, and is available either as a cation or anion exchanger. The benefit of Dowex is that it can be reused after regeneration and does not require the absence of light. Two methods of platinum aquation were attempted using Dowex; simple stirring of cisplatin in a beaker with Dowex followed by filtration and rotary evaporation, and/or elution of cisplatin through Dowex columns of varying lengths, with the resultant solutions rotary evaporated to dryness. Samples produced by both methods were then analysed by ^{195}Pt NMR.

Platinum NMR is used for a number of applications including structure elucidation, relaxation studies, kinetic and mechanistic studies and drug binding studies. Platinum has been studied by NMR since the 1960s after it was discovered that the chemical shift (δ) of the ^{195}Pt isotope was affected by structural changes. The ^{195}Pt isotope is the only NMR active platinum isotope. This isotope has favourable properties for use in NMR studies including a spin quantum number, I =1/2, and relative sensitivity of 0.00994 (^{1}H=1). The range of values recorded for ^{195}Pt span 13000 ppm and a change of more than 100 ppm is observed through varying the ligand substitutions.

When studying the effect of ligand substitution on the chemical shift of ^{195}Pt, there are a number of difficulties that can occur when referencing the complex of interest: the large temperature dependence of the chemical shift, interactions with internal reference material if used, uncertainties due to isotopomers and small mathematical errors. The reference complexes normally used in platinum NMR are $[PtCl_6]^{2-}$ or $[PtCl_4]^{2-}$ in D_2O but $[Pt(CN)_6]^{2-}$ can also be used. The peak in NMR for potasssium tetrachloroplatinate, $[PtCl_4]^{2-}$, occurs at -1631 ppm and is used in our experiments as an external reference. The ranges for platinum(0), platinum(II) and platinum(IV) complexes have been determined.

The calculated chemical shifts for platinum(II) complexes are higher than those for platinum(0) complexes due to the deshielding that results from removal of electrons. The peaks for platinum(IV) complexes occur at the high-frequency end of the NMR spectrum but considerable overlap occurs with the platinum(II) and platinum(IV) ranges.

The effect of different types of ligands bound to platinum has been investigated. Substitution of ligands with halogens, amines, phosphines, heterocylces (pyridine and macrocycles), arsenic and sulphur has allowed general trends to been established for different classes of complexes. The order of increasing shielding in the ^{195}Pt NMR for related amine complexes is $OSO_3^{2-} < OH^- < H_2O < Cl^- < NO_2 < Br^- < NH_3 <$ SCN < I < solid thiourea < Me_2SO-S. The signals for the platinum complexes cis-$[Pt(NH_3)(OH_2)_2]$, cis-$[Pt(NH_3)(NO)_2]$ and cis-$[Pt(NH_3)_2(SCN)_2]^{2-}$ appear at -1593, -2214 and -3016 ppm in accordance with the established trend. The NMR signal for cisplatin is observed at approximately -2100 ppm and replacing the chlorido ligands with water ligands, through the aquation reaction, will have a deshielding effect and result in a downfield shift of the ^{195}Pt signal.

The resulting complexes indicate that Dowex is only partially able to aquate cisplatin, Figure 2.2. In the ^{195}Pt NMR spectra three individual resonances are always observed at -2150, -1838 and -1600 ppm which represent cisplatin in the bis-chlorido form, mono-

aquated and bis-aquated cisplatin, respectively.[11] In some instances additional broad resonances are observed at -1520, -1730 and -1750 ppm, which most likely represent mono and bis-aquated cisplatin with hydroxyl rather than water ligands.[11] The amount of unreacted cisplatin in all cases is very low (less than 1%), peack c Figure 2.2, with the ratios of mono and bis-aquated complexes roughly observed as a 50%:50% mix, Figure 2.2 peaks a and b. Attempts to drive the reaction further to the bis-aquated product through further elution on additional Dowex columns or further stirring with Dowex were however unsuccessful. Whilst this method is not able to produce a solution containing only bis-aquated cisplatin it may still have industrial application, or in the laboratory, in reducing the amount of $AgNO_3$ required.

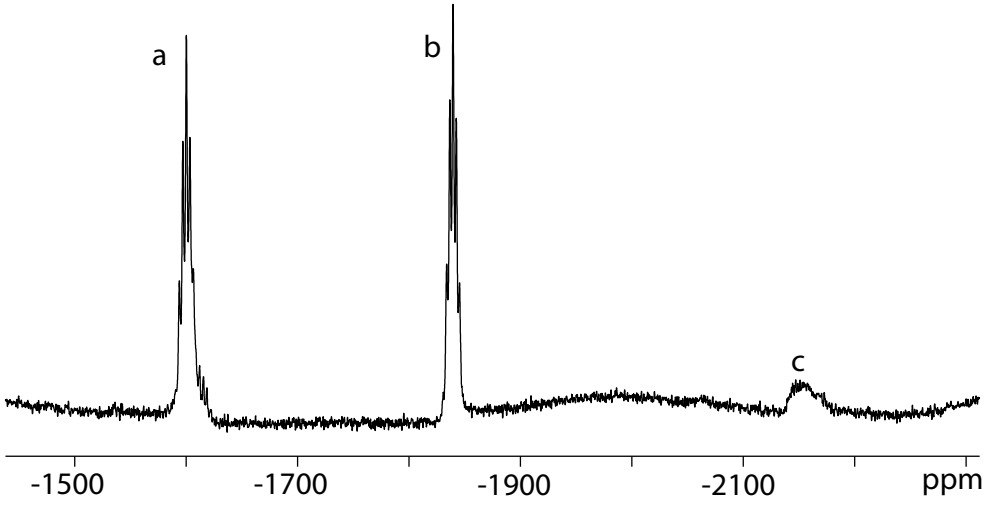

Figure 2.2 The ^{195}Pt NMR spectrum (85.8 MHz, D_2O) of the product of aquated cisplatin, at pH 7, made using Dowex anion exchange resin, showing a. bis-aquated cisplatin, b. mono-aquated and c. unreacted cisplatin.

Subsequently, samples used for binding to dendrimers in this study were either partly aquated with Dowex before complete aquation using $AgNO_3$, or were completely aquated using $AgNO_3$.

2.2.2 Synthesis and characterisation of dendrimer-platinate complexes

All dendrimers were combined in unbuffered water with four equivalents of triethylamine (TEA) and a half equivalent of bis-aquated cisplatin (both to the number of dendrimer surface groups). These solutions were then stirred for 5 h changing them from colourless to yellow coloured solutions. Unbound cisplatin and the TEA were removed by centrifuging the samples through Vivaspin columns with a molecular weight cut off of 5 kDa, leaving the dendrimer-platinate complexes in the top of the column, Figure 2.1. The dendrimer-platinates are highly soluble in water, although if dried, they are difficult to get back into solution. As such, samples were generally diluted to a known concentration with either H_2O or D_2O immediately after centrifuge purification and kept frozen until needed. Samples were initially kept frozen for up to one week for the first three months then fresh samples were prepared each time as required

Following the coupling reaction it is important to quantify the number of drug molecules bound to the dendrimer. Ideally all of the binding sites on the dendrimer will be occupied; however this is not likely to be the case and to carry out accurate *in vivo* and *in vitro* tests the actual figure must be determined. A number of techniques exist for the analysis of metals and non-metals in samples including atomic absorption spectroscopy (AAS), inductively coupled plasma spectroscopy techniques (ICP) and ^{195}Pt NMR.

Under normal conditions electrons will be in the ground state.[12, 13] When light of the correct wavelength (energy) is absorbed by the electrons they are promoted to the excited state. The amount of light emitted by a species diminishes if an absorbance occurs.[13] This reduction in the amount of light given off is proportional to the number of atoms absorbing it and through the application of the Beer-Lambert (Eq 1) law the absorption can be used to determine the atom concentration.[12, 13]

$$\text{Eq 1: } A = \log \frac{I_o}{I} = k_v l \log e$$

The absorbance is A, the intensity of the incident light is I_o, intensity of the transmitted light is I, K_v is the absorption coefficient and l is the path length.

A number of AAS techniques are currently used for the analysis of samples including Flame, FAAS, and Electrothermal AAS.[13] These analytical techniques have particularly low limits if detection, FAAS has a detection limit of 0.09 μg mL^{-1} for platinum.[12, 13] The use of element specific radiation sources provides spectral lines with narrow bandwidths which means that overlap of one atomic absorption line with another is negligible and the techniques are highly selective.[12, 13]

To maintain the selectivity, hollow cathode lamps lined with the metal of interest or electrodless discharge lamps containing the element of interest or a salt of that element are used.[13] Although the selectivity is high, and the detection limit is low there are some problems associated with AAS including: chemical interferences, ionisation interferences, and physical and spectral interferences.[12, 13] Chemical interferences occur as a result of two mechanisms: the atomisation of the analyte elements is not completed in the solid or liquid phase or the vaporised atoms react with other atoms, elements or radicals to form new compounds with different thermochemical properties.[12, 13] Ionisation interferences occur when the analyte is only partially ionised leading to depressed absorption signals.[12, 13] Physical interferences are a result of the physical characteristics of the solution being analysed as viscosity, surface tension, vapour pressure and temperature all influence sample intake and therefore the absorption signal.[12, 13] Although rare, spectral interferences can occur when the resonances emitted from the light source overlaps with the spectral line of another element in the atomiser.[12, 13]

It is also possible to use ^{195}Pt NMR to determine the concentration of platinum in a sample. The use of another platinum complex as an internal standard, added at a known

concentration, will allow a direction comparison of the peak for the NMR complexes. The integral of the analyte peak can be expressed as a percentage of the integral of the peak for the internal standard and if the exact concentration of the internal standard is known the percentage can be used to calculate the concentration of platinum. In order to use this technique the internal standard must be chosen very carefully to avoid the appearance of peaks in the same range as the analyte.

One technique that has been developed recently is Inductively Coupled Plasma (ICP) spectroscopy. Inductively coupled plasma can be used with different detectors such as ICP- Mass Spectrometry (MS) and ICP- Atomic Emission Spectroscopy/ Optical Emission Spectroscopy (AES/OES) to accurately determine the amount of metal present and, when used in conjunction with mass spectrometry, can measure concentrations as low as parts per trillion.[14, 15] These techniques have become popular as they can be used with sample volumes less that 1 mL, coupled to other techniques to decrease sample consumption which reduces possible interferences and used to analyse several elements simultaneously.[16]

The detection through atomic emission spectroscopy is made possible due to the emission of light ($h\nu$) as electrons return from an excited state to a ground state, Figure 2.3.[14] Plasma is an electronically neutral, highly ionised gas consisting of electrons, ions and atoms and ICP-AES uses plasma to atomise and excite the species of interest.[14, 17] The energy used to maintain the plasma is derived from an electric or magnetic field. The plasma is used in conjunction with inert gases such as helium or argon in order to prevent combustion.[14] The temperature of the plasma used in ICP analysis ranges from 600-8000 K, comparable to the temperature on the surface of sun, 10 000 K, and the range at which the analysis is performed is between 5000 and 8000 K as this ensures that most samples are completely atomised.[14, 17]

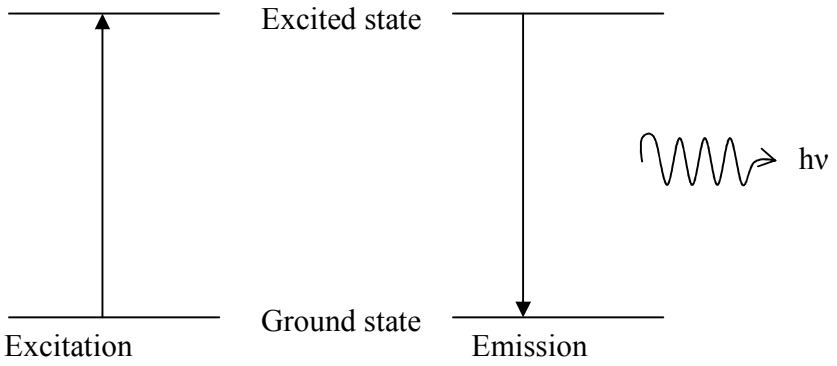

Figure 2. 3 The emission of light resulting from the relaxation back to the ground state.

In order to analyse the samples they must first be introduced into the plasma, Figure 2.4. The samples are introduced to the plasma *via* a nebuliser which converts the aqueous solutions to an aerosol consisting of particles that are 1-10 μm in diameter.[14, 16] Direct injection of a liquid sample into the plasma would result in the plasma being extinguished or cause the atoms to be improperly desolvated making excitation and extinction less efficient.[14]

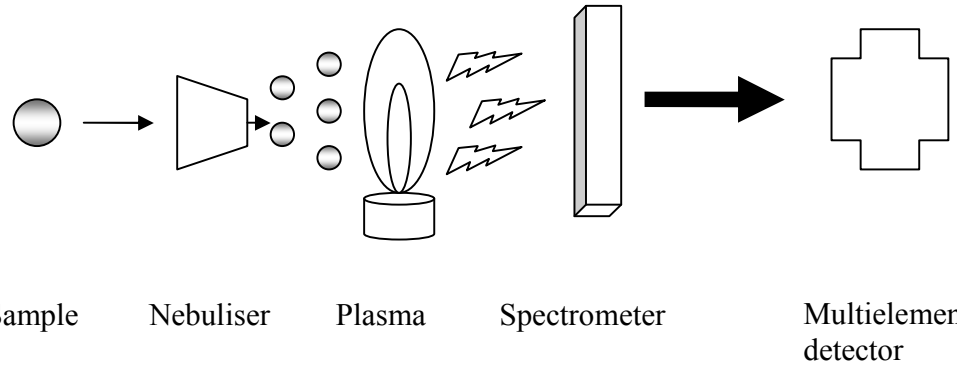

Figure 2.4 The schematic representation of sample analysis using an ICP-AES system.

Typically, the emission from the samples being analysed is collected through four different types of detector including photomultiplier tubes, photo diode arrays and charge coupled devices.[14] These detectors are normally combined in one of four

configurations: sequential, simultaneous with single point detection, simultaneous with one-dimensional detection and simultaneous with two-dimensional detection.[14] Sequential systems can only measure one wavelength at a time whilst more efficient systems make use of polychromators to analyse a number of wavelengths. More recent systems use solid state detectors which can allow spectral windows to be analysed, with charge coupled devices being used in conjunction with a prism and grate to carry out multielement analysis using more than one wavelength per element.[14]

ICP-AES analysis can be adversely affected due to interferences that can arise during sample preparation or from the operating conditions of the plasma itself.[14, 17] The interferences that arise from the plasma may occur due to two or more elements emitting radiation at the same wavelength or the formation of undesired species such as ions or metal oxides.[14, 17] Despite these potential interferences, the limit of detection for ICP-AES is as low as parts per billion (ng mL^{-1} or $\mu g\ L^{-1}$).[14, 17] The limit of detection may also be influenced by the positioning of the plasma torch as horizontal placement can increase the sensitivity of the technique.[14]

The number of cisplatin molecules bound to each dendrimer was determined using ICP-AES. This technique was selected over the others as it has high selectivity, very low detection limits and was the only technique readily available at the time of analysis. The sensitivity of the instrument used in the analysis can be affected by a number of different factors including room temperature. In order to ensure repeatability, reliability and comparability between different runs the machine must be calibrated prior to each run and at intervals during prolonged use. This was achieved using a multielement standard containing 0 - 1000 ppb platinum in 1% nitric acid. The standard was diluted to concentrations of 1, 10 and 50 ppm in 1% nitric acid and these were used to obtain a calibration curve for the experiment, a range over which the results are known to be accurate, Figure 2.5. The calibration was also run after every ten samples of the experiment to ensure the accuracy of the results.

Originally the dendrimer-platinates were examined directly, but decomposition and deposition of the dendrimer in the machine blocked the ports and gave unreliable results. As such, the Vivaspin centrifuge filtrate was analysed to determine the concentration of unbound aquated cisplatin, and from this, the amount of bound cisplatin. Each dendrimer binds a different number of cisplatin molecules, consistent with the increasing number of carboxylate surface groups with increasing dendrimer generation, Table 2.1. Cisplatin binding efficiency decreases with increasing dendrimer size with 22 cisplatin molecules for the G3.5 dendrimer representing binding of 68% of the theoretically available surface groups, increasing to 94 cisplatin molecules for the G6.5, which represents binding to only 37% of the available carboxylate groups. The lower binding efficiency of the higher generation dendrimers may be a function of the increased steric crowding of the surface groups making them less accessible to the platinum drug and/or the difficulty in deprotonating so many closely packed carboxylic acids.

The spherical structure of the dendrimers and their reported monodispersity mean that a predictable number of binding sites are available on the surface of the dendrimer. If the structure is not monodisperse then it is difficult to say with accuracy that the number of binding sites is consistent. This can affect the results for loading and release. Despite attempts to prove the monodispersity of the structure using Matrix Assisted Laser Desorption/Ionisatin mass spectroscopy we were unable to confirm the relative monodispersity of the structure and as such the results presented assume the idealised dendrimer structure.

Table 2.1. Binding and release characteristics of the active component of cisplatin to the anionic half generation PAMAM dendrimers G3.5 to 6.5.

Generation	**No of surface groups (Theoretical binding sites)[a]**	**No. of bound Pt molecules[b]**	**No. of releasable Pt molecules**	**Particle size**			
				D **(×10^{-10} m^{2}s^{-1})[c]**		**Diameter (nm)**	
				Free	**Bound**	**Free**	**Bound**
3.5	64 (32)	22 ± 4	4 ± 1	1.30	2.15	2.74	1.66
4.5	128 (64)	37 ± 3	11 ± 3	0.91	1.12	3.91	3.17
5.5	256 (128)	54 ± 8	19 ± 3	0.66	1.06	5.44	3.37
6.5	512 (256)	94 ± 11	59 ± 7	0.60	0.89	5.93	4.01

a. Number of binding sites assumes cisplatin binding to the dendrimer is in a bidentate manner. b. Determined by indirect quantification. c. Diffusion coefficient of the dendrimer.

Previously it has been shown that the inert DNA intercalating platinum complex, [Pt(5,6-dimethyl-1,10-phenanthroline)(1S,2S-diaminocyclohexane)]$^{2+}$ (56MESS),[18] which binds anionic PAMAM dendrimers solely through electrostatic interactions, was able to bind these dendrimers just as efficiently; 28 and 96 56MESS molecules for G3.5 and G6.5 dendrimers respectively.[1] Our result is consistent with the results obtained for 56MESS, but significantly lower than the result obtained by Malik *et al* who found their cisplatin-G3.5 dendrimer-platinate complex contained 24% w/w platinum by analysis, which represents as many as 57 cisplatin molecules per dendrimer.[3] No results for G4.5 or higher generation PAMAM dendrimers have previously been reported.

The dendrimer-platinates were further characterised using one dimensional and diffusion ^{1}H NMR spectroscopy. Each dendrimer, as provided by the manufacturer, shows two groups of resonances; one group of relatively high intensity peaks between 2.2 and 3.8 ppm and a group of much smaller intensity between 5.6 and 6.2 ppm, Figure 2.6. Upon centrifuging in a Vivaspin column the resonances around 5-6 ppm disappear leaving only a group of 9-10 resonances in the aliphatic region. These results indicate that the dendrimers, as supplied by Sigma-Aldrich and Dendritech, contains lower molecular mass impurities that can be removed by Vivaspin centrifuge. Therefore, all commercial PAMAM dendrimers should be purified first before reaction with platinum drugs.

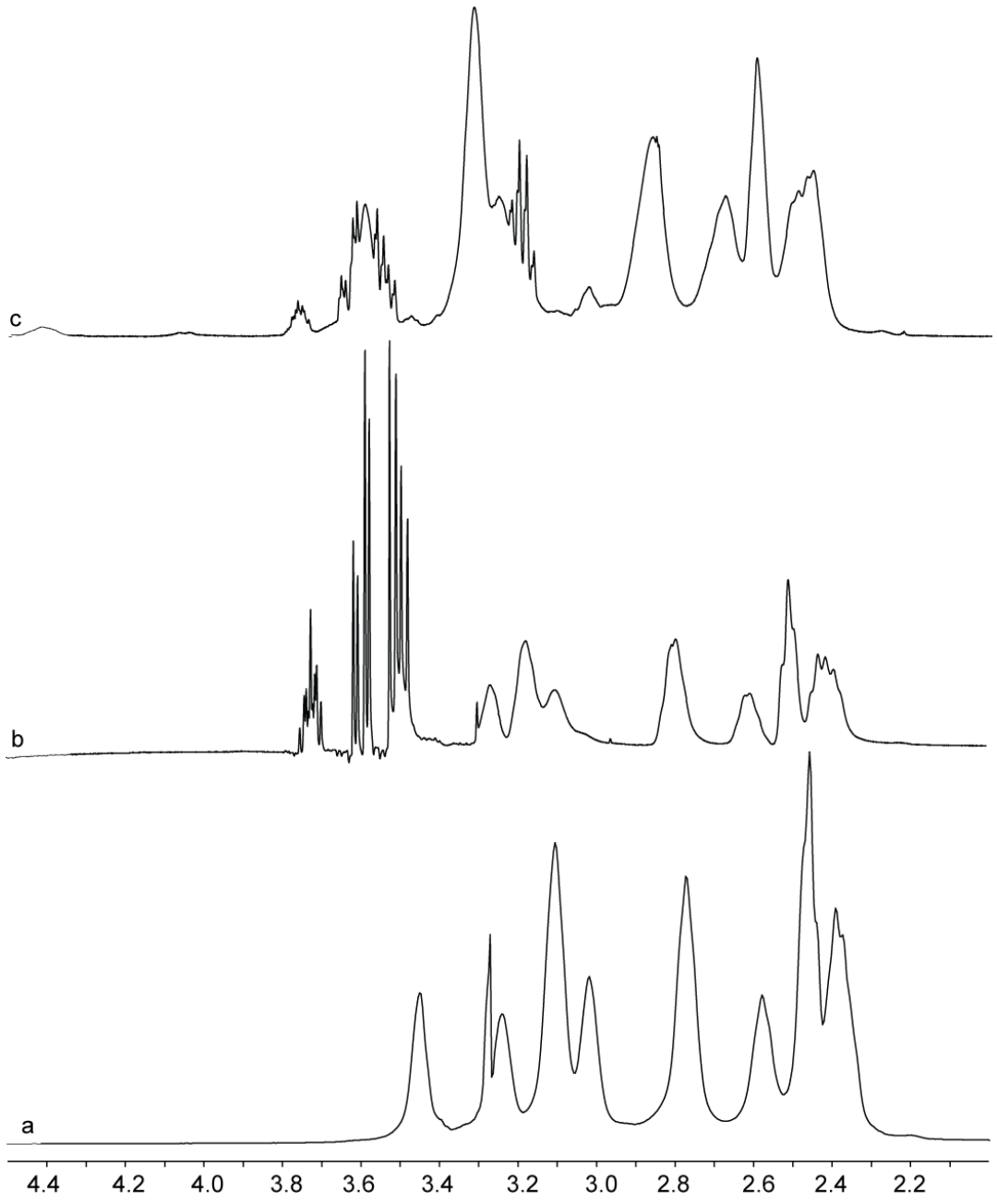

Figure 2.6. The ^{1}H NMR spectra (400 MHz, D_2O) of a. unpurified G4.5 dendrimer, b. G4.5 dendrimer purified on a Vivaspin column with a 5 kDa filtration membrane and c. purified G4.5 cisplatin dendrimer-platinate complex.

Addition of cisplatin to each dendrimer induces changes in the dendrimer ^{1}H NMR spectra, Figure 2.6. Five broad resonances are observed between 2.4 and 3.4 ppm, leaving three relatively sharps resonances at 2 and between 3.6 to 3.8 ppm.

Brownian motion describes the random movement of particles through solution, Figure 2.7. The motion is caused by millions of collisions occurring between the particle and solution molecules every second. These collisions cause a net change in the magnitude and direction of motion of the particle and result in the diffusion of the particle through the solution.

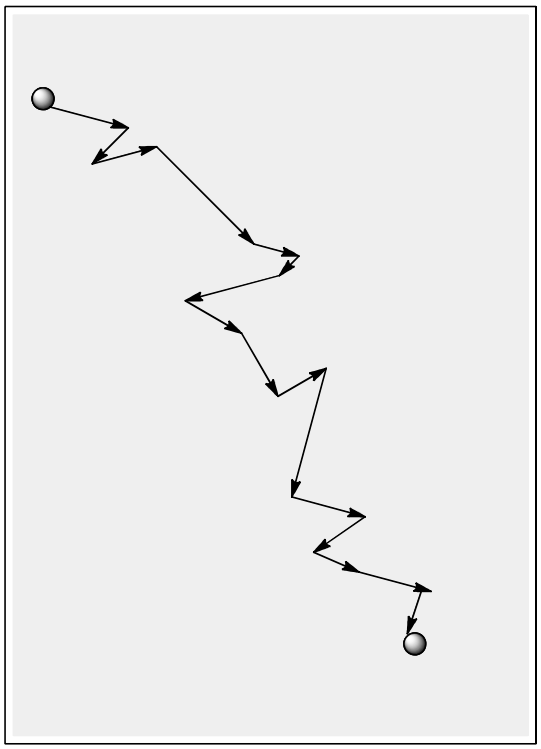

Figure 2.7 The random Brownian motion of a particle through solution.

The diffusion of molecules through a solution can be used in conjunction with NMR to obtain data on a wide range of physical molecular properties including: molecular size, shape, aggregation, encapsulation, complexation and hydrogen bonding.[19] The NMR

measurements taken to determine these properties rely on the application of field gradients to encode the physical location of the molecule or complex in the solution and so characterise its diffusion along the direction of the applied field.[19]

The Brownian motion of a molecule through a solution allows the determination of its diffusion coefficient, D. This diffusion coefficient can be related to its molecular size through the relationship:[19]

$$\text{Eq 2:} \qquad D = \frac{k_b T}{f}$$

K_b is the boltzman constant, and T the absolute temperature, and f is the hydrodynamic friction coefficient which reflects the size and shape of the molecular species.[19, 20] In the ideal case of the diffusion of a sphere through a solution f can be related to the Stokes radius of the sphere, r_s, and the viscosity of the solution, η:

$$\text{Eq 3} \qquad f = 6\prod \eta r_s$$

When substituted into the previous relationship the Stokes-Einstein relationship is obtained: [20, 21]

$$\text{Eq 4: } D = \frac{k_b T}{6\Pi \eta r_s}$$

The relationship between D and r_s shows that the diffusion coefficient is inversely related to the radius of the molecule such that larger molecules will have smaller diffusion coefficients, *i.e.* larger molecules will diffuse through the solution at a slower rate.[19, 22]

NMR experiments can be used to determine the value of the diffusion coefficient if the viscosity of the solution is known as well as the absolute temperature at which the

experiment was carried out.[19] Once this value has been obtained the Stokes-Einstein equation can be solved to give the hydrodynamic radius of the dendrimer and the particle size of the complex.[19, 22]

The data required to calculate D is obtained by using a diffusion ordered spectroscopy, 1D-DOSY, NMR with parameters: Δ (delta), the diffusion delay; and δ, the length of the gradient pulses, Figure 2.8.[19] Delta can be changed to increase or decrease the amount of time the complex has to diffuse though the solution and δ can be altered to increase or decrease the degree of dephasing in the sequence.[19] If these parameters are not optimised correctly the decay profile may not reflect the true diffusion coefficient of the complex.[19] If the signal attenuation is too fast the later data points in the data set will not contribute to the profile and if it is too slow there won't be enough data points for accurate determination of the diffusion coefficient.[19] Two pulses are used in the 1D-DOSY NMR, the first to tag the protons and the second to measure the intensity of the peaks.

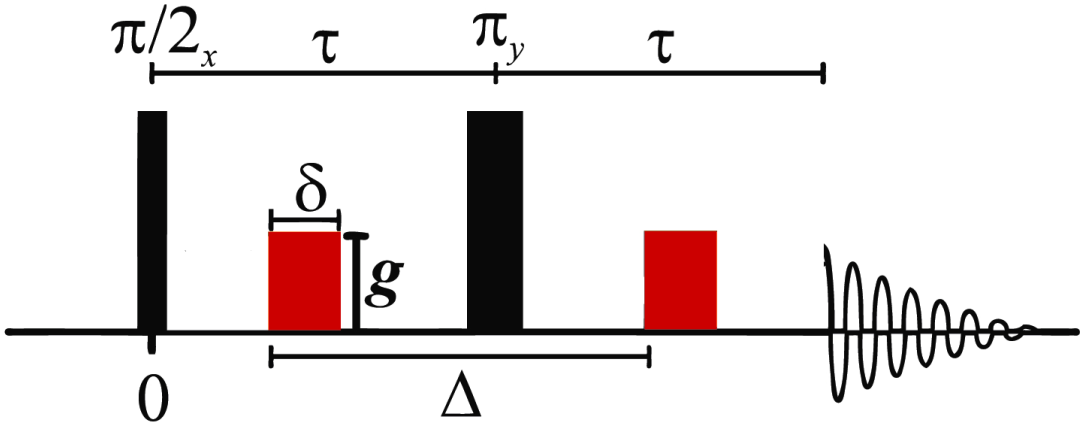

Figure 2.8 A pulse gradient spin echo sequence.

The parameters are optimised and the DOSY NMR is recorded as two-dimensional data points but are essentially a series of one-dimensional scans. The 1D-DOSY NMR

monitors the decrease in the intensity of the NMR peaks that result due to diffusion of the analyte. The magnetic field gradients are pulsed after a specific time, Δ, and the decrease in the intensity signals can be used to determine the diffusion coefficient through the following equation (Eq 5).

$$\text{Eq 5: } I = I_o e^{-\gamma^2 G^2 D \delta^2 \left(\Delta - \frac{\delta}{\Pi^2}\right)}$$

I is the intensity of the signal in the presence of the gradient, I_o is the intensity of the signal in the absence of the gradient, γ is the proton gyromagnetic ratio, G and δ are the amplitude and duration of the two pulse field gradients. By plotting the signal intensity ratio, as $\ln(I/I_o)$, against $-(G\gamma\delta)^2 D(\Delta-\delta/3)$ a diffusion decay curve, Figure 2.9, is produced and by applying a best fit line to the data, the diffusion coefficient can be determined.

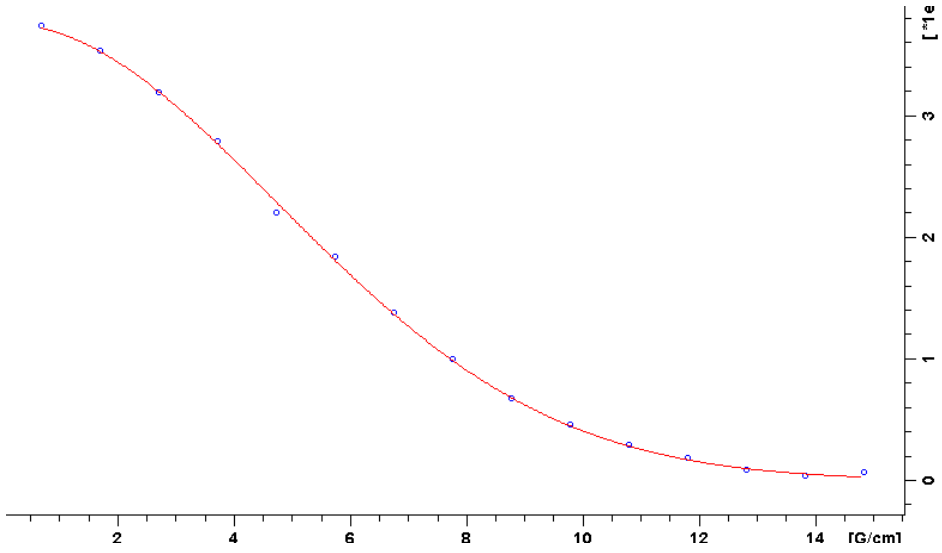

Figure 2.9 The diffusion curve for the G5.5 dendrimer platinate.

The size of the free dendrimers and the dendrimer-platinate complexes were determined using diffusion NMR, Table 2.1. The diffusion coefficient of the free dendrimers decreases, with increasing dendrimer generation, consistent with larger particle sizes.[23] The dendrimers range in diameter from 2.7 to 5.9 nm, which are significantly less than

those previously reported.[1] Full generation PAMAM dendrimers G4-G7, have previously been shown to have diameters of 4-8 nm,[24] similar to the results reported by Wiwattanapatapee *et al*.[25] for G3.5 (4.0 nm) and G5.5 (6.7 nm) dendrimers and are roughly in agreement with our results. In all cases, addition of cisplatin results in a decrease in the size of each dendrimer. In their free form, the anionic carboxylate groups of the dendrimers most likely hydrogen bond with one or more shells of water molecules, thus greatly increasing the dendrimers' effective hydrodynamic radius. When cisplatin binds to the dendrimers they become significantly less charged, and whilst the ammine groups of cisplatin can still hydrogen bond with water, they may do so with much less efficiency, which may explain the reduction in dendrimer size upon cisplatin attachment. The results obtained from the diffusion NMR may be affected by the ionic strength and pH of the unbuffered D_2O solution as this will influence the amount of hydrogen bonding between the complex and solution. The degree of hydrogen bonding which can be achieved with the surrounding D_2O molecules will affect the rate of diffusion and therefore the measured size of the complex.

2.2.3 Drug release and DNA binding

To act as drug delivery vehicles, it is important that the dendrimers are not only able to bind platinum drugs, but they must also be able to release the drugs so that they can bind to their cellular target, DNA. To do this we have examined platinum release from the dendrimers using guanosine binding experiments.

Each dendrimer-platinate complex was incubated with two equivalents of 5′-guanosine monophosphate (based on cisplatin concentration) in D_2O and the solutions heated at temperatures up to 60 ^{o}C for periods of up to seven days. Cisplatin release from the dendrimers and binding to guanosine is observed through the downfield shift of the guanosine H8 resonance from 8.1 to 8.6 ppm, Figure 2.10.[26] Free cisplatin is known to react with guanosine/DNA in a relatively short time period ($t_{1/2}$ = 0.5-4 h).[27, 28] For our dendrimer-platinate complexes the cisplatin release is significantly slower and in fact

never goes to theoretical completion, Table 2.1. From the ^{1}H NMR spectra it appears only a fraction of the bound cisplatin is released from the dendrimer: G3.5, 18% of bound cisplatin; G4.5, 30%; G5.5, 35% and G6.5, 63%. The reason for the lack of cisplatin release may be due to cisplatin binding to the amine and amide groups within the dendrimer branches. Previously, Pellechia *et al.* demonstrated that K_2PtCl_4 when incubated with hydroxyl terminated, full generation G2 and G4 PAMAM dendrimers, the platinum formed a number of dendrimer adducts, including single ($PtCl_3N$), double ($PtCl_2N_2$) and triple ($PtClN_3$) amine adducts,[4] and these are likely to also be formed by our aquated cisplatin.

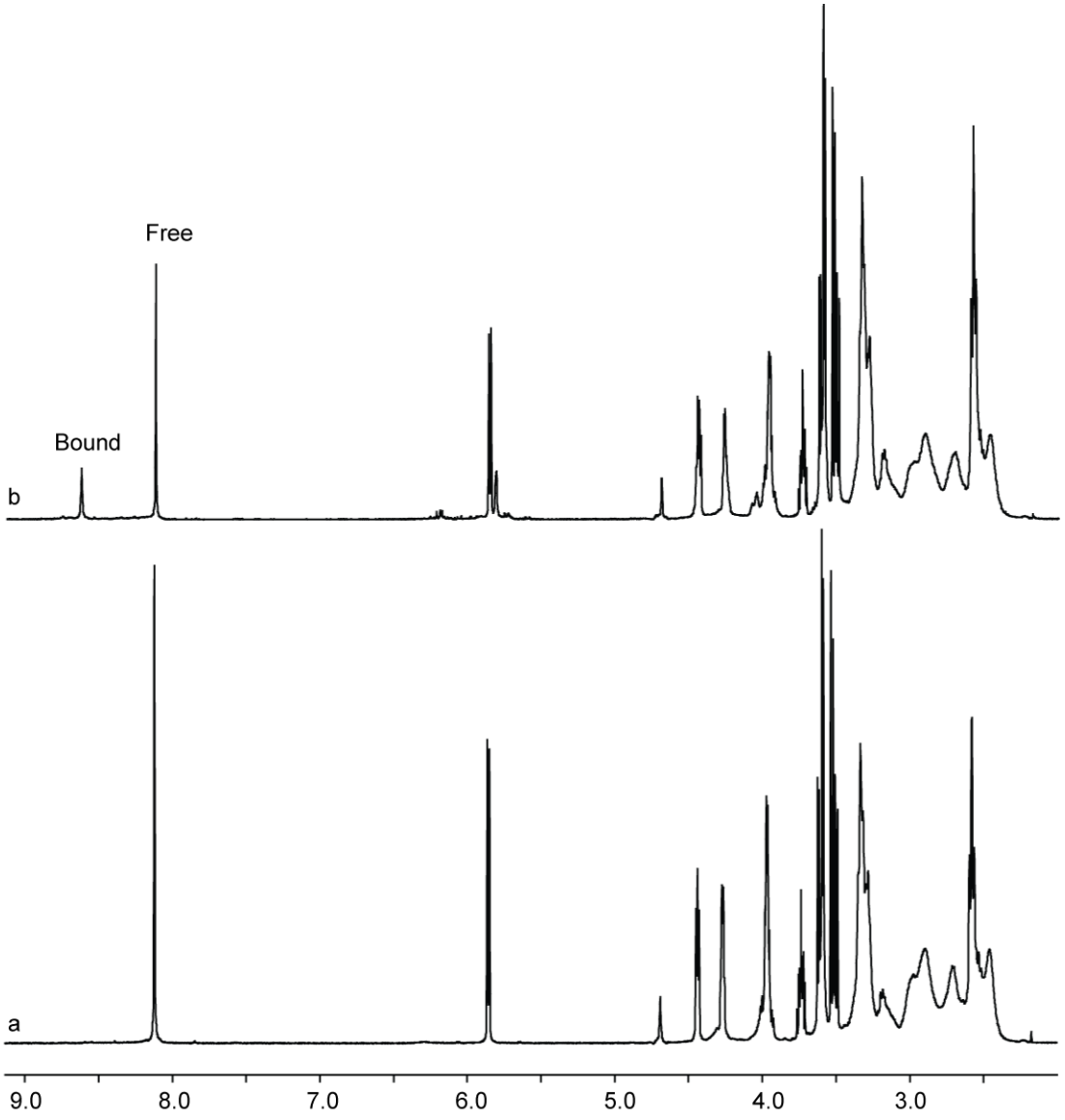

Figure 2.10. The ^{1}H NMR spectra of the G4.5 drug-dendrimer complex and guanosine at a. 0 hours and b. 7 days, showing the large downfield shift of the guanosine H8 resonance upon binding by cisplatin (8.1→8.7 ppm) as it is released from the dendrimer.

To examine if non-reversible amine binding is a probable explanation of the incomplete drug release from the dendrimer, we examined the reaction of aquated cisplatin with 3-(diethylamino)propionate, Figure 2.11, by ^{1}H NMR which we use as a representative "fragment" of a dendrimer arm. This small molecule contains the functional groups of

interest in the half-generation PAMAM dendrimers; a terminal carboxylate group separated from a tertiary amine by an ethyl chain. As purchased, the amine of the fragment is protonated. Upon addition of four equivalents of triethylamine (the same ratio used in the full dendrimer experiments), the four resonances of the fragment shift downfield by 0.24 to 0.65 ppm, which is consistent with deprotonation of the amine, Figure 2.12. Incubation of the fragment with one equivalent of aquated cisplatin has an immediate effect, with selective upfield shifts of the fragment's resonances. The two methyl groups closest to the amine shift by more than 0.2 ppm, whilst the resonance of the methyl protons closest to the carboxylate group only shifts 0.11 ppm, Figure 2.12. This suggests coordination to the amine group rather than the carboxylate. The rapid binding of aquated cisplatin to the dendrimer fragment's amine group is possibly a function of the group's accessibility, which is why no binding to the carboxylate is observed. In the full dendrimer, where steric effects limit access to the amine groups, this binding would be expected to be slower. On further incubation of the fragment and aquated cisplatin at 37 ^{o}C for time periods of up to 48 hours, no further changes are observed, beyond those seen upon the immediate addition of the platinum, Table 2.2.

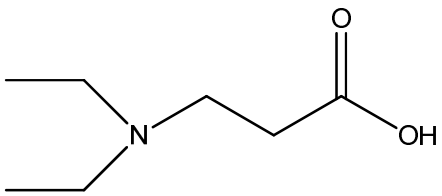

Figure 2.11 The chemical structure of 3-(diethylamino)propionate which contains the two key functional groups of the dendrimer arms, a tertiary amine and a carboxylic acid/carboxylate.

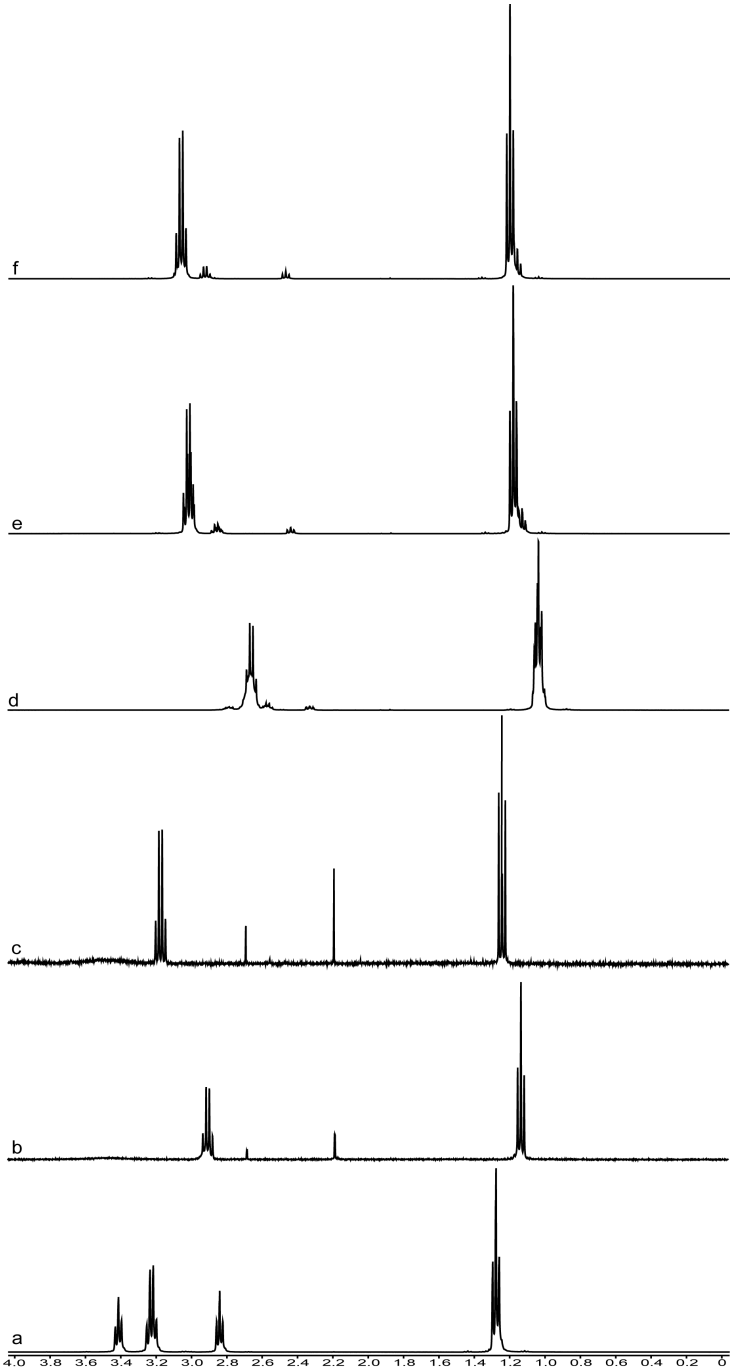

Figure 2.12 The ^{1}H NMR spectra of (bottom – top): a. 3-(diethylamino)propionate, b. TEA, c. TEA+ cisplatin, d. 3-(diethylamino)propionate + TEA, e.3-(diethylamino)propionate + TEA+ cisplatin 0 h and f. 3-(diethylamino)propionate + TEA+ cisplatin 48 h.

Table 2.2 The δ values of the peaks of the protons analysed in the fragment binding experiment.

Analysed Sample	Δ					
	TEA 1	TEA 2	Frag 1	Frag 2	Frag 3	Frag 4
	CH_3	CH_2	CH_3	CH_2-O	CH_2-NQ	CH_2-NT
Free TEA	1.14	2.92	-	-	-	-
Free Fragment	-	-	1.28	2.84	3.22	3.42
TEA+ Fragment	1.04	2.66	1.04	2.33	2.57	2.78
TEA+ Cisplatin	1.24	3.16	-	-	-	-
TEA + Frag + Cisplatin 0 h	1.18	3.01	1.14	2.44	2.86	-
TEA + Frag + Cisplatin 48 h	1.21	3.05	1.17	2.47	2.92	3.08
Δδ			0.13	0.14	0.35	0.3

The results indicate that binding of the platinum atom to the tertiary amines in the full dendrimer arms is possible and may explain the incomplete drug release. What is likely to occur when the aquated cisplatin is coupled to the dendrimer is initial binding to a single carboxylate group. Then, over time, it is likely that a 5-membered chelate ring is formed, involving a carboxylate oxygen and a tertiary amine nitrogen. With longer time, the percentage of platinum bound to the amines will increase and there may even be formation of 5-membered rings involving both the amine and amide nitrogen atoms, and some cross linking of the dendrimer arms.

The guanosine binding results demonstrate that the amount of platinum released is dependent on dendrimer generation; the higher the generation, the more platinum that is released. This may be due to the dense surface of higher generation dendrimers which prevents access of the platinum atom to the internal amine/amide groups, thus ensuring a higher proportion of carboxylate attached drug molecules.

The binding of platinum to the dendrimer amine/amide groups is problematic in that it will make synthesis of consistent dendrimer-platinate complexes very difficult. If PAMAM dendrimers are used for drug delivery then our results suggest that higher generation dendrimers, >G5 are preferable to lower generation dendrimers <G4. Alternatively, the problem of amine binding might be overcome through the use of different dendrimer structures (*i.e.* not PAMAM dendrimers) that do not contain competitive binding sites for cisplatin. Other commercially available dendrimers could be functionalised with carboxylate groups through simple polyamide or click chemistry.

2.2.4 Kinetics of drug release

Once established that the platinum is released from the dendrimers and able to bind to the guanosine, Figure 2.10, it is important to determine the rate at which the platinum is released. Most established drug delivery vehicles deliver a high percentage of their drug as an initial burst release followed by a slow release of the remaining drug. The identification of a slower, sustained release delivery vehicle, with no initial burst, can be beneficial for patients undergoing treatment. In addition to being able to reduce the possible side effects of the drug it could also reduce the number of times the drug has to be administered. Very little of the platinum drug actually survives intact to reach the cancer cell and therefore has to be given in high doses to ensure the effectiveness of the treatment. A delivery vehicle which can deliver sustained release will ensure higher concentrations of the drug are present over a longer period of time.

The rate of release of platinum from the dendrimers was anlaysed through ICP-AES. The dendrimer-platinate complexes were dissolved in pH 7.4 phosphate buffered saline (PBS) and incubated at 37 ^{o}C. Aliquots of 1 mL were taken from the saline solution hourly for the first 12 hours, to check for an initial burst release of platinum, then at 24 hour intervals to determine if a sustained release of platinum is observed. The samples were centrifuged for 15 min in a Vivaspin column and the free platinum collected for analysis. It is unlikely that all of the platinum bound to the dendrimer is released from

the dendrimer collected during sampling. After the sample was centrifuged in the Vivaspin column, the dendrimer retained in column was reconstituted in 1 ml of fresh PBS and returned to the solution containing the drug-dendrimer complex. The volume of PBS solutions containing the residual platinum was corrected to 10 mL and then analysed, along with a sample of fresh PBS, by ICP-AES, Table 2.2.

The analysis was originally carried out using the G3.5 dendrimer-platinate complex. Samples were taken every hour for 12 hours then at periods of 24, 48 and 72 hours. The rate of release of platinum remains slow for the first 10 hours then rapidly increases, Figure 2.13. A similar trend is observed when the percentage of releaseable platinum released is compared to the same time period during the guanosine binding experiments, Figure 2.13. The total releaseable platinum, however, is obtained much quicker in the pH 7.4 PBS solution than in the D_2O/guanosine solution used for the NMR study. When the experiment was repeated with all four drug-dendrimer complexes a sharp peak in platinum concentration was observed after 1 hour; however subsequent samples showed very little platinum. The differences in the results between the first execution of the experiment and the subsequent attempts cannot be explained.

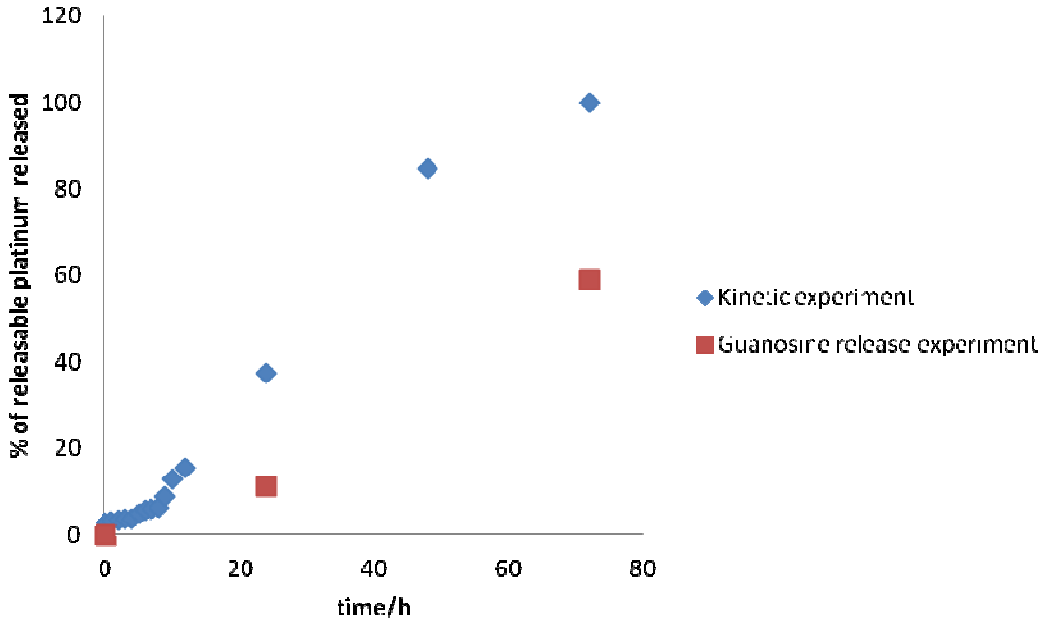

Figure 2.13 The % of releasable platinum released, over a period of 72 h, from the G3.5 cisplatin-dendrimer complex incubated in PBS at 37 ^{o}C or D_2O/guanosine NMR solution

2.2.5 In vitro Cytotoxicity

The effectiveness of a drug can be expressed in a number of ways including IC_{50}, EC_{50} and LD_{50}. The IC_{50} value, the half maximal inhibitory concentration, is the concentration of an inhibitor required to inhibit 50% of its target whilst the EC_{50} value, the median effective concentration, is the concentration of a drug complex required to achieve half the maximum effective and the LD_{50} value, the median lethal dose, is the concentration of a drug complex that is lethal to 50% of the population exposed to the complex.[29, 30]

The IC_{50} values for a complex can be determined through *in vitro* assays. Cells are incubated with increasing concentrations of the complex for a predetermined length of time. In the same experiment a sample of the cells is incubated in the absence of the

complex which allows the cells to grow freely. Dyes such as MTT, (3-(4,5-dimethylthiazol-2yl)-2,5-diphenyltetrazolium bromide, or WST-1, (4-(3-(4-iodophenyl)-2-(4-nitrophenyl)-2H-tetrazol-3-ium-5-yl)benzene-1,3-disulfonate), are then added to determine the amount of cells still viable. These dyes undergo structural changes in the presence of reductases and the ultra violet absorbance from the dyes can be measured at specific wavelengths, Figure 2.14. The absorbance value recorded at these wavelengths directly correlates to the number of viable cells and the absorbance of the samples containing the complex is compared to that of the sample with no complex. Plotting the absorbance against the complex concentration allows for the determination of the IC_{50} value.

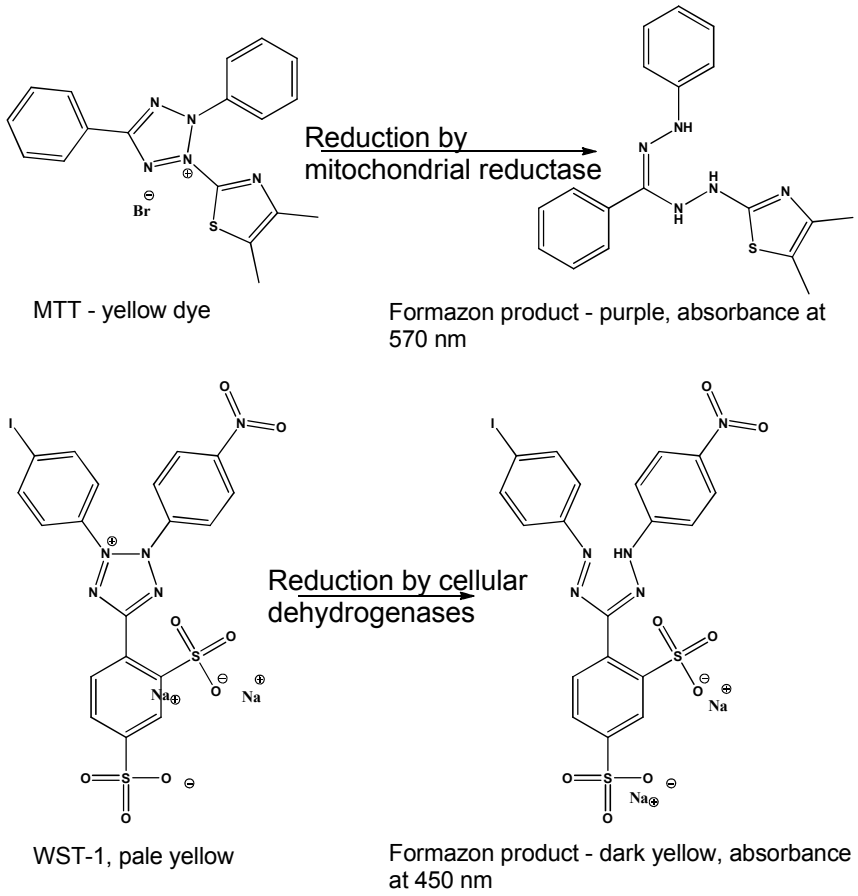

Figure 2.14. The structures of the MTT and WST-1 dyes, their formazon products and the wavelength measured to determine IC_{50}.

The cytotoxicity of the free dendrimers and the drug-dendrimer complexes were determined in the human ovarian carcinoma cell line A2780 and its cisplatin-resistant daughter lines, A2780cis and A2780cp. Anionic half generation dendrimers have previously been shown to be significantly less cytotoxic compared with cationic full generation dendrimers,[31] and our results demonstrated that the free PAMAM dendrimers have no significant cytotoxicity (IC_{50} >100 μM).

The dendrimer platinates are tested *in vitro* at different concentrations to determine if they have any effect on the cancer cell lines in which they were incubated. Following a set period of incubation the cells are stained, fixed and then the UV absorbance measured at a particular wavelength, dictated by the type of stain used. The higher the number of viable cells present the higher the absorbance will be and through comparison with a sample where the cells have been allowed to grow freely an IC_{50} value for the dendrimer-platinates can be determined.

Due to the slow release of cisplatin from the dendrimers, the cancer cell lines were incubated with dendrimer-platinate complexes for time periods between 24 and 96 h. When the assays were conducted with the WST-1 stain in the A2780 and A2780cis lines, it was found the dendrimer complexes were inactive, with IC_{50} values greater than 100 μM in all cases. Conversely, moderate cytotoxicity is observed when the A2780 and A2780cp lines are stained with MTT, Table 2.3, which indicates that WST-1 is not a suitable stain for screening platinum drugs *in vitro*. Previously it has also been shown that Alamar Blue is not a suitable stain for platinum drug screening.[32]

Table 2.3. The in vitro cytotoxicity of the dendrimer-platinate complexes in the human ovarian cancer cell line A2780 and its cisplatin resistant daughter line A2780cp at 96 h.

Drug/complex	IC_{50} (μM)[a]		Resistance factor (Rf)[b]
	A2780	A2780cp	
Cisplatin	0.14 ± 0.01	1.90 ± 0.37	13.6
cisplatin-G3.5	0.40 ± 0.07	24.5 ± 4.4	61.3
cisplatin-G4.5	0.62 ± 0.05	18.8 ± 1.0	30.3
cisplatin-G5.5	1.48 ± 0.20	26.8 ± 0.6	18.1
cisplatin-G6.5	1.07 ± 0.38	25.2 ± 1.7	23.6

a. Based on the total "releasable" cisplatin concentration per mole of dendrimer, measured by indirect quantification. b. Defined as the IC_{50} value in the resistant line divided by the IC_{50} value in the sensitive line; the lower the Rf the better the complex is at overcoming resistance.

All four dendrimer-platinate complexes display moderate activity in the A2780 cell line, although they are 2- to 11-fold less active than cisplatin. In the cisplatin-resistant line, all four complexes are significantly less cytotoxic and are not able to overcome resistance in the A2780cp line (as observed by larger resistance factors compared with normal cisplatin). The smaller dendrimer-platinate complexes (G3.5/4.5) are more active in the sensitive line than the larger dendrimers (G5.5/6.5) but conversely also more cross-resistant. Within the margin of error both the G5.5 and G6.5 dendrimer-platinate complexes are equally cytotoxic and cross-resistant in the two cell lines.

2.2.6 In vivo effectiveness

Whilst disappointing, the in vitro results were not surprising as previously Malik *et al.*[3] found that a PAMAM G3.5 dendrimer with the active component of cisplatin attached was almost inactive in CCRF, COR L23 and B16F10 cells when tested *in vitro.* Significant activity was only observed *in vivo* in L1210 murine leukaemia and B16 melanoma bearing mice. In another study, *in vitro* cytotoxicity was only observed when

a dendrimer-platinate complex was incubated with cells for very long periods of time: 75 to 225 h.[33] Therefore the *in vitro* results do not necessarily imply that the dendrimer-platinate complexes developed in this study are not active and different methods for determining cytotoxicity, including *in vivo* experiments, may be necessary for dendrimer-based delivery systems to be investigated properly. Whilst not ideal to use mice in drug studies, it is a necessary step in the development process. The number of mice should be at levels where the minimum is used to achieve the complete the experiment.

To this effect, we then determined the effectiveness of the cisplatin-G6.5 dendrimer-platinate *in vivo* using an A2780 tumour xenograft. The G6.5 complex was chosen because with the G5.5 dendrimer-platinate, it was most effective at overcoming resistance. Additionally, it is able to release more cisplatin molecules than the other three dendrimers and because its larger size meant it was more likely to be trapped within the tumour vasculature compared with the other dendrimer-platinate complexes.

In vivo experiments are commonly used in both industry and academic settings to demonstrate proof of principal, pharmaceutically-tractable, molecules to be tested in a living environment.[34] Since the 1950s *in vivo* experiments have been used a screening system to predict the efficacy and identify toxicity of chemotherapeutic agents before they enter clinical trials.[35] There are typically two types of *in vivo* experiments that are carried out: the grafts of tumour material (xenografts) into immunocompetent or immunodeficient animals such as nude, athymic, mice and the use of genetically engineered mice that recapitulate a specific cancer genotype.[34, 35] The first studies were carried out by the National Cancer Institute (NCI) and involved the use of mice carrying sarcoma 180, L1210 lukemia and carcinoma 755 lines to represent colon, lung and ovarian cancers.[34, 36] These first studies demonstrated the concept of fractional cell kill: the observation that the population of tumour cells killed by a given dose of a drug was relatively constant.[36] These studies also demonstrated a number of other useful relationships which are exploited when carrying out an *in vivo* study: the dose-response

relationship and the therapeutic index (a demonstration of antitumour efficacy at doses below those causing severe toxicity).[34, 36]

The value of *in vivo* studies are a matter of debate as the results from these studies are sometimes difficult to correlate with the results observed during *in vitro* experiments and those seen in a clinical setting.[34-36] The *in vitro* studies carried out by the NCI failed to predict activity in xenograft models which in turn didn't predict the activity in clinical therapy.[35] A retrospective study carried out by the NCI showed that for 39 compounds, which have xenograft data and phase II clinical trail data available, the phase II activity was predicted for a third of the compounds and other studies of have also shown a good predictability between the xenograft models and the phase II results for ovarian and non-small-cell lung cancers.[34, 35] The usefulness of *in vivo* studies has also been supported by the response pattern observed with more recent drugs such as paclitaxel, gemcitabine, docetaxel, vindesine and topotecan as similar results are observed in xenografts as in montherapy in clinical trials.[34] In the 1980s many groups established a series of disease specific xenografts derived from patient biopsies and this approach has since been used extensively to develop more effective analogues of cisplatin and carboplatin.[34] The eventual development of platinum sensitive and resistant xenograft models allowed the identification of some of the major mechanisms of resistance to the platinum drugs.[34]

The design of *in vivo* experiment, using xenografts, involves the consideration of a number of different variables including the origin of the tumour material implanted into the animal.[34] There are two different sources of material which can be implanted into animals, such as nude mice, as the material obtained from a patient biopsy can be directly implanted or material obtained from inoculation or a continuous cell can be implanted.[34] The material derived from a biopsy is considered to be a more accurate representation of human cancer as it retains the morphological and molecular marker properties of those of the source tumour, however these can be difficult to establish in the animal.[34] The implantation of material from cell lines is often preferred as the

xenograft is easier to establish and shows a more homogeneous and undifferentiated histology.[34]

The site of implantation has to be considered when developing the study in order to balance the ease of assessment and the differences in biological behaviour in a particular area of the body.[34] The majority of *in vivo* studies are carried out using subcutaneous implantation, as this allows easier access to the tumour for analysis of tumour volume or diameter.[34] After the xenograft has been implanted the growth properties of the tumour have to be monitored as this affects usability. If the growth is to slow, inconsistent, eratic or non-linear with time, or posess necrotic or cystic areas, then the tumour tissue can be compromised by up to 80%.[34]

After the tumour the xenograft has been established the start and end points of treatment have to be clearly defined. There are three strategies which are used to identify the time at which the first dose of the drug is delivered: chemoprevention, early stage and advanced stage.[34] In the chemoprevention strategy the drug is administered at the same time as the tumour implanted, early stage dosing occurs when the tumour becomes palpable at approximately 5 mm diameter or around 60 mm^3 and advanced stage dosing occurs when the tumour reaches approximately 8-10 mm.[34] Advanced stage dosing is thought to be the most representative of the clinical treatment of cancer as it is unlikely that identification will occur early enough to resemble the conditions of the early stage strategy.[34] The end point of the study has to be predetermined before being initiated and is usually achieved through measuring the tumour weight or volume in an untreated mouse against those which have been dosed with the drug of interest after a set number of days.[34] Amongst the most commonly employed endpoints is the time taken to reach a predetermined increase in volume, 3-4 fold, and this is normalised to the untreated mouse in order to determine the effect of the drug on the tumour.[34]

When free cisplatin and the G6.5 dendrimer-platinate were administered at equimolar doses of 6 mg/kg (based on the number of releasable cisplatin molecules from the G6.5

dendrimer), both demonstrated similar, and statistically significant, effectiveness in delaying tumour growth, Figure 2.15. Conversely, the free G6.5 dendrimer had no effect on tumour growth. When administered at a higher dose (8 mg/kg) the dendrimer-platinate demonstrated similar systemic side-effects, as determined by the relative decrease in the mice's body weight, but was significantly better at delaying tumour growth. Seven days after administration the tumour volumes of the cisplatin and dendrimer-platinate complex (6 mg/kg) were 67% and 68%, respectively, of the tumour volume of the untreated control group ($P < 0.001$). The dendrimer-platinate complex (8 mg/kg) significantly delayed growth to an even greater extend with a tumour volume of only 55% compared to the control group ($P < 0.001$). The tumour doubling times were: control group 3.17 ± 0.15 days; cisplatin, 4.87 ± 0.14 days; dendrimer-platinate 6 mg/kg 5.2 ± 0.35 days; and dendrimer-platinate 8 mg/kg, 6.32 ± 0.37 days. This result further supports our hypothesis that *in vitro* assays are not a suitable screen alone for platinum drug-nanoparticle delivery vehicle systems and *in vivo* experiments are required to determine their effectiveness properly.

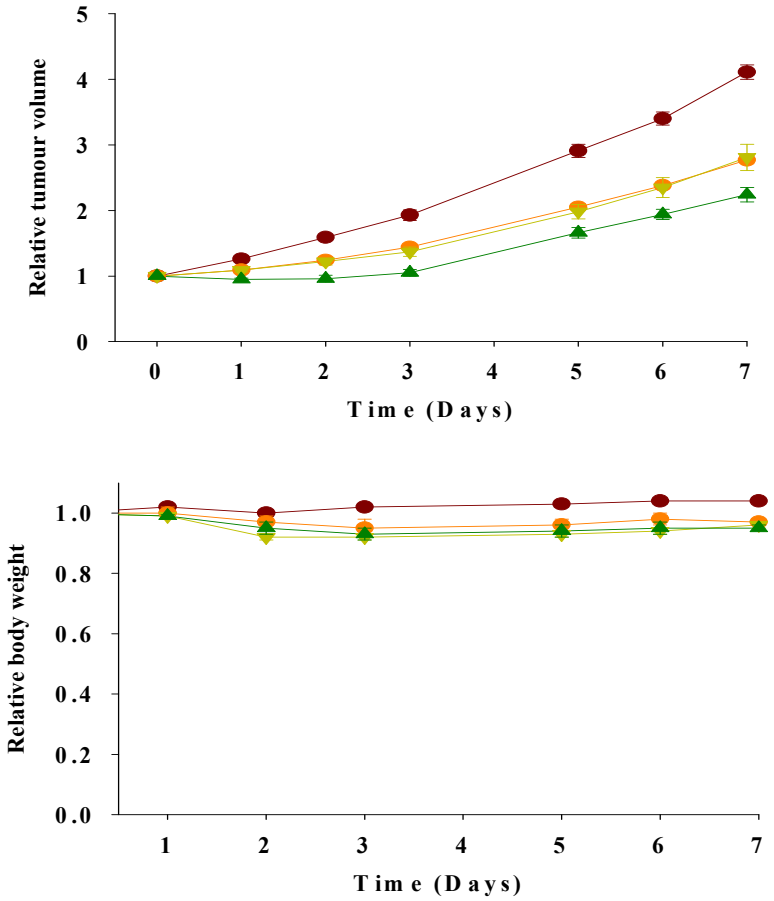

Figure 2.15. (Top) Effect of control (●, saline), cisplatin (●, 6 mg/kg), *cis*-^{27}-G6.5 complex (▼, 6 mg/kg) and *cis*-^{27}-G6.5 complex (▲, 8 mg/kg equivalent) on the growth of an A2780 ovarian tumour xenograft after a single IP administration on day 0. (Bottom)

The loss of body weight of the mice after a single IP injection of saline or drug, demonstrating the similar systemic toxic effect of the drugs.

2.3 CONCLUSIONS

A systematic examination of half generation anionic PAMAM dendrimers as drug delivery vehicles has been concluded. Aquated cisplatin was dissolved in water with generation 3.5 to 6.5 dendrimers and stirred for 5 h before being purified on Vivaspin centrifuge columns. The amount of cisplatin bound to the dendrimers increases with dendrimer size, although the binding efficiency decreases. Cisplatin release from the dendrimers was demonstrated using guanosine binding experiments. Only a fraction of the dendrimer bound cisplatin is released which may be a function of the drug forming non-reversible coordinate bonds to the amine and amide groups within the dendrimer branches. The dendrimer-platinate complexes display moderate cytotoxicity in the A2780 and A2780cp cell lines, but effectiveness was only properly observed when examined *in vivo* using an A2780 tumour xenograft. The results of our study demonstrate that half-generation PAMAM dendrimers may be effective, but not ideal, for the delivery of platinum drugs. Further study of dendrimers should focus on carboxylate terminated dendrimers with no competing binding groups within their branches. Further studies need to also include different methods for determining cytotoxicity, including *in vivo* experiments, in order to evaluate fully the success of any nanoparticle-based drug delivery system.

2.4 References

1. Pisani, M. J.; Wheate, N. J.; Keene, F. R.; Aldrich-Wright, J. R.; Collins, J. G. Anionic PAMAM dendrimers as drug delivery vehicles for transition metal-based anticancer drugs. *J. Inorg. Biochem.* **2009,** 103, 373-380.

2. Howell, B. A.; Fan, D.; Rakesh, L. Thermal decomposition of a generation 4.5 PAMAM dendrimer platinum drug conjugate. *J. Therm. Anal. Calor.* **2006,** 85, 17-20.

3. Malik, N.; Evagorou, E. G.; Duncan, R. Dendrimer-platinate: a novel approach to cancer chemotherapy. *Anti-Cancer Drugs* **1999,** 10, 767-776.

4. Pellechia, P. J.; Gao, J.; Gu, Y.; Ploehn, H. J.; Murphy, C. J. Platinum ion uptake by dendrimers: An NMR and AFM study. *Inorg. Chem.* **2004,** 43, 1421-1428.

5. Tarazona-Vasquez, F.; Balbuena, P. B. Pt(II) uptake by dendrimer outer pockets: 1. Solventless ligand exchange reaction. *J. Phys. Chem. B* **2008,** 112, 4172-4181.

6. Zhao, X.; Loo, S. C. J.; Lee, P. P.-F.; Tan, T. T. Y.; Chu, C. K. Synthesis and cytotoxic activities of chloropyridylimineplatinum(II) and chloropyridyliminecopper(II) surface-functionalized poly(amidoamine) dendrimers. *J. Inorg. Biochem.* **2010,** 104, 105-110.

7. Chen, G.; Kumar, J.; Gregory, A.; Stenzel, M. H. Efficient synthesis of dendrimers via a thiol-yne and esterification process and their potential application in the delivery of platinum anti-cancer drugs. *Chem. Commun.* **2009**, 6291-6293.

8. Haxton, K. J.; Burt, H. M. Hyperbranched polymers for controlled release of cisplatin. *Dalton Trans.* **2008**, 5872-5875.

9. Jansen, B. A. J.; van der Zwan, J.; Reedijk, J.; den Dulk, H.; Brouwer, J. A tetranuclear platinum compound designed to overcome cisplatin resistance. *Eur. J. Inorg. Chem.* **1999**, 1429-1433.

10. Dabrowiak, J. C. *Metals in Medicine*. Wiley: Chippenham, 2009; p 334.

11. Still, B. M.; Kumar, P. G. A.; Aldrich-Wright, J. R.; Price, W. S. 195Pt NMR theory and application. *Chem. Soc. Rev.* **2007,** 36, 655-686.

12. Ebdon, L.; Evans, E. H.; Fisher, A.; Hill, S. J. *An Introduction to Analytical Atomic Spectrometry*. Wiley & Sons: Chichester, 1998.

13. Lajunen, L. H. J.; Peramaki. *Spectrochemical Analysis by Atomic Absorption and Emission*. 2nd ed.; The Royal Society of Chemistry: Cambridge, 2004.

14. Manning, T. J.; Grow, W. R. Inductively Coupled Plasma- Atomic Emission Spectrometry. *Chem. Educator* **1997,** 2, 1-19.

15. Nageswara Rao, R.; Kumar Talluri, M. V. N. An overview of recent applications of inductively coupled plasma-mass spectrometry (ICP-MS) in determination of inorganic impurities in drugs and pharmaceuticals. *J. Pharmaceut. Biomed.* **2007,** 43, 1-13.

16. Todolí, J. L.; Mermet, J. M. Sample introduction systems for the analysis of liquid microsamples by ICP-AES and ICP-MS. *Spectrochim. Acta B* **2006,** 61, 239-283.

17. Becker, J. S.; Dietze, H.-J. Inorganic trace analysis by mass spectrometry. *Spectrochim. Acta B* **1998,** 53, 1475-1506.

18. Wheate, N. J.; Taleb, R. I.; Krause-Heuer, A. M.; Cook, R. L.; Wang, S.; Higgins, V. J.; Aldrich-Wright, J. R. Novel platinum(II)-based anticancer complexes and molecular hosts as their drug delivery vehicles. *Dalton Trans.* **2007**, 5055-5064.

19. Claridge, T. D. W. *High-resolution NMR Techniques in Organic Chemistry*. Elsevier Ltd: Oxford, 1999.

20. Korzhnev, D. M.; Billeter, M.; Arseniev, A. S.; Orekhov, V. Y. NMR studies of Brownian tumbling and internal motions in proteins. *Prog. in Nucl. Mag. Res. Sp.* **2001,** 38, 197-266.

21. Walderhaug, H.; Söderman, O.; Topgaard, D. Self-diffusion in polymer systems studied by magnetic field-gradient spin-echo NMR methods. *Prog. in Nucl. Mag. Res. Sp.* 56, 406-425.

22. Stockman, B. J.; Dalvit, C. NMR screening techniques in drug discovery and drug design. *Prog. in Nucl. Mag. Res. Sp.* **2002,** 41, 187-231.

23. Cohen, Y.; Avram, L.; Frish, L. Diffusion NMR spectroscopy in supramolecular and combinatorial chemistry: An old parameter-new insights. *Angew. Chem. Int. Ed.* **2005,** 44, 520-554.

24. Svenson, S.; Tomalia, D. A. Dendrimers in biomedical applications - reflections on the field. *Adv. Drug Del. Rev.* **2005,** 57, 2106-2129.

25. Wiwattanapatapee, R.; Carreno-Gomez, B.; Malik, N.; Duncan, R. Anionic PAMAM dendrimers rapidly cross adult rat intenstine in vitro: a potential oral delivery system? *Pharm. Res.* **2000,** 17, 991-998.

26. Lippert, B. *Cisplatin: Chemistry and Biochemistry of a Leading Anticancer Drug*. Wiley-VCH: Weinheim, 1999; p 563.

27. Wheate, N. J.; Evison, B. J.; Herlt, A. J.; Phillips, D. R.; Collins, J. G. DNA binding of the anti-cancer platinum complex trans-[{$Pt(NH_3)_2Cl$}$_2$u-dpzm]$^{2+}$. *Dalton Trans.* **2003**, 3486-3492.

28. McGregor, T. D.; Hegmans, A.; Kasparkova, J.; Neplechova, K.; Novakova, O.; Penazova, H.; Vrana, O.; Brabec, V.; Farrell, N. A comparison of DNA binding profiles of dinuclear platinum compounds with polyamine linkers and the trinuclear platinum phase II clinical agent BBR3464. *J. Biol. Inorg. Chem.* **2002,** 7, 397-404.

29. Dabrowiak, J. C. *METALS IN MEDICINE*. John Wiley & Sons: 2009.

30. Patrick, G. L. *An Introduction to Medicinal Chemistry*. Second ed.; Oxford University Press: Oxford, 2001; p 123-152.

31. Jevprasesphant, R.; Penny, J.; Attwood, D.; McKeown, N. B.; D'Emanuele, A. Engineering of dendrimer surfaces to enhance transepithelial transport and reduce cytotoxicity. *Pharm. Res.* **2003,** 20, 1543-1550.

32. Wheate, N. J.; Abbott, G. M.; Tate, R. J.; Clements, C. J.; Edrada-Ebel, R.; Johnston, B. F. Side-on binding of p-sulphonatocalix[4]arene to the dinuclear platinum complex trans-[{$PtCl(NH_3)_2$)}$_2$u-dpzm]$^{2+}$ and its implications for anticancer drug delivery. *J. Inorg. Biochem.* **2009,** 103, 448-454.

33. Kapp, T.; Dullin, A.; Gust, R. Platinum(II)-dendrimer conjugates: Synthesis and investigations on cytotoxicity, cellular distribution, platinum release, DNA, and protein binding. *Bioconjugate Chem.* **2010,** DOI: 101.1021/bc900406m.

34. Kelland, L. R. "Of mice and men": values and liabiliteis of the athymic nude mouse model in anticancer drug development. *Eur. J. Cancer* **2004,** 40, 827-836.

35. Morten, C. L.; Houghton, P. J. Establishment of human tumor xenografts in immunodeficient mice. *Nat. Protoc* **2007,** 2, 247-250.

36. Bibby, M. C. Making the most of rodent tumour systems in cancer drug discovery. *Brit. J. Cancer* **1999,** 79, 1633-1640.

Chapter 3: $\{Pt(R,R\text{-dach})\}^{2+}$ dendrimer-platinates

3.1 Introduction

The discovery of oxaliplatin and its subsequent activity in cisplatin resistant cell tumours represented another breakthrough in platinum drug chemotherapy (see 1.2.3). The resistance of tumours towards the platinum drugs such as cisplatin had previously limited the range of tumours which could be treated with the drugs. Increasing the cytotoxicity of oxaliplatin and enhancing the ability to overcome resistance are currently being explored through the use of drug delivery vehicles such as dendrimers.

Previous studies of oxaliplatin with dendrimers, as with those of cisplatin, are limited in scope and are concerned with, in most cases, a singular size of dendrimer. This chapter will look in more detail at the interactions and characteristics of activated component of oxaliplatin ([Pt(*R,R*-diaminocyclohexane)]$^{2+}$), Figure 3.1, coupled with G3.5-G6.5 half generation PAMAM dendrimers. The complexes where analysed through ^{1}H NMR, 1D-DOSY NMR and ^{195}Pt NMR. Quantification of platinum content was confirmed using ICP-MS and drug release was monitored through guanosine binding experiments coupled with ICP-MS. *In vitro* cytotoxicity studies were carried out using A2780 and A2780cp cell lines.

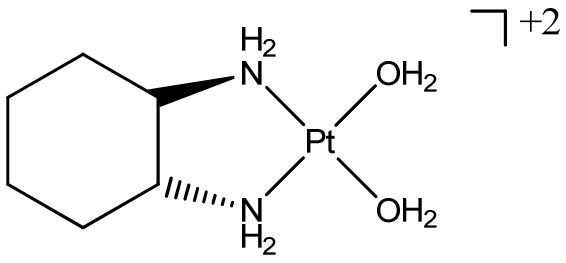

Figure 3.1 The active component of oxaliplatin, [Pt(*R,R*-dach)]$^{2+}$

3.2 Results and Discussion

3.2.1 Synthesis and aquation of [$PtCl_2$(*R,R*-dach)] to form [$Pt(OH_2)_2$(*R,R*-dach)]

In order to obtain an oxaliplatin complex capable of binding to the dendrimer it is necessary to synthesise the di-chloro precursor of oxaliplatin. This complex is formed as an intermediate during the synthesis of the complete oxaliplatin drug structure and can be readily obtained by reacting potassium tetrachloroplatinate with 1,2-*R,R*-diaminocyclohexane, Scheme 3.1.

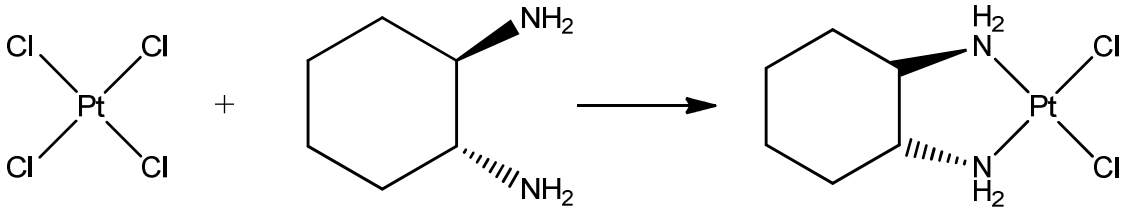

Scheme 1. The synthesis of the dichloro precursor of oxaliplatin.

Aqueous potassium tetrachloroplatinate was reacted with one mole equivalents of the amine for 3 h, at room temperature, during which time a yellow precipitate formed. The solution was then chilled for a further 1 h to maximise the yield of the product obtained. The precipitate was collected by vacuum filtration and washed with water and ethanol to remove traces of unreacted starting material. The ^{1}H NMR of the free and platinum bound ligands are shown below, Figure 3.2.

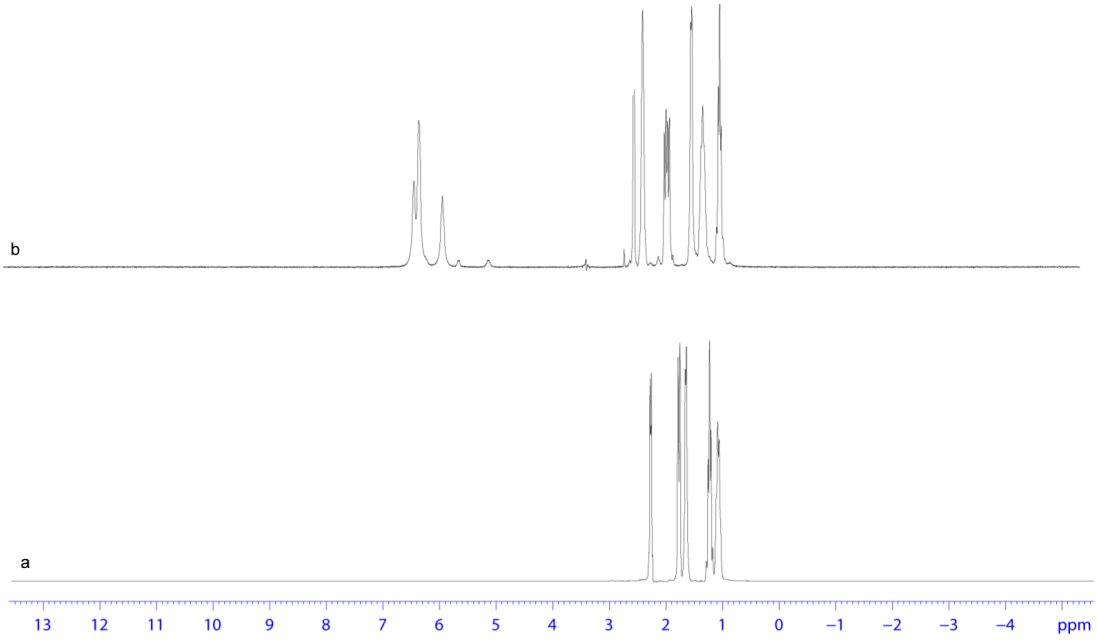

Figure 3.2 The ^{1}H NMR spectra of a. free R,R-dach ligand and b. platinum bound *R,R*-dach ligand.

The deshielding and subsequent downfield shift of the amine protons to 6 ppm and 6.3 ppm results from binding to platinum through the lone pair of electrons on the nitrogen atoms. This chemical shift is indicative of the successful synthesis of the desired [Pt Cl_2 (*R,R*-dach)] complex.

Following the successful synthesis of the chloro complex the aquation reaction with $AgNO_3$ was carried out to facilitate the platinum complex with the means to coordinate with the carboxylate groups on the dendrimer. To this end [Pt Cl_2 (*R,R*-dach)] was refluxed with 1.9 equivalents of $AgNO_3$ overnight before being filtered to remove the AgCl precipitate. The filtrate was then rotatary evaporated to dryness to yield [Pt$(OH_2)_2$ (*R,R*-dach)].2NO_3 as a yellow solid. The ^{195}Pt NMR of the aquated complex, Figure 3.3, shows a downfield shift from -2100 ppm to -1880 ppm and some remaining starting material at approximately -2100 ppm. The downfield shift is of a similar nature to that observed for the mono-aquated cisplatin platin complex, however as no other peak is

observed for the aquated product it is assumed that this peak represents the di-aquo complex.

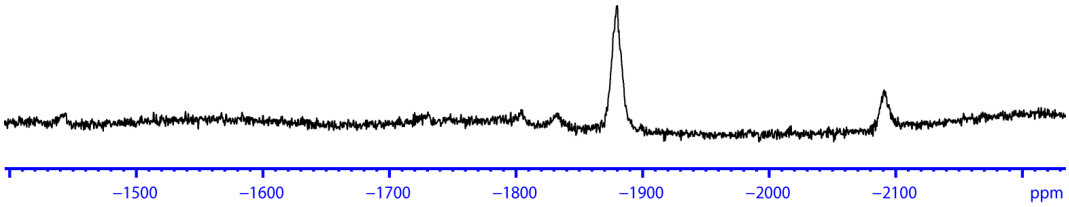

Figure 3.3 The ^{195}Pt NMR spectrum of [Pt(OH_2)$_2$ (*R,R*-dach)].

3.2.2 Synthesis and Characterisation of [Pt (*R,R*-dach)]-dendrimer complexes

The different generation dendrimers were combined in unbuffered water with four equivalents of TEA and a half equivalent of bis-aquated oxaliplatin. These solutions were then stirred for 5 h changing them from uncoloured to yellow coloured solutions. Unbound oxaliplatin and the TEA were removed by centrifuging the samples on Vivaspin columns with a molecular weight cut off of 5 kDa, leaving the drug-dendrimer complexes in the top of the column. The oxaliplatin-dendrimer complexes are highly soluble in water, although if dried, they are difficult to get back into solution. As such, samples were generally diluted to a known concentration with either H2O or D2O immediately after centrifuge purification and kept until needed.

The binding of the oxaliplatin to the dendrimer was confirmed through the use of ^{1}H NMR of the dendrimer complex collected after centrifuge purification. Successful conjugation of the dendrimer with oxaliplatin is made evident through the appearance of the signals from the hydrogen atoms that make up part of the cyclohexane ring of oxaliplatin. The ^{1}H NMR of the free dendrimer was compared to that of the oxaliplatin bound dendrimer, Figure 3.4, and the introduction of the three peaks between 1.11 and 2.1 ppm result from the successful binding of oxaliplatin.

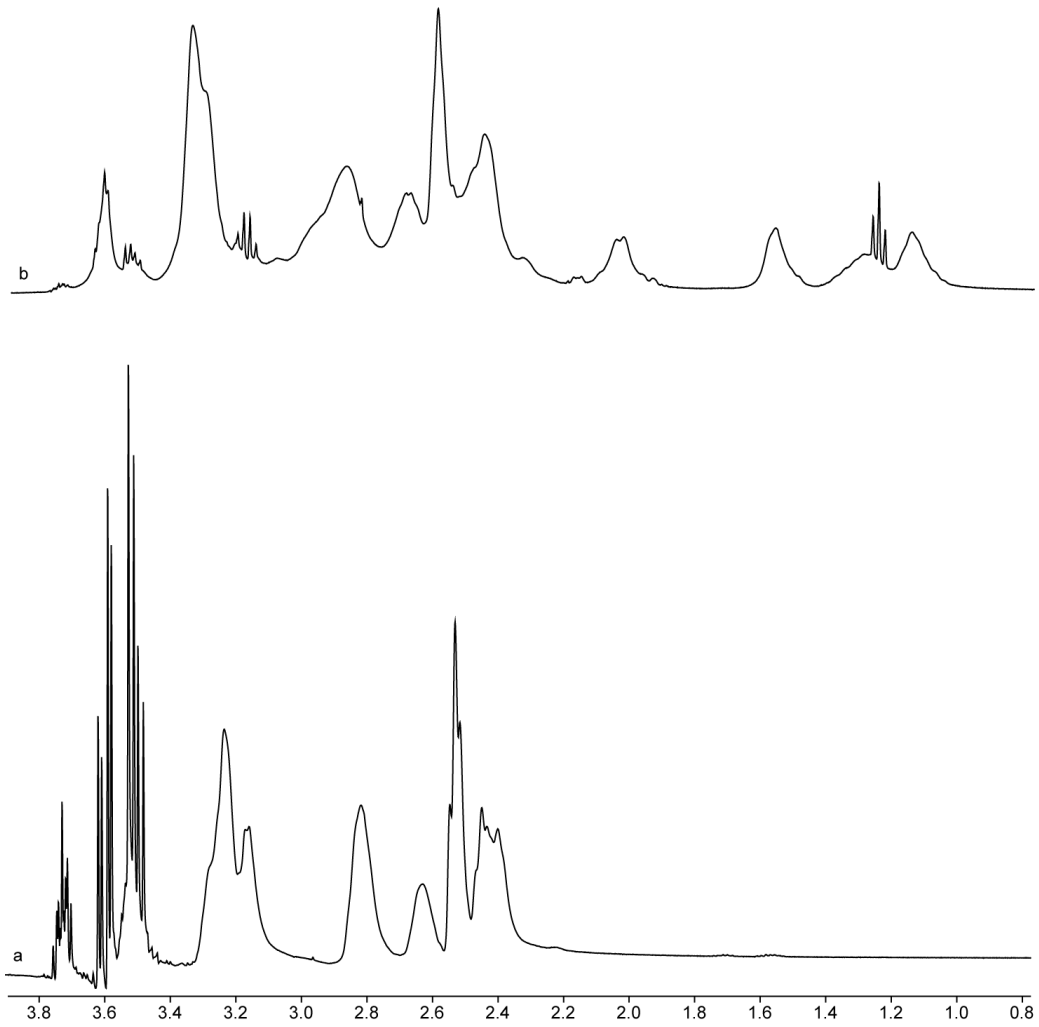

Figure 3.4 The ^{1}H NMR of a. free G5.5 dendrimer and b. $\{Pt(R,R\text{-dach})\}^{2+}$ conjugated G5.5 dendrimer showing the peaks due to the cyclohexane ring at 1.1, 1.5 and 2.1 ppm.

Following the synthesis of the dendrimer-oxaliplatin complexes it is necessary to quantify the number of platinum molecules bound to each dendrimer. The ideal situation, as it was with cisplatin, is the bidentate binding of oxaliplatin to all of the surface groups of the dendrimer. In order to quantify the number of platinum molecules 10 μL of a 100 mM solution, 1 μmol, of 3-(trimethylsilyl)-1-propane sulfonic acid (TMS), Figure 3.5, was added to the oxaliplatin-dendrimer solution as an internal standard. The signal from the protons of the methyl groups in TMS appear at exactly 0

ppm and the integration of this peak can be used to determine the number of oxaliplatin molecules when compared with the integration of the peaks from the cyclohexane ring, Figure 3.6.

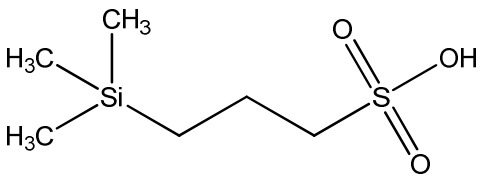

Figure 3.5 The chemical structure of TMS showing the methyl protons which give rise to the signal at 0 ppm.

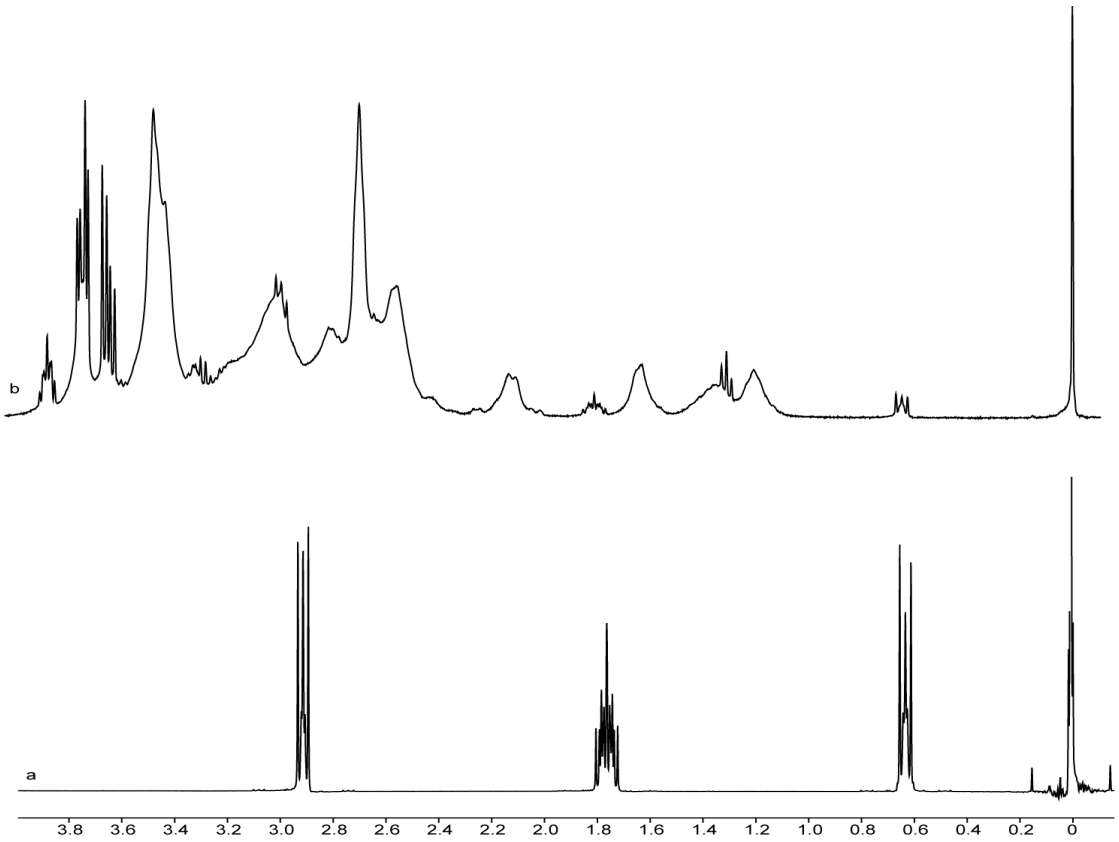

Figure 3.6 The ^{1}H NMR of a. free TMS and b. G4.5 {Pt(*R,R*-dach)}$^{2+}$-dendrimer complex showing the TMS peak at 0 ppm and the oxaliplatin peaks at 1.2, 1.7 and 2.1 ppm.

The integration of the oxaliplatin peak at 1.7 ppm was measured and compared to that of the peak from the 3 methyl groups in TMS at 0 ppm. The number of protons which determine these peaks are: 2 protons for the $\{Pt(R,R\text{-dach})\}^{2+}$ peak and 9 for the TMS peak. If the equivalent number of moles of oxaliplatin and TMS are present in the sample then the ratio of integrations would be 2:9 and any deviation from this ratio would determine the number of moles of $\{Pt(R,R\text{-dach})\}^{2+}$ in the sample which could then be translated into the number of platinum molecules per dendrimer. In all cases the ratio of peaks allowed the number of platinum molecules per dendrimer to be determined, Table 3.1. The number of platinum groups conjugated to the dendrimer was also confirmed using ICP-MS, either by direct analysis of the dendrimer complex and quantification of the unbound platinum.

Table 3.1: The number of $\{Pt(R,R\text{-dach})\}^{2+}$ moieties per dendrimer.

Dendrimer	**Number of surface groups**	**Number of binding sites**	**Oxaliplatin moieties/ dendrimer[a]**	**Oxaliplatin moieties/ dendrimer[b]**	**Binding efficiency**
3.5	64	32	12 ± 4	10 ± 3	38%
4.5	128	64	19 ± 3	16 ± 5	30%
5.5	256	128	35 ± 20	34 ± 17	27%
6.5	512	256	63 ±30	60 ±32	24%

a. Direct analysis of the dendrimer-platinate b. Indirect quantification using unbound platinum

The number of $\{Pt(R,R\text{-dach})\}^{2+}$ groups on the dendrimers follows the same pattern expressed by the cisplatin moieties, however none of the complexes achieved the same degree of conjugation experienced with cisplatin. The G3.5 again has the highest degree of conjugation with 12 $\{Pt(R,R\text{-dach})\}^{2+}$ complexes bound to the dendrimer, 38% of binding sites, however this is approximately a 50% reduction from the number of cisplatin molecules achieved.

The size of the dendrimer platinates was investigated using diffusion NMR , Part 2.2.2. The NMR experiment was modified from that used to measure the sizes of the cisplatin dendrimer complexes. In order to obtain better spectra, and therefore more resolved peaks, for calculation of the diffusion coefficient; a presaturation sequence was run before the diffusion spectra. The diffusion coefficient was again used in the Stokes-Einstein equation to determine the hydrodynamic radius and thus diameter of the complexes. In contrast to the results observed with the cisplatin complexes, Table 2.1, the trend exhibited by the [Pt(*R,R*-dach)]-dendrimer complexes was an increase in size upon addition of the oxaliplatin, Table 3.2.

Table 3.2 The diffusion coefficients and hydrodynamic diameter of the [Pt(*R,R*-dach)]-dendrimer complexes.

Generation	**Particle Size**			
	D **($\times 10^{-10}$ m^2s^{-1})**		**Diameter (nm)**	
	Free	**Bound**	**Free**	**Bound**
3.5	1.30	0.88	2.74	4.03
4.5	0.91	0.56	3.91	6.33
5.5	0.66	0.46	5.44	7.71
6.5	0.60	0.24	5.93	14.51

The size of the G3.5-4.5 oxaliplatin complexes are approximately 1.5 times the size of the equivalent free dendrimer whilst the G6.5 dendrimer more than doubles in size when coupled with oxaliplatin. The reason for the increase in size of these complexes is the likely aggregation that occurs due to the hydrophobic character of the cyclohexane ring of the *R,R*-dach group. This hydrophobic character will orientated the complexes such that as many of the cycohexane rings as possible are not in contact with the surrounding water and this would be achieved by aggregation of the dendrimer complexes.

3.2.3 Drug release and kinetics of drug release.

The release of the platinum from the dendrimers was measured using guanosine experiments similar to those described previously. In this instance however, the solution containing the $\{Pt(R,R\text{-dach})\}^{2+}$ dendrimer-complexes and guanosine monophosphate in D_2O was incubated for one week then centrifuged in a Vivaspin column to collect the guanosine bound platinum. The content of released platinum was then determined using ICP-MS, Table 3.3.

Table 3.3 The number of $\{Pt(R,R\text{-dach})\}^{2+}$ moieties released from the dendrimer as determined by guanosine binding and ICP-MS analysis.

Dendrimer	**Number of $\{Pt(R,R\text{-dach})\}^{2+}$ molecules per dendrimer[a]**	**Number of $\{Pt(R,R\text{-dach})\}^{2+}$ molecules released**	**Release efficiency (%)**
3.5	8	2	25
4.5	16	6	38
5.5	53	36	67
6.5	63	43	69

a. determined by indirect quantification of unbound platinum

The trend exhibited by the $\{Pt(R,R\text{-dach})\}^{2+}$ dendrimer platinate complexes mirrors that observed with the $\{Pt(NH_3)_2\}^{2+}$ bound dendrimer-platinates. In each case, however, the percentage released is greater for the $\{Pt(R,R\text{-dach})\}^{2+}$ dendrimer-platinate complexes and is likely a result of increased reversible binding of the platinum at the surface of the dendrimer. Despite this increase, the lower numbers of platinum moieties available in the $\{Pt(R,R\text{-dach})\}^{2+}$ dendrimer-platinates results in less free platinum being available than in equivalent cisplatin dendrimer-platinates.

The rate of release of platinum from the dendrimer was also investigated using the guanosine monophosphate binding. The dendrimer platinate was dissolved in 5 mL of phosphate buffered saline and 2 mol equivalents (to the number of platinum molecules present) of guanosine added. The solution was then incubated at 37 ^{o}C for 1 week and

200 µL samples taken from the solution every hour for the first 5 h then at periods of 24 h for 1 week. These samples were immediately centrifuged in a Vivaspin column, released platinum collected and the residual dendrimer reconstituted up to 200 µL and returned to the dendrimer guanosine solution. The samples containing the unbound platinum were made up to 10 mL using 2% nitric acid and the platinum content analysed by ICP-MS, Figure 3.7.

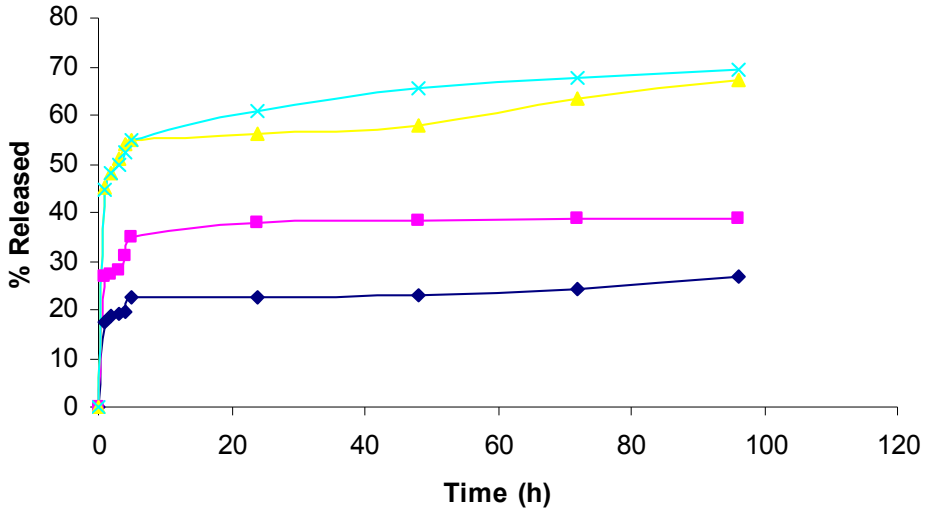

Figure 3.7. The rate of release of platinum from the G3.5 (◆), G4.5 (□), G5.5 (△) and G6.5 (X) dendrimer-platinate complexes .

In all cases there was a burst of platinum within the first 5 hours followed by sustained slow release. The initial burst release accounts for approximately 85% of all of the released platinum in all cases whilst the remaining 15% was observed over the following 95 hours.

3.2.4 In Vitro Cytotoxicity

In order to determine if the $\{Pt(R,R\text{-dach})\}^{2+}$ dendrimer-platinates were active *in vitro* they were incubated overnight with A2780 and A2780cis ovarian cancer cells. The IC_{50} values were determined by MTT assay, Table 3.4.

Table 3.4 The IC_{50} values of $\{Pt(R,R\text{-dach})\}^{2+}$ and $\{Pt(R,R\text{-dach})\}^{2+}$ dendrimer platinates

Complex	IC_{50} (μM)[a]		Resistance factor (Rf)[b]
	A2780	A2780cp	
$\{Pt(R,R\text{-dach})\}^{2+}$	1.82 ± 0.24	28.0 ± 1.1	15.38
G3.5$\{Pt(R,R\text{-dach})\}^{2+}$	0.164 ± 0.014	2.27 ± 0.03	13.84
G4.5$\{Pt(R,R\text{-dach})\}^{2+}$	0.031 ± 0.003	0.468 ± 0.018	15.01
G5.5$\{Pt(R,R\text{-dach})\}^{2+}$	0.368 ± 0.011	4.41 ± 0.10	11.98
G6.5$\{Pt(R,R\text{-dach})\}^{2+}$	0.55 ± 0.005	0.690 ± 0.017	1.25

a. Based on the total "releasable" cisplatin concentration per mole of dendrimer. b. Defined as the IC_{50} value in the resistant line divided by the IC_{50} value in the sensitive line; the lower the Rf the better the complex is at overcoming resistance.

In all cases the dendrimer-platinates were more active in both the sensitive and resistant cell lines. This is the opposite of the effect observed with the cisplatin dendrimer-platinates and is possibly a result of aggregation of the. The dendrimer-platinate complexes were less active in the resistant cell line however, they retained a smaller degree of cross-resistance than that observed with the free $\{Pt(R,R\text{-dach})\}^{2+}$. Similarly to the results observed with the cisplatin dendrimer-platinates, the larger $\{Pt(R,R\text{-dach})\}^{2+}$ dendrimer-platinates showed the least cross-resistance between cell lines.

3.3 Conclusions

The active component of oxaliplatin was successfully synthesised and coupled to G3.5-G6.5 PAMAM dendrimers. The resulting complexes were found to contain between 12 and 63 $\{Pt(R,R\text{-dach})\}^{2+}$ moieties and were shown to aggregation upon conjugation of the platinum complex. The dendrimer-platinates were shown to release between 2 and 43 platinum molecules and that 85% of these molecules were released in the first 2 hours

when incubated with guanosine monophosphate. The resulting dendrimer-platinates were more cytotoxic than the free platinum complex in A2780 and A2780cis cells and exhibited a smaller degree of cross resistance between the cell lines.

Chapter 4: Dendrimer-platinate complexes with the dendrimer as the amine ligand of ligand of cisplatin

4.1 Introduction

Full generation PAMAM dendrimers with amine functionality share some of the same physical characteristics as their half generation analogues. They are both monodisperse and spherical in shape, however, full generation dendrimers are cationic in aqueous solutions, with the charge density being restricted to the amine surface groups, Figure 4.1.[1] These dendrimers have been utilised for a range of purposes including: gene delivery, metal ion conjugation for imaging and therapy and catalysts in the synthesis of lactams and lactones.[1-4] A number of other types of dendrimers have previously been explored as delivery vehicles for platinum drugs including the half generation PAMAM dendrimers. Malik *et al* previously reported no interaction between cisplatin and the amine groups of a G3.5 dendrimer, however, Pellechia *et al* have subsequently shown interactions between K_2PtCl_4 and the amine groups in the branches of hydroxyl terminated dendrimers. [5, 6] These interactions should therefore be possible with the amine groups on the surface of the full generation PAMAM dendrimers. In this study, the G4 full generation dendrimer was reacted with K_2PtCl_4 to develop a cisplatin-like drug where the amine groups of cisplatin replaced by the dendrimer (Figure 4.1).

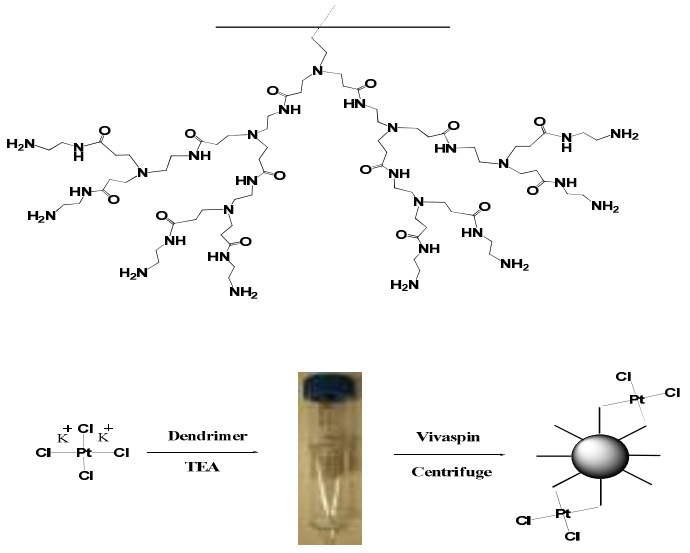

Figure 4.1 The chemical structure of a G2 dendrimer showing only one hemisphere (Top) and the reaction with K_2PtCl_4 to form the cisplatin analogue (bottom).

4.2 Results and Discussion

4.2.1 Synthesis of Dendrimer-$PtCl_2$ complexes

The G4 dendrimer was combined water with 5-32 mol. equivalents of triethylamine (TEA) and 5-32 mol. equivalents of K_2PtCl_4 in unbuffered. The solutions were then stirred for 6 h in which time a colour change from red to brown was observed. Solutions containing 20-32 mol. equivalents of K_2PtCl_4 formed a brown precipitate, which was collected by vacuum filtration. The solutions containing 5-15 mol. equivalents of K_2PtCl_4 did not form a precipitate and unbound cisplatin and the TEA were removed by centrifuging the samples on Vivaspin columns with a molecular weight cut off of 5 kDa, leaving the drug-dendrimer complexes in the top of the column (Figure 4.1). The dendrimer platinum complexes were recovered and placed in a fume cupboard to allow any remaining water to evaporate at which point a yellow gel like solid was obtained. The precipiates formed from the 20-32 equvialent solutions proved to be insoluble as they failed to dissolve in water, DMSO, DMF or MeOH. The yellow solid obtained from the 5-15 equivalent reactions proved difficult to get back into solution and these were subsequently kept solvated following centrifugation. ^{1}H NMR spectra were obtained for the free and platinum bound dendrimers, Figure 4.2.

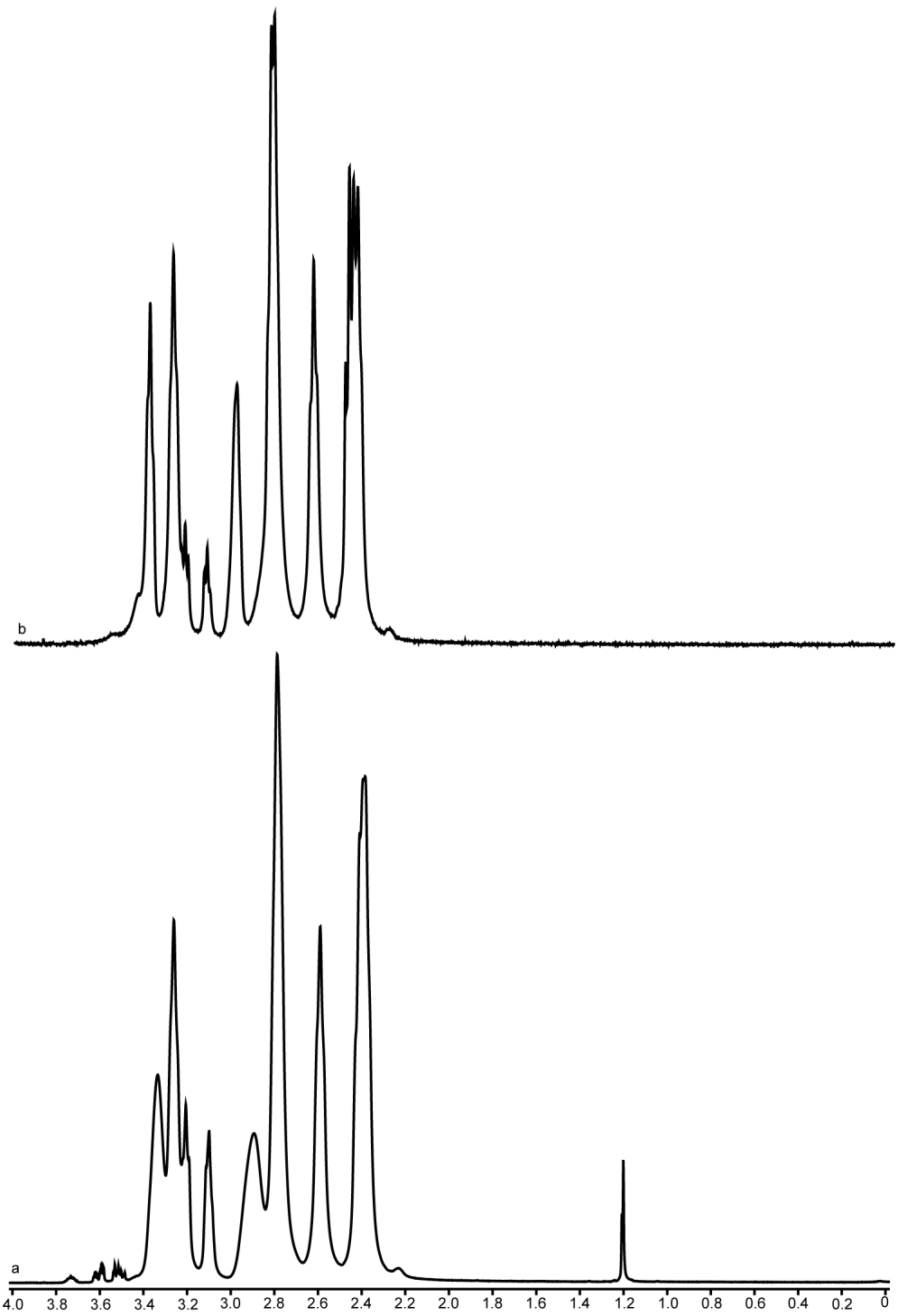

Figure 4.2 The ^{1}H NMR of free a. G4 dendrimer and b. the G4 dendrimer reacted with 5 equivalents of K_2PtCl_4.

4.2.2 Drug release and binding studies with guanosine

To determine whether the platinum bound to the dendrimers can be released as a complex that retains the same DNA binding capabilities as cisplatin, the products obtained from the 5-15 equivalent reactions were reacted with 10-30 equivalents of guanosine monophosphate. The ^{1}H spectra of guanosine with the dendrimer palatinate complexes were recorded and subsequently heated for 2 days at 60 ^{o}C with the ^{1}H NMR spectra being recorded after 1 day incubation and then 2 day incubation, Figure 4.3.

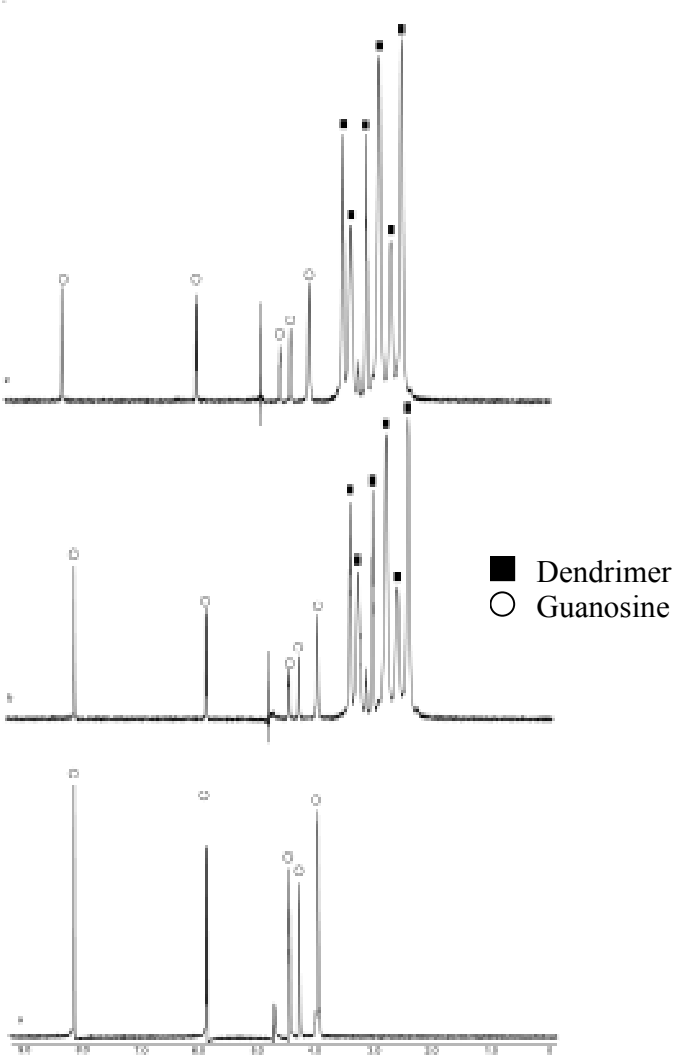

Figure 4.3 The ^{1}H NMR spectra of a. free guanosine; b. guanosine + G4-5 eq at time 0 and c. guanosine + G4 -5eq after 2 days incubation at 60 ^{o}C.

The ^{1}H NMR spectra recorded after day 1 and 2 of incubation showed no downfield shift of the H8 peak to 8.6 ppm which indicates that no binding between the platinum and the N7 of guanosine occurred. The absence of peak at 8.6 ppm suggests that the dendrimer-platinum complex is not able to bind to the N7 position in this form.

4.3 Conclusions

The formation of the brown precipitate with 20-32 equivalents of platinum and the eventual formation of the yellow solid from the 5-15 equivalents of platinum suggest that the desired dendrimer platinum complexes were formed. The lack of solubility of these complexes prevented confirmation by other methods. The lack of solubility of the complexes formed from higher molar ratio of platinum to dendrimer prohibited further testing of these complexes meaning that quantification of platinum content and binding capability could not be ascertained. The products from the lower molar ratio reactions also proved to be difficult to reconstitute into solution and were subsequently kept solvated. The binding reactions with guanosine showed that no binding was taking place, indicative of the platinum present is not in a form capable of binding to DNA. The lack of solubility and binding from all complexes formed prevent further analysis from being undertaken.

4.4 References

1. Biricova, V.; Laznickova, A. Dendrimers: Analytical characterization and applications. *Bioorg. Chem.* **2009,** 37, 185-192.

2. Eichman, J. D.; Bielinska, A. U.; Kukowska-Latallo, J. F.; Baker, J. R. The use of PAMAM dendrimers in the efficient transfer of genetic material into cells. *Pharm. Sci.Technol. To.* **2000,** 3, 232-245.

3. Nanjwade, B. K.; Bechra, H. M.; Derkar, G. K.; Manvi, F. V.; Nanjwade, V. K. Dendrimers: Emerging polymers for drug-delivery systems. *Eur. J. Pharm. Sci.* **2009,** 38, 185-196.

4. Touzani, R.; Alper, H. PAMAM dendrimer-palladium complex catalyzed synthesis of five-, six- or seven membered ring lactones and lactams by cyclocarbonylation methodology. *J. Mol. Catal. A-Chem.* **2005,** 227, 197-207.

5. Pellechia, P. J.; Gao, J.; Gu, Y.; Ploehn, H. J.; Murphy, C. J. Platinum ion uptake by dendrimers: An NMR and AFM study. *Inorg. Chem.* **2004,** 43, 1421-1428.

6. Malik, N.; Evagorou, E. G.; Duncan, R. Dendrimer-platinate: a novel approach to cancer chemotherapy. *Anti-Cancer Drugs* **1999,** 10, 767-776.

Chapter 5: Experimental

5.1 Materials

Dendrimers were purchased from Dendritech or Sigma-Aldrich. Cisplatin, Dowex™ 1×4-400 anion exchange resin, sodium nitrate, 5′-guanosine monophosphate and pH 6.5 phosphate buffered saline tablets were purchased from Sigma-Aldrich. D_2O (99.9%) was purchased from Cambridge Isotope Laboratories. All aqueous solutions were prepared using water filtered by a Millipore purification unit. Vivaspin™ columns used in centrifuge experiments were supplied by Sartorius Biolab or VWR.

5.2 NMR

^1H NMR spectra were obtained on a JEOL AS-400, a Bruker AV-500 or Bruker AV-400 spectrometer and ^{195}Pt spectra were recorded using a Bruker AV-400 spectrometer. All platinum containing samples were prepared as saturated solutions in 600 μL D_2O and all other solutions prepared at various concentrations. ^1H presaturation NMR spectra were recorded using 16-64 scans over a spectral width of 12 ppm with an irradiation offset value of 4.78 ppm. ^{195}Pt spectra were recorded using 80,000 scans over a spectral width of 75,000 Hz and externally referenced to K_2PtCl_4 at -1631 ppm.[97]

5.3 Diffusion NMR

The diffusion coefficients of the free dendrimers and the drug-dendrimer complexes were determined using a standard Bruker 1D- pulse sequence. Spectra were obtained using a Δ of 100 ms, a δ of 5 ms with 32 scans and a relaxation delay of 2 s. The diameter of the dendrimers was determined using the Stokes-Einstein equation:

$$D = \frac{kT}{6\pi\eta r}$$

where D is the diffusion coefficient (m^2s^{-1}), k is Boltzmann constant ($J\ K^{-1}$), T is temperature (K), η is solvent viscosity (1.232×10^{-3} Pa s) at 25 ^oC and r is the hydrodynamic radius of the dendrimer (m).

5.4 ICP-AES

Analysis was carried out on a Thermo Electron X-Series II quadrupole ICP-AES with a Cetac ASX-520 autosampler. The instrument used a concentric nebuliser containing a Peltier cooled conical single-pass spray chamber with impact bead and an integral peristaltic pump for sample uptake. A hexapole for CCT ED (Collision Cell Technology with Energy Discrimination) mode was used to remove polyatomic interferences. Instrumental operating conditions used were 1400W RF forward power, 13 L min^{-1} plasma flow, 1.0 L min^{-1} nebulizer flow and 0.8 L min^{-1} auxiliary flow. A sample flush time of 60 s, a wash time of 60 s and a peak jump mode was used with a dwell time per isotope of 10 ms. Platinum concentration was determined using the ^{194}Pt and ^{195}Pt isotopes. The instrument was calibrated using solutions prepared from a Spex CertiPrep certified standard diluted as required with 2% Fisher Primar Plus nitric acid.

5.5 Aquation of cisplatin

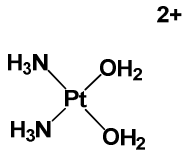

Dowex anion exchange resin (1×4-400, 25 g) was converted to the nitrate salt either by stirring in 200 mL 5 M $NaNO_3$ for approx. 5 h, filtered and washed with water, or the Dowex was loaded into a glass column, washed with water, 200 mL 5 M $NaNO_3$ and then again with water. Cisplatin (100-200 mg) was then dissolved in water and either stirred with the Dowex in a beaker for several hours with heating, or eluted down a Dowex column. In some instances, individual samples were eluted or stirred multiple times with fresh Dowex. All samples were rotary evaporated to dryness before analysis by ^{195}Pt NMR. Alternatively, cisplatin was fully dissolved in water, wrapped in foil to prevent degradation by light before being stirring for 24 h with $AgNO_3$ (2 mol. equiv.). The resultant AgCl precipitate was removed by filtration through a 0.2 μm nylon filter and the filtrate rotary evaporated to dryness.

5.6 Synthesis of dendrimer-drug complexes

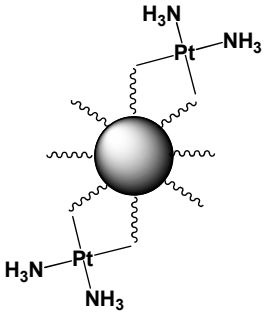

Dendrimer in water (0.5-7.9 mM, 100-210 μL) was stirred with aquated cisplatin or oxaliplatin (32-256 mol. equi.) overnight in water (10 mL). The solutions were then centrifuged in Vivaspin™ columns with a 5 kDa molecular weight cut off membrane for 40 min at 3500 rpm. The drug-dendrimer complexes were collected separately into small sample vials and placed in a fume cupboard to evaporate the remaining water to yield a brown solid or instead diluted in H_2O/D_2O to a known concentration. The eluted water fractions from the bottom of the column were collected then evaporated to dryness and the residue reconstituted in water (10.00 mL) for analysis by ICP-AES.

5.7 Guanosine binding

The drug-dendrimer complexes were dissolved in D_2O (520 μL) and placed in an NMR tube. 5′-Guanosine monophosphate in D_2O (2 mol. equiv to total platinum content) was added and the solution heated for 1 week at temperatures up to 60 ^{o}C, and the ^{1}H NMR spectra recorded at intervals of 0, 24, 96 and 168 h . The spectra were monitored for a shift in the peak at 8.2 ppm to 8.6 ppm which was then used to calculate the number of platinum molecules binding to the guanosine.

5.8 Kinetics of drug release

A phosphate buffer tablet was dissolved in 200 ml of water to form 200 mL of pH 7.4 phosphate buffered saline (PBS). The drug-dendrimer complexes were then individually

dissolved in 10 mL of the saline solution. 1 mL of the resulting solution was immediately extracted and centrifuged for 15 min at 8000 rpm in a Vivaspin column, to collect any platinum that has been released, whilst the remaining solution was incubated at 37 ^{o}C. . 1 mL samples of the drug-dendrimer saline solutions were extracted every hour for the first 12 hours and then after 24, 48, 72, 96, 120 h and the free platinum collected. The volume of the PBS containing the free platinum was made up to 10 mL using 1% nitric acid and then analysed through ICP-AES.

5.9 *In vitro* growth inhibition assays

A2780, A2780cis and A2780cp ovarian cancer lines were grown in RPMI media containing 10% foetal calf serum, penicillin streptomycin and *L*-glutamate in a 5% CO_2 atmosphere. The cells were trypsinised, counted and adjusted to 500-1000 cells per well for the MTT stain assays and 2000 cells per well for the WST-1 stain assays (both in 96 well plates). Cisplatin, free dendrimer and drug-dendrimer complex stock solutions were diluted with RPMI to prepare a dilution series based on the total platinum concentration (0.1 – 100 μM cisplatin). 10 μL aliquots were taken from these solutions and added in triplicate to each well along with RPMI only. The plate was then cultured for 24, 48, 72 or 96 h and 50 μL of WST-1, followed by further incubation for 1 h. The absorbance of the WST-1 was measured using a plate reader at 450 nm, and the cells fixed with 4% paraformaldehyde with crystal violet used to stain the viable cells. The absorbance of the crystal violet stain was measured at 540 nm. For assays using the MTT stain: on the final day MTT (50 μL of a 5 mg/mL solution) was added to the 200 μL of medium in each well and the plates were incubated at 37 ^{o}C for 4 h in the dark. Medium and MTT was then removed and the MTT-formazan crystals dissolved in 200 μL DMSO. Glycine buffer (25 μL per well, 0.1 M, pH 10.5) was added and the absorbance measured at 570 nm in a multiwell plate reader.

5.10 *In vivo* tumour growth inhibition

The human ovarian tumour cell line A2780 was used. These form well vascularised tumours that have a doubling time of about 3 days. Cells were injected subcutaneously into the right flank of female athymic nude mice. After about 10 days, once tumours had reached a mean diameter of at least 5mm, mice were randomised into groups of 5. They were weighed and tumours measured by callipers daily. Mice were then treated (Day 0) with a single intraperitoneal injection of either phosphate buffered saline (control), cisplatin (6 mg/kg in PBS), cisplatin-G6.5 dendrimer complex equivalent to 6 mg/kg or 8 mg/kg cisplatin or G6.5 dendrimer alone. Tumour volumes are calculated assuming spherical geometry and results are plotted as relative tumour volume or relative body weight. This method gives all weights and volumes a value of 1 on Day 0 and all other measurements are then related to the initial measurement. This was done because it is not possible to start with all tumours of equal size; however, the growth rate is consistent regardless of starting size provided it is greater than 5mm.

5.11 Synthesis of [$PtCl_2$(*R,R*-dach)]

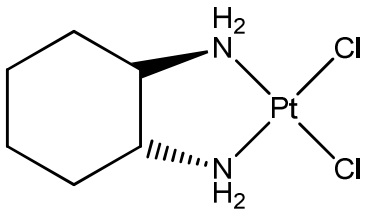

K_2PtCl_4 (0.602 mmol) was dissolved in 100 mL of water and stirred with one equivalent of (1*R*,2*R*)-(-)-diaminocyclohexane for 5 h then placed in the freezer for a further 1 h. During this time a yellow precipitate was formed and collected by vacuum filtration. The yellow powder was then washed with 2x 25 ml ethanol and 2x 25 ml diethyl ether and then aired dried. Yield: 90%.

5.12 Aquation of [$PtCl_2$(*R,R*-dach)]

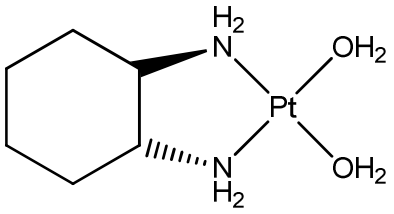

100 mg (0.263 mmol) of [$PtCl_2$(*R,R*-dach)] was added to 1.9 equivalent of $AgNO_3$ in 200 ml of water. The solution was then wrapped in foil and refluxed overnight before being filtered to remove the AgCl precipitate. The solution containing the [$Pt(OH_2)_2$ (*R,R*-dach)]was then evaporated to yield a yellow solid. Yield: 85%.

5.13 Synthesis of G4-platinate dendrimer complexes

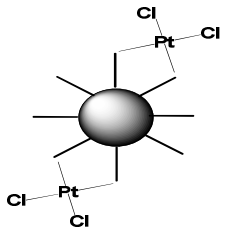

Dendrimer in water (15.24 mM, 230 μL) was stirred with K_2PtCl_4 (5-32 mol. equiv.) and TEA (5-32 mol. equiv.) for 6 h at 70 ^oC. A brown precipitate formed during the synthesis of samples containing 20 mol equiv. or above of K_2PtCl_4. The solutions were then filtered to collect any precipitate formed or centrifuged to remove excess platinum. Centrifuged samples were placed in a fume cupboard to evaporate any residual water. Attempts to dissolve the products were then made in water, DMSO, DMF, MeOH and H_2SO_4.

Part 2: Active Targeting of dendrimer-platinates

Chapter 6: Targeting groups

6.1 Introduction

Section one of this thesis discussed the exploitation of the EPR effect in order to passively target cancer cells using dendrimers as delivery vehicles of sufficient size. In addition to passive targeting it is possible to actively target a therapeutic agent to its target location e.g. cancer cells.[1] Active targeting is the inclusion of a chemical or biological moiety in a drug structure which will recognise and target cellular characteristics of specific cell types e.g. receptors and cell surface peptides.[1, 2] Active targeting can also provide additional benefits over passive targeting such as a reduction in the quantity of a drug required to achieve therapeutic activity and side effects resulting from less accumulation of the drug in non-target cells.[3]

The selection of a targeting moiety is, in part, driven by the type of target being exploited. In the development of targeted anticancer agents there are essentially two types of targeting strategy: antiangiogenesis and antiproliferation.[1, 4] Angiogenesis is a viable, and important, target for directed therapeutics as this process is a major contributor to the tumours ability to grow and become metastatic.[1, 5] Antiangiogenesis drugs, designed to prohibit the growth of new vasculature to supply nutrients to a tumour, would typically be directed towards proangiogenic factors such as the vascular endothelial growth factor and $\alpha_v\beta_3$ integrins, and this targeting strategy provides a number of benefits: removal of the physiological barrier that limits the proliferation of drugs throughout the tumour, it decreases the growth and metastatic capabilities of the tumour, the neovascular endothelial cells are less likely to undergo phenotypic variation and this reduces the likelihood of developing secondary acquired resistance and tumour vasculature is universal and not limited by the type of cancer.[1, 5, 6]

The prevention of the uncontrolled proliferation of tumour cells is one of the most significant active targeting strategies currently being investigated.[1] This method of targeting utilises the upregulation of receptors that promote cell growth; such as the epidermal growth factor receptor and transferrin receptors.[7, 8] The epidermal growth

factor receptor has been shown to be present at increased levels in numerous cancers, including breast and lung cancers, and has been implicated in abnormal cell growth.[7] Transferrin receptors are expressed in many tumours providing a viable target for cancer therapy and their presence in the blood brain barrier also makes them an interesting target for directing drugs to the brain.[9]

The active targeting of cancer cells can be achieved through the conjugation of drugs with a number of different types of structure including: aptamers, peptides, steroids and vitamins.[10]

6.2 Antibodies

Antibodies have been of interest as targeting agents for a number of different types of complexes including radiotherapy and chemotherapy agents.[11] Antibodies enable the targeting of cells through specific receptors which are present in larger quantities in the target cells compared with healthy cells, Figure 6.1. The types of cellular receptors which can be targeted by antibodies include the hypoxia inducible factor 1α receptor which is expressed in cancer cells to enable them to survive in the hypoxic conditions of a tumour.[3] In most cases monoclonal antibodies, or fragments of these antibodies, are used as the targeting moiety and in some cases the antibody may also provide the therapeutic effect e.g. they bind to the receptor and disrupt signal transduction pathways and prevent proliferation of cancer cells.[4]

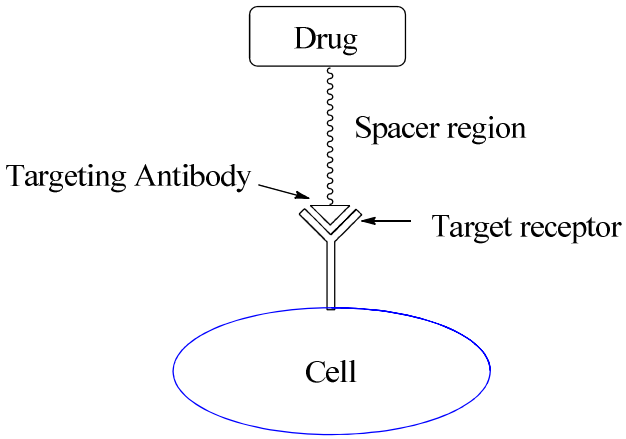

Figure 6.1 A generalised summary of active targeting of a cell using antibodies.

Although antibodies can be used as the therapeutic agent, this description of their use will be restricted to only complexes where they have been used as a targeting moiety. Mylotarg was the first antibody-drug conjugate, the antibody is conjugated to the drug ozogamicin and was approved for clinical use; however, this approval has since been rescinded after it failed to show a clinical benefit to patients and an increase in patient deaths. Despite this set back efforts are still being made in to the development of antibody targeted drugs. Wagner *et al*. have described their efforts to target albumin nanoparticles containing doxorubicin using a monoclonal antibody, DI17E6, which targets αvβ3 integrins.[12] The complex was shown to have an increased cytotoxic effect, compared to the nanoparticle with doxorubicin alone, when incubated with melanoma cells expressing the integrin receptor.[12] The DI17E6 antibody used to construct the complex has a dual function, prevention of tumour growth and inhibition of angiogensis, which can increase the uptake of the cytotoxic drug payload.[12] A similar study carried out by Song *et al*. using paclitaxel encapsulated in nanomicelles with an anti-HIF-1α antibody demonstrated an ability to selectively kill stomach cancer cells, MGC-803, and decrease the side effects of paclitaxel.[3]

Calcium phophosilicate composite nanoparticles conjugated with an anti-CD71 antibody have been developed in an attempt to selectively target both human breast and pancreatic cancers.[13] The antibodies in this study were targeted against transferring receptors for breast cancer or gastrin receptors for pancreatic cancer, and in both cases they showed an ability to selectively accumulate in the desired cells, and in the case of the gastrin targeted conjugates, cross the blood brain barrier.[13] Antibodies have also been explored as a means to overcome drug resistance in some cancer cells. The antibody of P-glycoprotein was conjugated to carbon nanotubes loaded with doxorubicin and the resulting complex was tested *in vitro* against multidrug resistant leukemia cells, K562R.[14] The antibody complex was shown to improve the cytotoxicity of doxorubicin in the resistant cells as well as demonstrating an ability to suppress the proliferation of these leukemia cells. The use of antibodies for targeted therapy is not limited to cancer; anti cross-linked fibrin antibodies have been explored for the delivery of antirestenotic drugs to prevent arteries from becoming blocked after surgery and to remove plaque build up.[15]

Despite having been shown to enhance the properties of some drug complexes, antibodies have some disadvantages which can prove detrimental to their ability to act as targeting agents. The antibodies themselves can be immunogenic which results in adverse reactions during use and their large size can reduce their ability to penetrate tumours effectively.[16] Fragmented antibodies can penetrate more readily into the tumour but these are subject to rapid clearance from the body.[16] The actual process of conjugating the antibody to a linker or drug can compromise the targeting ability of the antibody as it may result in loss of specificity and/or affinity for the target.[17] It can also prove difficult to access antibodies which are specific to the target cell types.[17]

6.3 Aptamers

Aptamers are short sequence single strand DNA or RNA oligonucleotides which adopt a specific and stable three dimensional conformation which allows for specific tight binding to protein targets.[18, 19] These sequences are isolated from synthetic nucleic acid libraries by an *in vitro* selection process called systematic evolution of ligands by exponential enrichment (SELEX), Figure 6.2.[18-20] The SELEX process is an iterative process which readily yields highly selective aptamers.[18] The oligonucleotide sequences combine the advantages of antibodies: high affinity, selectivity, low toxicity with a high degree of stability across a wide range of conditions including pH and temperature.[20, 21] The stability in these varying conditions and the ease of synthesis through the SELEX process allows for the aptamers to be tailored for certain physiological conditions.[18] Although aptamers can bind target proteins with high specificity and affinity, they themselves are poor antigens due to their size (20-80 bases) and similarity to endogenous molecules.[18] The bioavailability of aptamers is limited due to their rapid clearance, but modification with anchor groups such as cholesterol and polyethylene glycol can act to enhance availability and pharmacokinetics.[18, 19]

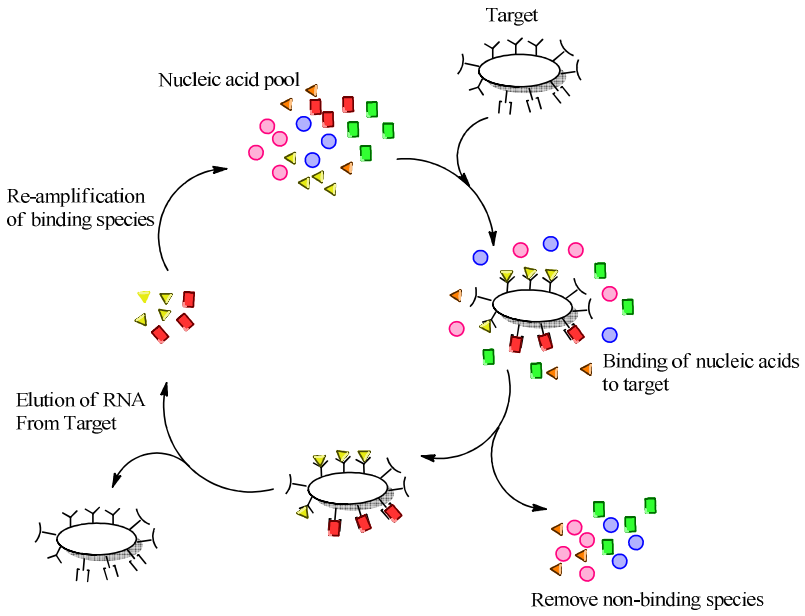

Figure 6.2 The SELEX cycle for the synthesis of aptamers.

A number of studies into the use of aptamers as targeting groups for therapeutics are currently underway but they have already been shown to be viable as anti-infectives, anticoagulation, anti-inflammation, antiangiogenesis, antiproliferation and immune therapies.[18] The first aptamer drug approved was Macugen (pegaptamib) for the treatment of age related macular degeneration; however, a number of studies are focused on the use of aptamers in cancer treatment.[19-21] Huang *et al* prepared aptamer-doxorubicin conjugates using the aptamer sgc8c and these conjugates maintained specificity of the aptamer and efficacy of doxorubicin whilst exhibiting high specificity for cancer cells.[20] Another study by Farokhzad *et al*. involved the synthesis of docetaxel nanoparticles functionalised with the A10 2′-fluoropyrimidine RNA aptamer as a therapeutic against prostate cancer.[21] The aptamer functionalised nanoparticles were shown to be more cytotoxic than the unfunctionalised nanoparticles *in vitro*, 61 ± 5% vs 42 ± 2% cell viability for unfunctionalised nanopatricle vs functionalised nanoparticle.[21] The same functionalised nanoparticles were also shown to be more active *in vivo* in LNcaP xenografts than the unfunctionalised nanoparticles.[21] The aptamer complex

furthest along the drug pipeline for cancer treatment is AS1411 which exhibited anticancer activity in human phase I and II trials as well as a favourable tolerance profile.[19] Unfortunately, more recent phase IIb studies of AS1411 have been abandoned as early data showed that the results were likely to be inclusive, with no benefit being achieved over standard therapy.

Despite being promising candidates for use in targeted therapies aptamers also must be carefully studied before they can be fully utilised. It is possible that nucleic acid aptamers may be subject to nuclease degradation in cells or blood serum making them ineffective.[22] Complexes containing aptamers may also be limited to local administration only due to possible interactions with proteins in untargeted regions of the body resulting in adverse effects.[22]

6.4 Peptides

Small peptides have been explored as drug targeting molecules as they may provide a means to overcome the problems associated with targeting antibodies as well as providing effective tissue penetration and selectivity.[23] The other advantages provided by peptides are near invisibility to the immune system and lack of infectious materials present in other microorganisms, such as phages and adenoviruses, used to transport material into cells.[23, 24] The selection and synthesis of peptides which can specifically target biological markers, such as those for tumour cells and immunoglobins, both *in vitro* and *in vivo* is readily achievable through the use of peptide libraries.[23] Typically there are two classes of peptides being considered for therapeutic use: cell penetrating peptides (CPPs) and cell targeting peptides (CTPs).[24, 25]

Cell penetrating peptides were developed after the observation that several proteins can spontaneously translocate through the membrane and into the cell.[24] Further investigation of these proteins allowed the identification of a minimal domain required for translocation, 10 – 27 amino acids, which were subsequently used to develop the

highly cationic mutants and analogues which constitute the CPP family.[24, 25] CPPs penetrate cells through a receptor independent route, however, this process is not fully understood.[25] Amongst the most commonly studied CPPs are the SynB vectors, antennapedia and transactivation of transcription (TAT) peptides which are all heterogeneous in size and shape and are all positively charged.[25] The SynB vectors are derived from the antimicrobial peptide protegrin-1 (PG-1).[25] The PG-1 interacts with the lipid matrix of bacterial membranes and its analogues, without cystine residuesand are used to interact with cell surfaces and cross the plasma membrane.[25] The internalisation of these peptides is also independent of receptor chirality as the *D*-enantiomer penetrates as efficiently as the *L*-enantiomer.[25] Another short sequence peptide, penetratin (pAntp43-58) is able to penetrate various cells and again is not dependent on a stereospecific receptor; however, the means of interaction between this peptide and the cell surface is not known.[25] Analogues derived from the TAT peptides have been shown to translocate into the interior of various cell types within minutes and have been predominantly investigated as drug delivery vehicles to transport large cargoes into cells.[25] There are, however, some problems which must be addressed in order to make CPPs viable as they lack specificity *in vivo* and translocate into various cell types.[24] The cationic nature of CPPs may also result in toxic side effects when used.[24]

Cell targeting peptides are designed to target a specific cell type and are generally chosen for their binding to surface proteins involved in specific biological functions, such as cell surface receptors, growth factor receptors and cell adhesion molecules.[23] The inclusion of CTPs in a drug complex may allow targeting of over expressed receptors on the surface of particular cell types.[24]

The advantages presented by peptides have led to them being investigated for use in therapeutics aimed at a number of targets. In cancer research both CTPs and CPPs have been investigated as a means of improving drug efficiency. The receptor for lutenising hormone-releasing hormone (LHRH) is over expressed in breast, ovarian and prostate cancer whilst not being present at detectable levels in visceral organs.[26] Dharap *et al*.

designed a CTP based on LHRH as a means of targeting the receptors and they were able to demonstrate high anticancer activity of their complexes and a substantial reduction in the level of side effects.[26] Prakash *et al*. also developed a cyclic peptide to target stromal cells by binding specifically to platelet derived growth factor receptors which are unregulated in several cancers including: colorectal, pancreatic, ovarian, lung and breast.[27] In order to determine the suitability of their peptide as a drug carrier and targeting agent they coupled the drug doxorubicin to a complex of the peptide and human serum albumin.[27] Through *in vivo* experiments they were able to show that their conjugate was able to accumulate in C26 cells and that the complex was able to improve the therapeutic efficacy and had reduced side effects compared with free doxorubicin.[27] More recently peptides have been developed as ligands for cisplatin in order to achieve a charged platinum-peptide complex.[28] These complexes have been shown to form DNA adducts at concentrations up to 10 times lower than that required of free cisplatin which further supports further exploration with the platinum anticancer drugs.[28]

6.5 Estradiol

The estrogen receptor, ER, is useful as a potential target as it is expressed in a number of different cancers including 60-70% of breast cancer, 70% of uterus and 61% of ovarian cancers, which combined represent approximately 40% of all diagnosed cancer in women.[29] The high affinity between 17β-estradiol, Figure 6.3 and the estrogen receptor allows for the design of therapeutic agents which selectively target drugs towards the estrogen receptor by modification of the estradiol structure.[29, 30] Targeting groups based on estradiol have a high affinity for the ER and have been explored as a means for targeting platinum drugs.[29]

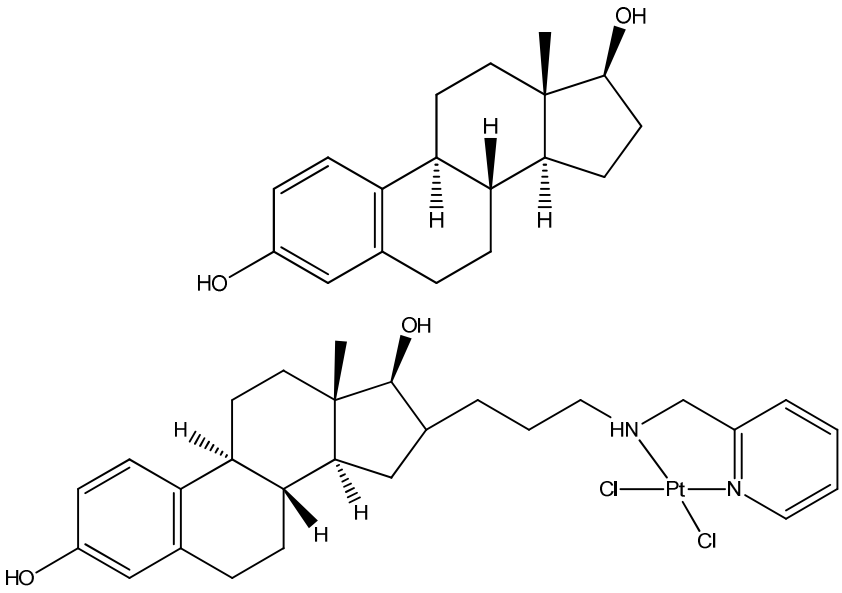

Figure 6.3 The structure of17β-estradiol (Top) and the high affinity 17β-estradiol-platinum(II) complex synthesised by Berube et al (Bottom).[31]

Berube and co-workers have developed a series of 17β-estradiol-platinum(II) complexes and these have been tested *in vitro* against estrogen receptor positive (ER^+, MCF-7) and estrogen receptor negative (ER^-, MDA-MB-231) human mammary carcinomas, Figure 6.3.[31] The estradiol-platinum(II) complexes with the greatest affinity for ERα were shown to exhibit greater cytotoxicity in breast cancer cells than tamoxifen and cisplatin, some were up to 32 times more cytotoxic than cisplatin in the MCF-7 cells and 25 times more cytotoxic than cisplatin in the MDA-MB-231 cells.[31] The same research group carried out a similar study with estradiol complexes attached to a platinum(II) complex via linker group, such as polyethylene glycol, however these complexes showed no specific cytotoxicity in ER^+ cell lines.[32]

6.6 Apoferritin

The protein ferritin is a native iron-storage protein found throughout the body. In its iron free form, Apoferritin forms a potentially useful cage like structure which could be used to deliver other metal-based drugs to the desired target, Figure 6.4.[33, 34] Apoferritin is made up of 24 subunits which arrange to form a hollow cage which is eight nm in diameter internally and 12 nm in diameter externally.[33, 34] Hydrophylic channels are formed at the intersection of the subunits and these allow access to the protein cavity.[33] The cavity has previously been shown to accommodate several types of complexes including: gadolimium contrast agents, desferrioxamine B, metal ions and nanoparticles of iron salts.[33] The difficulty with using native proteins for drug targeting is the need for chemical modification to increase the efficiency of drug loading and this decreases their affinity for cellular targets.[33] Unusually apoferritin does not need modification in order to encapsulate the drug, as this can be controlled through pH. At low pH the subunits dissociate. When the pH is increased to near neutral they then reform the cage, entrapping any material in solution.[33, 34] Apoferritin has been shown to be useful in the synthesis of magnetic nanoparticles of cobalt, nickel and palladium with the metal(II) ions binding to the inner wall of apoferritin and subsequently reduced to metal(0) which can give rise to the nucleation of a metal nanoparticle, Figure 6.4.[35] The ability to synthesise and encapsulated magnetic nanoparticles *in situ* may also allow apoferritin to have a dual function as both a targeting group and a delivery vehicle. The ferritin binding sites and endocytosis of ferritin have been observed in cancer cells and some studies have shown this strategy may have potential in targeting anticancer drugs to the brain.[33, 34]

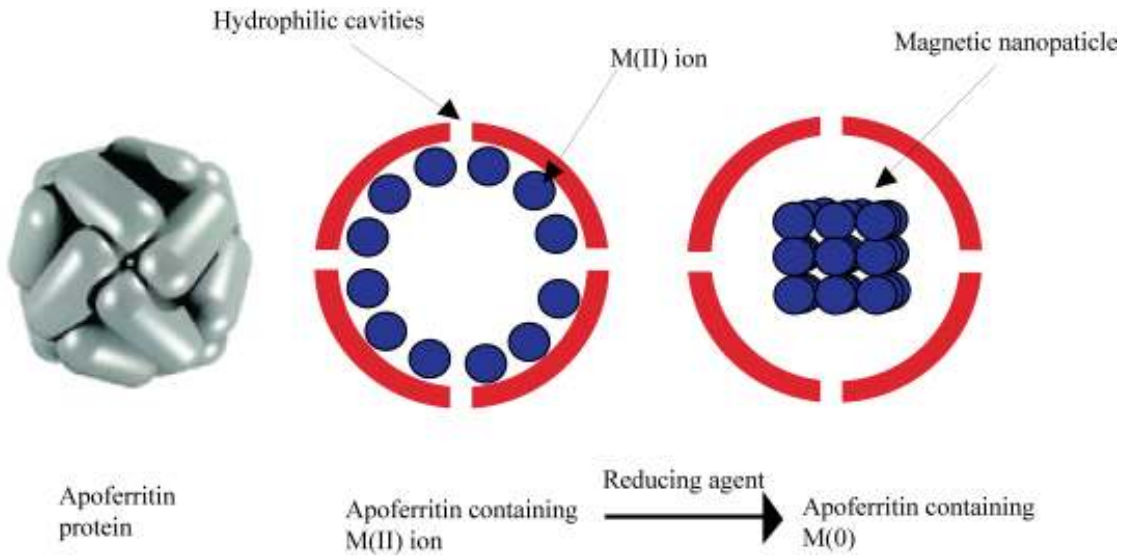

Figure 6.4 The protein structure and cavity of apoferritin and the synthesis of magnetic nanoparticles using apoferritin.[35]

Apoferritin has been studied for the encapsulation and delivery of the three major platinum drugs: cisplatin, carboplatin and oxaliplatin.[34] The drug contained within apoferritin-cisplatin complexes has been shown to be taken up at much higher levels than free cisplatin in pheochrimicytoma cells, PC12, and this indicates that the apoferritin-cisplatin complex may be internalised more readily by tumour cells.[34] This complex was shown to have a lower cytotoxic effect than free cisplatin. The cytotoxic effect of the complexes was observed gradually and continued to increased over time which contrasts with cisplatin as this acts rapidly and achieves maximum inhibition after 48 h.[34]

6.7 Folic Acid

The folate receptor, FR, is a glycosyl-phosphatidylinositol linked membrane protein which is expressed in limited quantities in normal tissue but overexpressed in malignant cells.[36] There are three isoforms of the folate receptor, FR-α, FR-β and FR-γ, and studies have shown that FR-α has a much greater affinity for the major serum folate, N^5-methyltetrahydrofolate, and as such, is considered the more efficient receptor for folate uptake.[37, 38] The three isoforms have specific binding and tissue distributions, however, the expression of FR- α is restricted in normal cells whilst present in high quantities in many cancers of epithelial origin.[38] The FR receptor is a suitable target for directed chemotherapy because it is upregulated in a number of cancers, including: ovarian, breast and brain cancers, and the expression of the receptor increases as the disease progresses.[39]

Folic acid, Figure 6.5, and its structurally related analogues, which have the same biochemical activity, are generally referred to as folate although this specifically relates to the deprotonated form of the molecule. Folate is involved in one carbon transfer reactions during the synthesis and replication of DNA.[38] They are also important in a number of cellular processes including: division, growth and survival and are particularly important for rapidly dividing cells, such as tumour cells.[38] Folic acid has been shown to retain receptor binding capability when conjugated with macromolecules when linked through the γ-carboxyl group.[40]

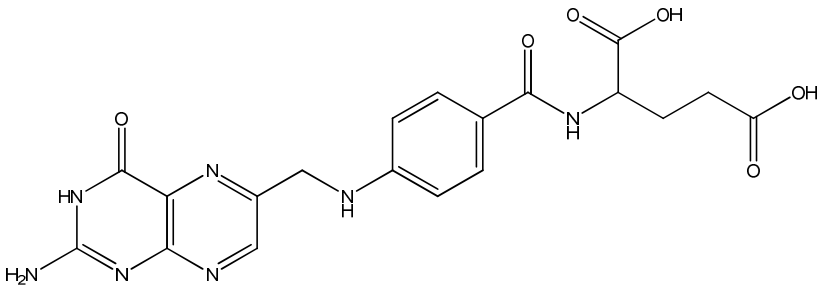

Figure 6.5 The structure of folic acid.

In the synthesis of drug complexes directed towards the FR, the folate is often not directly attached to the drug itself but through a linker, such as polyethylene glycol.[41, 42] In a study by Schroeder *et al*., quantum dots used for fluoresence tagging of tumour cells were encapsulated in phospholipids to form a stable nanoparticle and subsequently conjugated to a PEG-folate complex.[41] The final folate nanoparticle and its non-folate derivative were then tested *in vitro* against J6456-FR lymphoma cells, human nasopharyngeal epidermoid carcinoma KB-FR cells and non-FR expressing C26 colon cancer cells. Fluoresence was observed only in the cells which had been incubated with the folate targeted nanoparticle.[41] The same complexes were then tested *in vivo* against mice previously been injected with J6456-FR cells. The mice treated with the folate targeted nanoparticle displayed fluorescence in 80-90% of cells harvested whilst only 5-12% of cells from mice treated with the non-folate targeted nanoparticle displayed any fluoresence.[41]

Another study by Pinhassi *et al*. used ethylenediamine and tetra-peptide linkers to conjugate methotrexate, an anticancer drug based on the structure of folic acid, to a polysaccharide which was further conjugated to folic acid propylamine.[39] The presence of folic acid allows the polymer to target the folic acid receptor without losing the activity of the methotrexate. The folate-methotrexate polysaccharide was then incubated *in vitro* to determine if a complex based on the polysaccharide and folic acid could be specifically targeted to CHO-AA8-C5-FRα cells, Chinese hamster ovary derived cells that over express the FRα receptor.[39] The complexes were shown to be selectively taken up in the FRα cells, compared to the parent CHO-AA8-C5 cells, however, only the complex conjugated to the methotrexate via the tetra-peptide linker showed cytotoxicity.[39]

Studies have also been carried out in order to enhance the selectivity of established cancer drugs such as doxorubicin, paclitaxel and platinum drugs. Jhaveri *et al*. used antisense oligonucleotides, complementary to FRα, in order to sensitise MDA-MB-435

breast cancer cells to doxorubicin.[43] The results of this study that showed a 5-fold increase in the cells sensitivity to doxorubicin could be achieved using the oligonucleotide.[43] This study highlighted alternative routes of using the FRα receptor as a means of targeted therapy *i.e*. without including folate in the complex structure. Another study involving folate-based targeting of doxorubicin was carried out by Lee and Low using doxorubicin encapsulated in liposomes with a PEG spacer between the liposome and folic acid.[44] The liposomal doxorubicin was shown to selectively target the folate receptor *in vitro* when tested against KB cells.[44] A 40-fold increase was observed in the uptake of doxorubicin when the folate targeting moiety was introduced and this also represented an increase of 1.6-fold over free doxorubicin.[44] The cytotoxicity of doxorubicin was also increased when the folate targeting group was conjugated to the liposomes; the cytotoxicity of the targeted liposomal doxorubicin was 86-fold greater than the non-targeted and 2.7-fold greater than free doxorubicin.[44] In the same study, co-cultures of HeLa and W138 cells showed exclusive uptake of the folate targeted liposomal doxorubicin in the HeLa, cells which over express the FR receptor.[44]

Lee *et al*. carried out a study using the drug paclitaxel conjugated to folate in order to increase the efficacy of the drug.[45] Although the complexes used in their study retained binding affinity towards the receptor and exhibited lower toxicity than free paclitaxel, they failed to demonstrate selective killing of cells *in vitro* or improve the cytotoxicity of the drug *in vivo* when given at an equimolar dose.[45] Aronov et al explored the use polyethylene glycol (PEG), with a folate targeting group, as the carrier ligand for the platinum anticancer drug carboplatin.[46] PEG linker with the folic acid was introduced into the carboplatin structure in place of cyclobutane ring, Figure 6.6. The PEG was used to increase the time the drug is available in the blood which should in turn increase uptake by the tumour.[46] The folate targeting group was included in the structure to enhance the permeability of the drug after conjugation with the PEG which has previously been shown to be detrimental to permeation.[46]

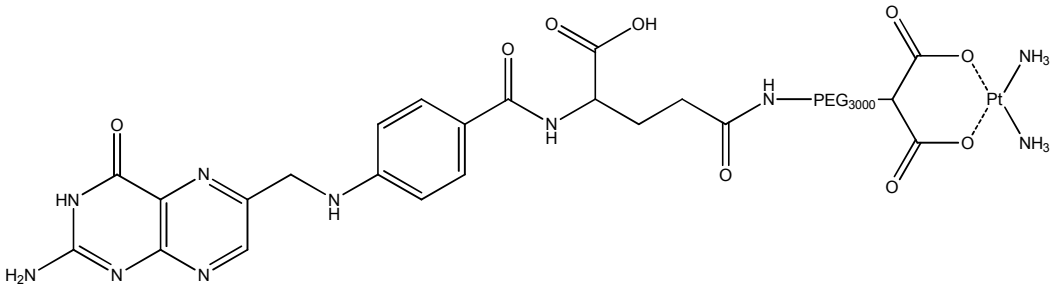

Figure 6.6 The structure of the folic acid-PEG-Pt complex used in the study by Aronov *et al*.[46]

Two PEG-folic acid conjugates were synthesised, FA-PEG-Pt and FA-PEG-FITC (Fluorescein isothiocyanate). The FA-PEG-FITC complex was used to determine if, by targeting the folate receptor, receptor mediated endocytosis could be used to overcome the decreased permeability of PEG complexes.[46] The complex was tested *in vitro* against folate receptor rich M109 lung cancer cells and the targeted PEG complex was shown to be taken up 3-fold more efficiently than the untargeted equivalent complex, PEG-FITC.[46] The FA-PEG-Pt complex was used to determine if increased cellular uptake improved the activity of the drug.[46] It was shown that whilst more of the FA-PEG-Pt complex was taken up by the FR expressing cells, the cytotoxic effect was lower by a factor of 1.7 than PEG-Pt. Further examination of the DNA adducts formed by the complexes showed that more adducts were formed by the PEG-Pt than the FA-PEG-Pt.[46] This was explained as a result of the folate receptor endocytosis process where the folate conjugates are not released into the cytosol but rather are directed to acidic vesicles. Release from these vesicles may be slow and inefficient resulting in less of the drug being available to form DNA adducts.[46]

Folate targeting groups have also been used in conjunction with delivery vehicles to construct complexes which can exploit both active and passive targeting mechanisms. Folate has been coupled, via a PEG linker, to a platinum(IV) complex that has also been conjugated to the surface of carbon nanotubes.[47] The resulting complex was shown to specifically target FR enriched cells and was also shown to be 8.6-fold more active than

cisplatin following intracellular reduction to platinum(II).[47] Folate has also be coupled, again via a PEG linker, to self-assembling amphiphilic block copolymers which are then used to form polymeric micelles with encapsulated adriamycin.[48] The concept behind this complex was to target the folate receptor expressing cells to increase the uptake of the micelle. Once in the cell localised pH is used to trigger the release of the encapsulated adriamycin.[48] The complex was tested *in vitro* and it was found that the complex was selectively taken up by KB cells and that increased cellular uptake resulted in enhanced growth inhibition of the drug.[48]

The use of folate targeted PAMAM dendrimers has also been studied and Quintana *et al* showed that coupling a small number, on average 2-3, folic acid groups to the dendrimer achieved significant internalisation.[49] Wiener *et al* also used folate to target a G4 PAMAM dendrimer conjugated to an MRI contrast agent, gadolinium(III). The observed fluoresence of FR positive cells increased dramatically after incubation with the complexes, reaching 378% after 1 minute and 648% after 30 minutes.[50] When incubated with FR negative cells no fluoresence was observed.[50]

6.8 Aims

The aim of this section of the thesis was to use folic acid as an active targeting agent on PAMAM dendrimers. This was to be achieved through conjugation of folic acid to the PAMAM dendrimer complexes prepared in section 1 via a suitable linker group. The resultant complexes were analysed to quantify the number of folic acid groups bound to the dendrimer as well the maximum number of platinum molecules which can be conjugated in the presence of the folic acid. The complexes were then tested *in vitro* against A2780 and A2780cis cells, grown in the absence of folic acid to increase the number of folic acid receptors available for binding, and to determine if the activity of the complexes can be increased through the inclusion of the folic acid group.

6.9 References

1. Byrne, J. D.; Betancourt, T.; Brannon-Peppas, L. Active targeting schemes for nanoparticle systems in cancer therapeutics. *Adv. Drug. Deliver. Rev.* **2008,** 60, 1615-1626.

2. Kirpotin, D. B.; Drummond, D. C.; Shao, Y.; Shalaby, M. R.; Hong, K.; Nielsen, U. B.; Marks, J. D.; Benz, C. C.; Park, J. W. Antibody Targeting of Long-Circulating Lipidic Nanoparticles Does Not Increase Tumor Localization but Does Increase Internalization in Animal Models. *Cancer Res.* **2006,** 66, 6732-6740.

3. Song, H.; He, R.; Wang, K.; Ruan, J.; Bao, C.; Li, N.; Ji, J.; Cui, D. Anti-HIF-1[alpha] antibody-conjugated pluronic triblock copolymers encapsulated with Paclitaxel for tumor targeting therapy. *Biomaterials* 31, 2302-2312.

4. Danhier, F.; Feron, O.; Préat, V. To exploit the tumor microenvironment: Passive and active tumor targeting of nanocarriers for anti-cancer drug delivery. *J. Control. Release* 148, 135-146.

5. Plate, K. H.; Breier, G.; Weich, H. A.; Risau, W. Vascular endothelial growth factor is a potential tumour angiogenesis factor in human gliomas in vivo. *Nature* **1992,** 359, 845-848.

6. Nisato, R.; Tille, J.-C.; Jonczyk, A.; Goodman, S.; Pepper, M. αv β 3 and αv β 5 integrin antagonists inhibit angiogenesis in vitro. *Angiogenesis* **2003,** 6, 105-119.

7. Radinsky, R.; Risin, S.; Fan, D.; Dong, Z.; Bielenberg, D.; Bucana, C. D.; Fidler, I. J. Level and function of epidermal growth factor receptor predict the metastatic potential of human colon carcinoma cells. *Clin. Cancer Res.* **1995,** 1, 19-31.

8. Ulbrich, K.; Hekmatara, T.; Herbert, E.; Kreuter, J. Transferrin- and transferrin-receptor-antibody-modified nanoparticles enable drug delivery across the blood-brain barrier (BBB). *Eur. J. Pharm. Biopharm.* **2009,** 71, 251-256.

9. Etrych, T.; Strohalm, J.; Kovár, L.; Kabesová, M.; Ríhová, B.; Ulbrich, K. HPMA copolymer conjugates with reduced anti-CD20 antibody for cell-specific drug targeting. I. Synthesis and in vitro evaluation of binding efficacy and cytostatic activity. *J. Control. Release* **2009,** 140, 18-26.

10. Ruiz-Sánchez, P.; Mundwiler, S.; Spingler, B.; Buan, N. R.; Escalante-Semerena, J. C.; Alberto, R. Syntheses and characterization of vitamin B_{12}-Pt(II) conjugates and their adenosylation in an enzymatic assay. *J. Biol. Inorg. Chem.* **2008,** 13, 335-347.

11. Ríhová, B.; Jelínková, M.; Strohalm, J.; Subr, V.; Plocová, D.; Hovorka, O.; Novák, M.; Plundrová, D.; Germano, Y.; Ulbrich, K. Polymeric drugs based on conjugates of synthetic and natural macromolecules.: II. Anti-cancer activity of antibody or (Fab')2-targeted conjugates and combined therapy with immunomodulators. *J. Control. Release* **2000,** 64, 241-261.

12. Wagner, S.; Rothweiler, F.; Anhorn, M. G.; Sauer, D.; Riemann, I.; Weiss, E. C.; Katsen-Globa, A.; Michaelis, M.; Cinatl Jr, J.; Schwartz, D.; Kreuter, J.; von Briesen, H.; Langer, K. Enhanced drug targeting by attachment of an anti [alpha]v integrin antibody to doxorubicin loaded human serum albumin nanoparticles. *Biomaterials* 31, 2388-2398.

13. Barth, B. M.; Sharma, R.; Altino glu, E.; Morgan, T. T.; Shanmugavelandy, S. S.; Kaiser, J. M.; McGovern, C.; Matters, G. L.; Smith, J. P.; Kester, M.; Adair, J. H. Bioconjugation of Calcium Phosphosilicate Composite Nanoparticles for Selective Targeting of Human Breast and Pancreatic Cancers In Vivo. *ACS Nano* **2010,** 4, 1279-1287.

14. Li, R.; Wu, R. a.; Zhao, L.; Wu, M.; Yang, L.; Zou, H. P-Glycoprotein Antibody Functionalized Carbon Nanotube Overcomes the Multidrug Resistance of Human Leukemia Cells. *ACS Nano* 4, 1399-1408.

15. Thomas, A. C.; Campbell, J. H. Conjugation of an antibody to cross-linked fibrin for targeted delivery of anti-restenotic drugs. *J. Control. Release* **2004,** 100, 357-377.

16. Jaracz, S.; Chen, J.; Kuznetsova, L. V.; Ojima, I. Recent advances in tumor-targeting anticancer drug conjugates. *Bioorg. Med. Chem.* **2005,** 13, 5043-5054.

17. Molema, G.; Meijer, D. K. F. Targeting of drugs to various blood cell types using (neo-)glycoproteins, antibodies and other protein carriers. *Adv. Drug Deliver. Rev.* **2008,** 14, 25-50.

18. Proske, D.; Blank, M.; Buhmann, R.; Resch, A. Aptamers - basic research, drug development and clinical applications. *Appl. Microbiol. Biotech.* **2005,** 69, 367-374.

19. Ireson, C. R.; Kelland, L. R. Discovery and development of anticancer aptamers. *Mol. Cancer Ther.* **2006,** 5, 2957-2962.

20. Huang, Y.-F.; Shangguan, D.; Liu, H.; Phillips, J. A.; Zhang, X.; Chen, Y.; Tan, W. Molecular assembly of an aptamer-drug conjugate for targeted drug delivery to tumor cells. *ChemBioChem* **2009,** 10, 862-868.

21. Farokhzad, O. C.; Cheng, J.; Teply, B. A.; Sherifi, I.; Jon, S.; Kantoff, P. W.; Richie, J. P.; Langer, R. Targeted nanoparticle-aptamer bioconjugates for cancer chemotherapy *in vivo*. *Proc. Natl. Acad. Sci. U.S.A* **2006,** 103, 6315-6320.

22. Lee, J. H.; Yigit, M. V.; Mazumdar, D.; Lu, Y. Molecular diagnostic and drug delivery agents based on aptamer-nanomaterial conjugates. *Adv. Drug Deliver. Rev.* **2010,** 62, 592-605.

23. Shadidi, M.; Sioud, M. Selective targeting of cancer cells using synthetic peptides. *Drug Resist. Update.* **2003,** 6, 363-371.

24. Vivès, E.; Schmidt, J.; Pèlegrin, A. Cell-penetrating and cell-targeting peptides in drug delivery. *BBA Rev. Cancer* **2008,** 1786, 126-138.

25. Temsamani, J.; Vidal, P. The use of cell-penetrating peptides for drug delivery. *Drug Discov. Today* **2004,** 9, 1012-1019.

26. Dharap, S. S.; Wang, Y.; Chandna, P.; Khandare, J. J.; Qiu, B.; Gunaseelan, S.; Sinko, P. J.; Stein, S.; Farmanfarmaian, A.; Minko, T. Tumor-specific targeting of an anticancer drug delivery system by LHRH peptide. *Proc. Natl. Acad. Sci. U.S.A* **2005,** 102, 12962-12967.

27. Prakash, J.; de Jong, E.; Post, E.; Gouw, A. S. H.; Beljaars, L.; Poelstra, K. A novel approach to deliver anticancer drugs to key cell types in tumors using a PDGF receptor-binding cyclic peptide containing carrier. *J. Control. Release* 145, 91-101.

28. Damian, M. S.; Hedman, H. K.; Elmroth, S. K. C.; Diederichsen, U. Synthesis and DNA Interaction of Platinum Complex/Peptide Chimera as Potential Drug Candidates. *Eur. J. Org. Chem.* **2010,** 2010, n/a-n/a.

29. Ott, I.; Gust, R. Preclinical and clinical studies on the use of platinum complexes for breast cancer treatment. *Anti-Cancer Agents Med. Chem.* **2007,** 7, 95-110.

30. Gagnon, V.; St-Germain, M.-E.; Descoteaux, C.; Provencher-Mandeville, J.; Parent, S.; Mandal, S. K.; Asselin, E.; Berube, G. Biological evaluation of novel estrogen-platinum(II) hybrid molecules on uterine and ovarian cancers-molecular modeling studies. *Bioorg. Med. Chem. Lett.* **2004,** 14, 5919-5924.

31. Perron, V.; Rabouin, D.; Asselin, E.; Parent, S.; C.-Gaudreault, R.; Berube, G. Synthesis of 17B-estradiol-linked platinum(II) complexes and their cytocidal activity on estrogen-dependent and -independent breast tumor cells. *Bioorg. Chem.* **2005,** 33, 1-15.

32. Provencher-Mandeville, J.; Descôteaux, C.; Mandal, S. K.; Leblanc, V.; Asselin, E.; Bérubé, G. Synthesis of 17beta-estradiol-platinum hybrid molecules showing cytotoxic activity on breast cancer cell lines. *Bioorg. Med. Chem. Lett.* **2008,** 18, 2282-2287.

33. Yang, Z.; Wang, X.; Diao, H.; Zhang, J.; Li, H.; Sun, H.; Guo, Z. Encapsulation of platinum anticancer drugs by apoferritin. *Chem. Commun.* **2007**, 3453-3455.

34. Xing, R.; Wang, X.; Zhang, C.; Zhang, Y.; Wang, Q.; Yang, Z.; Guo, Z. Characterization and cellular uptake of platinum anticancer drugs encapsulated in apoferritin. *J. Inorg. Biochem.* **2009,** 103, 1039-1044.

35. Galvez, N.; Sanchez, P.; Dominguez-Vera, J. M.; Soriano-Portillo, A.; Clemente-Leon, M.; Coronado, E. Apoferritin-encapsulated Ni and Co superparamagnetic nanoparticles. *J. Mater. Chem.* **2006,** 16, 2757-2761.

36. Weitman, S. D.; Lark, R. H.; Coney, L. R.; Fort, D. W.; Frasca, V.; Zurawski, V. R.; Kamen, B. A. Distribution of the folate receptor GP38 in normal and malignant cell lines and tissues. *Cancer Res.* **1992,** 52, 3396-3401.

37. Ross, J. F.; Chaudhuri, P. K.; Ratnam, M. Differential regulation of folate receptor isoforms in normal and malignant tissues in vivo and in established cell lines. *Cancer* **1994,** 73, 2432-2443.

38. Kelemen, L. E. The role of folate receptor alpha in cancer development, progression and treatment: Cause, consequence or innocent bystander? *Int. J. Cancer* **2006,** 119, 243-250.

39. Pinhassi, R. I.; Assaraf, Y. G.; Farber, S.; Stark, M.; Ickowicz, D.; Drori, S.; Domb, A. J.; Livney, Y. D. Arabinogalactanâˆ’Folic Acidâˆ’Drug Conjugate for Targeted Delivery and Target-Activated Release of Anticancer Drugs to Folate Receptor-Overexpressing Cells. *Biomacromolecules* **2009,** 11, 294-303.

40. Vyas, S. P.; Sihorkar, V. Endogenous carriers and ligands in non-immunogenic site-specific drug delivery. *Adv. Drug Deliver. Rev.* **2000,** 43, 101-164.

41. Schroeder, J. E.; Shweky, I.; Shmeeda, H.; Banin, U.; Gabizon, A. Folate-mediated tumor cell uptake of quantum dots entrapped in lipid nanoparticles. *J. Control. Rel.* **2007,** 124, 28-34.

42. Le Gourrierec, L.; Di Giorgio, C.; Greiner, J.; Vierling, P. Formulation of PEG-folic acid coated nanometric DNA particles from perfluoroalkylated cationic dimerizable detergents and in vitro folate-targeted intracellular delivery. *New J. Chem.* **2008,** 32, 2027-2042.

43. Jhaveri, M. S.; Rait, A. S.; Chung, K.-N.; Trepel, J. B.; Chang, E. H. Antisense oligonucleotides targeted to the human folate receptor inhibit breast cancer cell growth and sensitize the cells to doxorubicin treatment. *Mol. Cancer Ther.* **2004,** 3, 1505-1512.

44. Lee, R. J.; Low, P. S. Folate-mediated tumor cell targeting of liposome-entrapped doxorubicin in vitro. *Biochim. Biophys. Acta* **1995,** 1233, 134-144.

45. Lee, J. W.; Lu, J. Y.; Low, P. S.; Fuchs, P. L. Synthesis and Evaluation of Taxol-Folic Acid Conjugates as Targeted Antineoplastics. *Bioorg. Med. Chem.* **2002,** 10, 2397-2414.

46. Aronov, O.; Horowitz, A. T.; Gabizon, A.; Gibson, D. Folate-targeted PEG as a potential carrier for carboplatin analogs. Synthesis and in vitro studies. *Bioconjug. Chem.* **2003,** 14, 563-574.

47. Dhar, S.; Liu, Z.; Thomale, J.; Dai, H.; Lippard, S. J. Targeted single-walled carbon nanotube-mediated Pt(IV) prodrug delivery folate as a homing device. *J. Am. Chem. Soc.* **2008,** 130, 11467-11476.

48. Bae, Y.; Jang, W.-D.; Nishiyama, N.; Fukushima, S.; Kataoka, K. Multifunctional polymeric micelles with folate-mediated cancer cell targeting and pH-triggered drug releasing properties for active intracellular drug delivery. *Mol. Biosyst.* **2005,** 1, 242-250.

49. Quintana, A.; Raczka, E.; Piehler, L.; Lee, I.; Myc, A.; Majoros, I.; Patri, A. K.; Thomas, T.; Mule, J.; Baker, J. R. Design and function of a dendrimer-based therapeutic nanodevice targeted to tumor cells through the folate receptor. *Pharm. Res.* **2002,** 19, 1310-1316.

50. Wiener, E. C.; Konda, S.; Shadron, A.; Brechbiel, M.; Gansow, O. Targeting dendrimer-chelates to tumors and tumor cells expressing the high-affinity folate receptor. *Invest. Rad. Oncol.* **1997,** 32, 748-754.

Chapter 7: Folic acid targeted $\{Pt(NH_3)_2\}^{2+}$ and $\{Pt(R,R\text{-dach})\}^{2+}$ dendrimer-platinates

7.1 Introduction

Previous work has shown that the G3.5-6.5 PAMAM dendrimers can be successfully conjugated to the active components of both cisplatin and oxaliplatin. The G6.5 cisplatin dendimer-platinate complex was shown to be as active as free cisplatin at equimolar doses (6 mg/kg) *in vivo* and when the dendrimer complex is administered at higher doses (8 mg/kg) it is able to significantly retard tumour growth. Although these complexes exhibit greater cytotoxicity *in vivo* than the maximum tolerated dose of cisplatin the toxicity is comparable to cisplatin. In order to reduce the toxicity of the dendrimer platinate complexes it is proposed to target the folate receptor over expressed in cancer cells. This will be achieved by using folic acid coupled to the surface of the dendrimer via a 1,6-diaminohexane linker region, Figure 7.1.

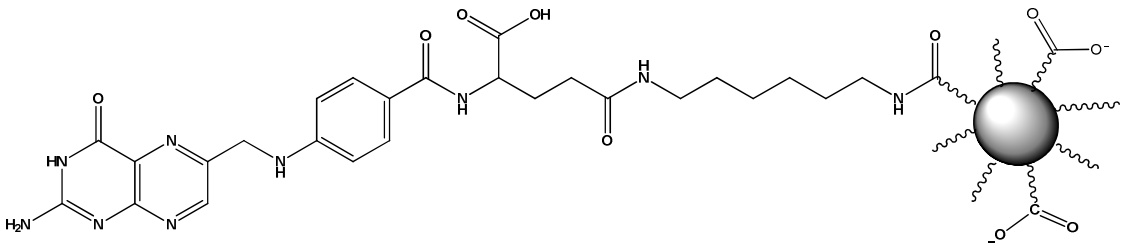

Figure 7.1 The proposed structure of the targeted dendrimer complexes.

7.2 Results and discussion

7.2.1 Synthesis of folic acid linker

In order to obtain the folic acid linked dendrimer it is first necessary to couple the 1,6-diaminohexane to the folic acid, Figure 7.2. The diamine is useful as a linker as it enables bis-amide bond formation with both the folic acid and the dendrimer surface groups. In order to facilitate the amide bond formation the coupling agent propylphosphonic anhydride (T3P) was used, Scheme 7.1.

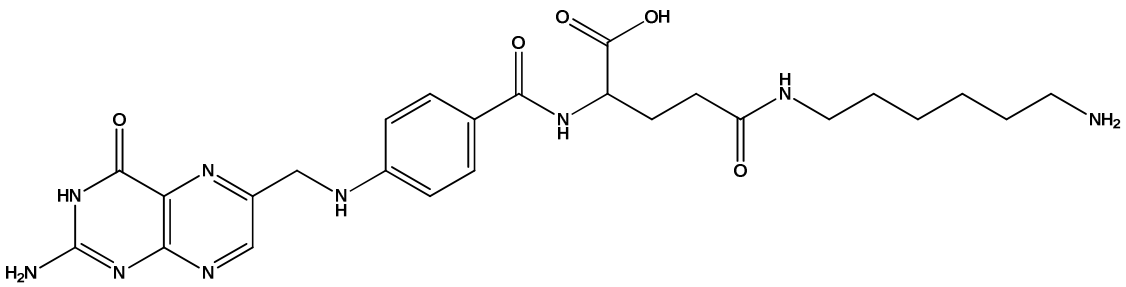

Figure 7.2 The structure of the folic acid linker required for coupling to the dendrimer.

Wissmann and Kleiner originally reported T3P as a coupling agent in 1980 and the lack of insoluble by-products, such as those that form with carbodiimides, and the high yields associated with it's use make this an ideal coupling agent for this reaction.[1] T3P activates the carboxylate of the acid, in this reaction the carboxylate group of the folic acid, which acts as good leaving group. The carboxyl carbon is then subjected to nucleophilic attack from the amine which results in the formation of the amide bond, water, and water soluble by-products, Scheme 7.1.

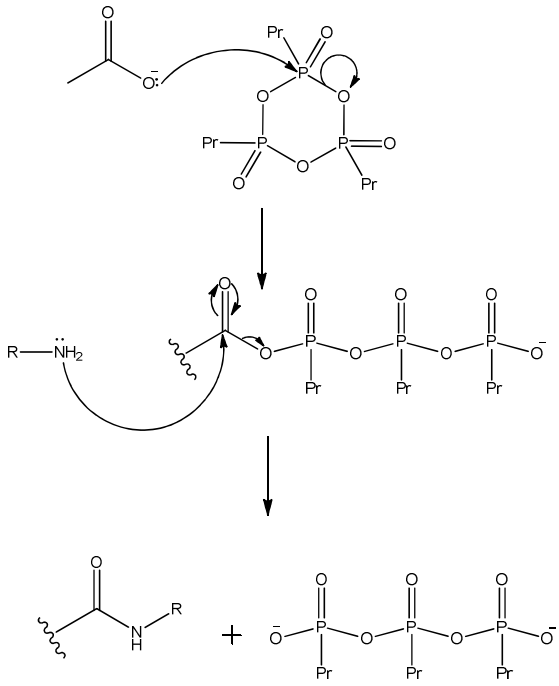

Scheme 7.1 The general mechanism for the formation of amide bonds using T3P.

Folic acid was dissolved in DMF, in an inert atmosphere, along with 1 mol. equivalent of the diamine and 2.5 mol. equivalents of TEA, to deprotonate the folic acid. The resultant solution was cooled to 0 ^{o}C for at which stage 1.2 mol. equivalents of T3P was added drop wise and then stirred for a further two days. The solution was slowly heated to room temperature and the coupling reaction quenched through addition of water. The product precipitated as an orange solid whilst the water soluble by-products and impurities remained in solution. The solid was then collected by filtration, and air dried. The product exhibited limited solubility, therefore analysis proved difficult. The ^{1}H NMR of both folic acid and the folic acid linker, Figure 7.3, shows the inclusion of the alkyl protons following the coupling reaction; a slight upfield shift of the amine proton at approx 8.3 ppm as well as the appearance of another peak in the same region. The data from the NMR spectra is suggestive of the successful formation of the desired product, however the isolated product is most likely a mixture of amine conjugated to the γ and α carboxyl groups.

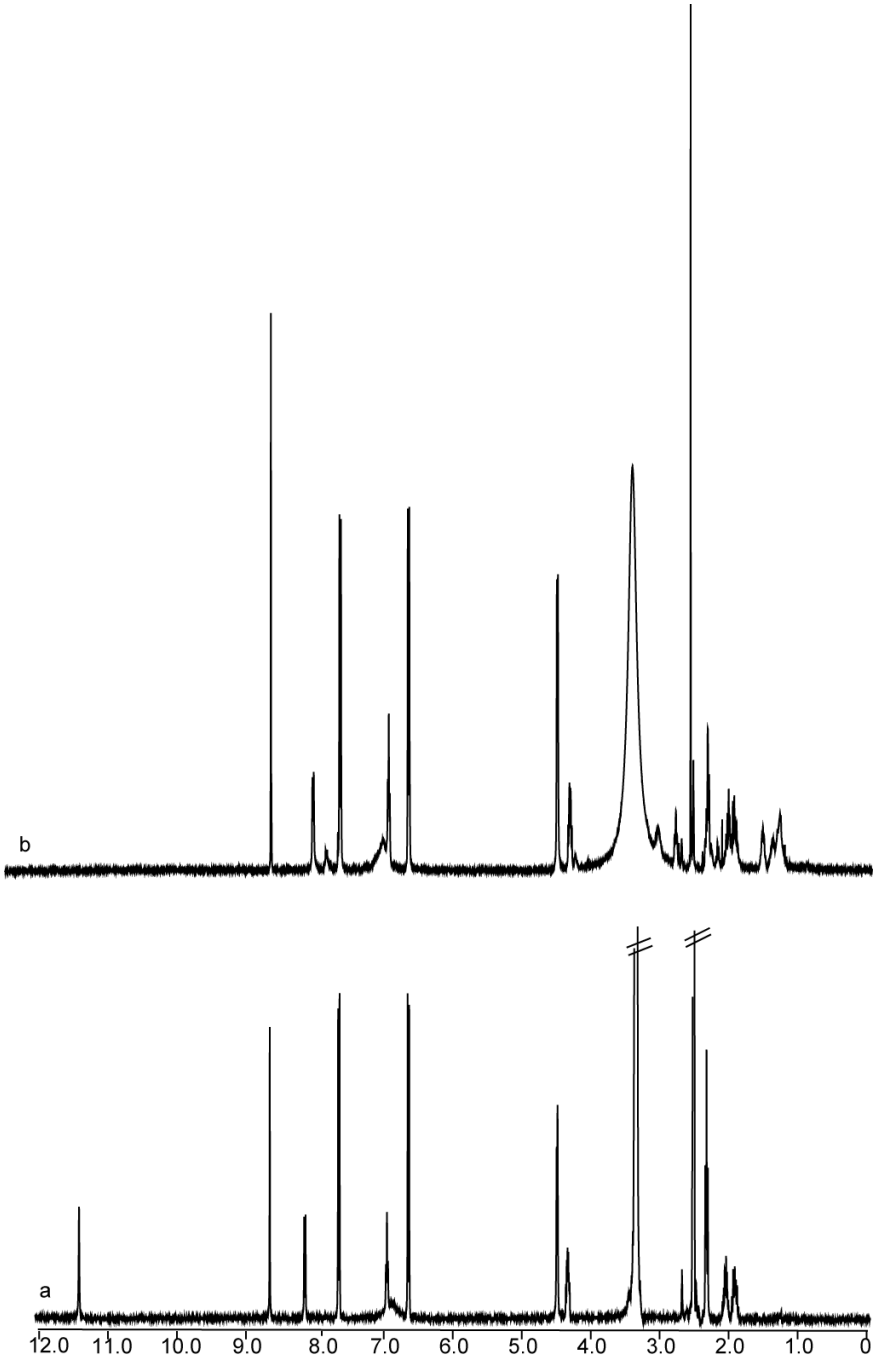

Figure 7.3 The ^{1}H NMR spectra for folic acid and the folic acid linker dissolved in DMSO at 400 MHz.

7.2.2 Synthesis of folic acid targeted dendrimers

Due to the presence of the remaining free amine on the linker it is possible to utilise the same coupling technique conjugate the FA-linker to the dendrimer carboxylates, scheme 7.1. To achieve maximum folate receptor coupling it is desirable to have as many of the linker groups attached to the dendrimer as possible without preventing the platinum drugs from binding at a later stage. It was decided that ten linker groups, regardless of dendrimer generation, would be the optimum number as the flexibility within the spacer region would allow maximum spatial coverage; ensuring that at least one folic acid group was in close proximity to the receptor. The length of the spacer region also means that the bulk of the FA-linker structure is far enough from the surface of the dendrimer to allow the platinum to bind. This is more important in the larger dendrimers where the branches are much closer together and a bulky FA group could block several binding sites if close to the dendrimer surface.

The dendrimers were dissolved in anhydrous DMF, in an inert atmosphere, with 10 mol equivalents of the folate linker and 256- 2048 mol. equivalents of TEA. The solution was then cooled to 0 ^{o}C and 1.2 mol. equivalents of T3P added dropwise before the solution was allowed to stir at low temperatures for one week. The solution was then allowed to come to room temperature and water added to quench the reaction. The solution was diluted to 300 mL, to ensure compatibility with the Viva spin columns, as DMF > 5% v/v dissolves the membrane of the column, then purified by centrifuge. The solution containing the dendrimer with the folic acid was then centrifuged twice more with 1 mL of D_2O with and the ^{1}H NMR recorded, Figure 7.4.

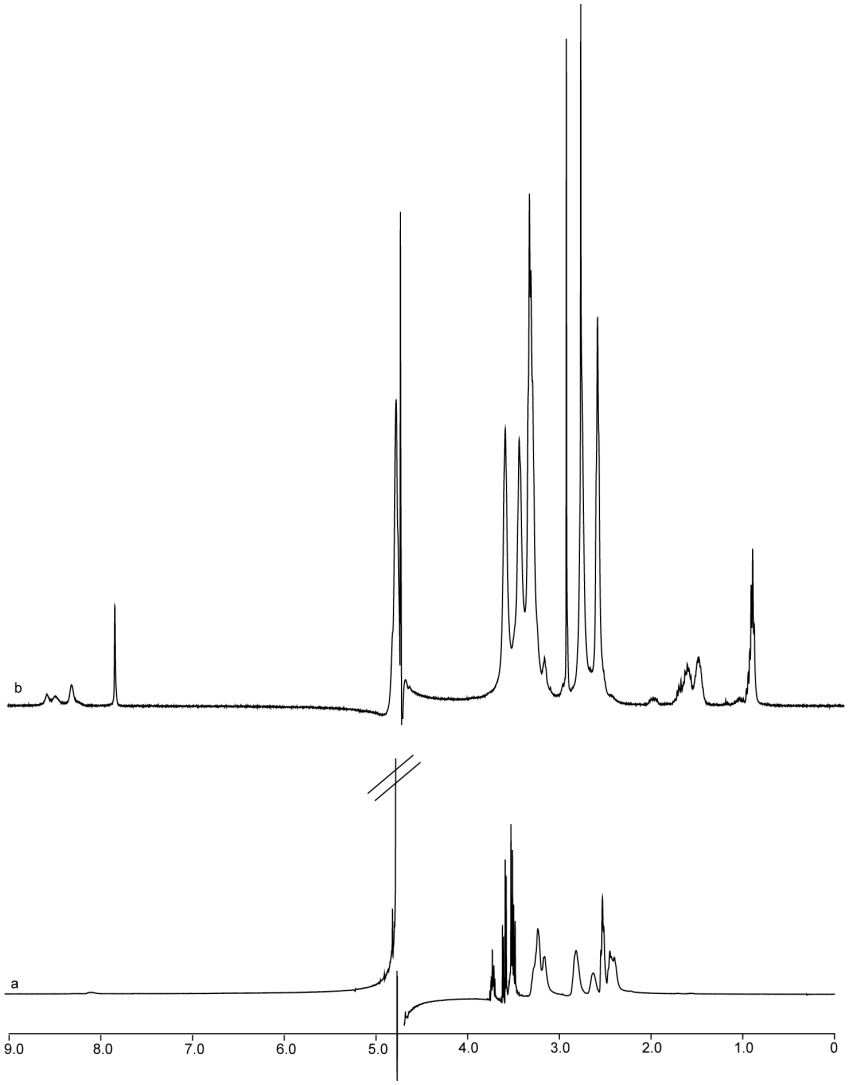

Figure 7.4 The ^{1}H NMR of the free G5.5 dendrimer and folic acid linker bound dendrimer.

The peaks of the FA-linker can be seen in the proton NMR spectrum between approx 7.9 and 8.6 ppm. The alkyl protons from the spacer region are also clearly visible in the NMR spectrum and occur at approx 1.5 – 2 ppm. The spectra above are similar to those present by Zhang *et al*. during their development of a folic acid conjugated G5 amine terminated PAMAM dendrimer, with the main difference arising in the aliphatic region due to the additional spacer group resonances.[2]

In order to quantify the number of folic acid groups present on the dendrimer it is possible to use UV-visible spectroscophotometry. The three aromatic rings within the pteroic acid section of the folic acid structure results in the linker absorbing strongly in the U.V. region and the U.V. profile, coupled with a suitable calibration curve, can be used to quantify the number of linker units, Figure 7.5.

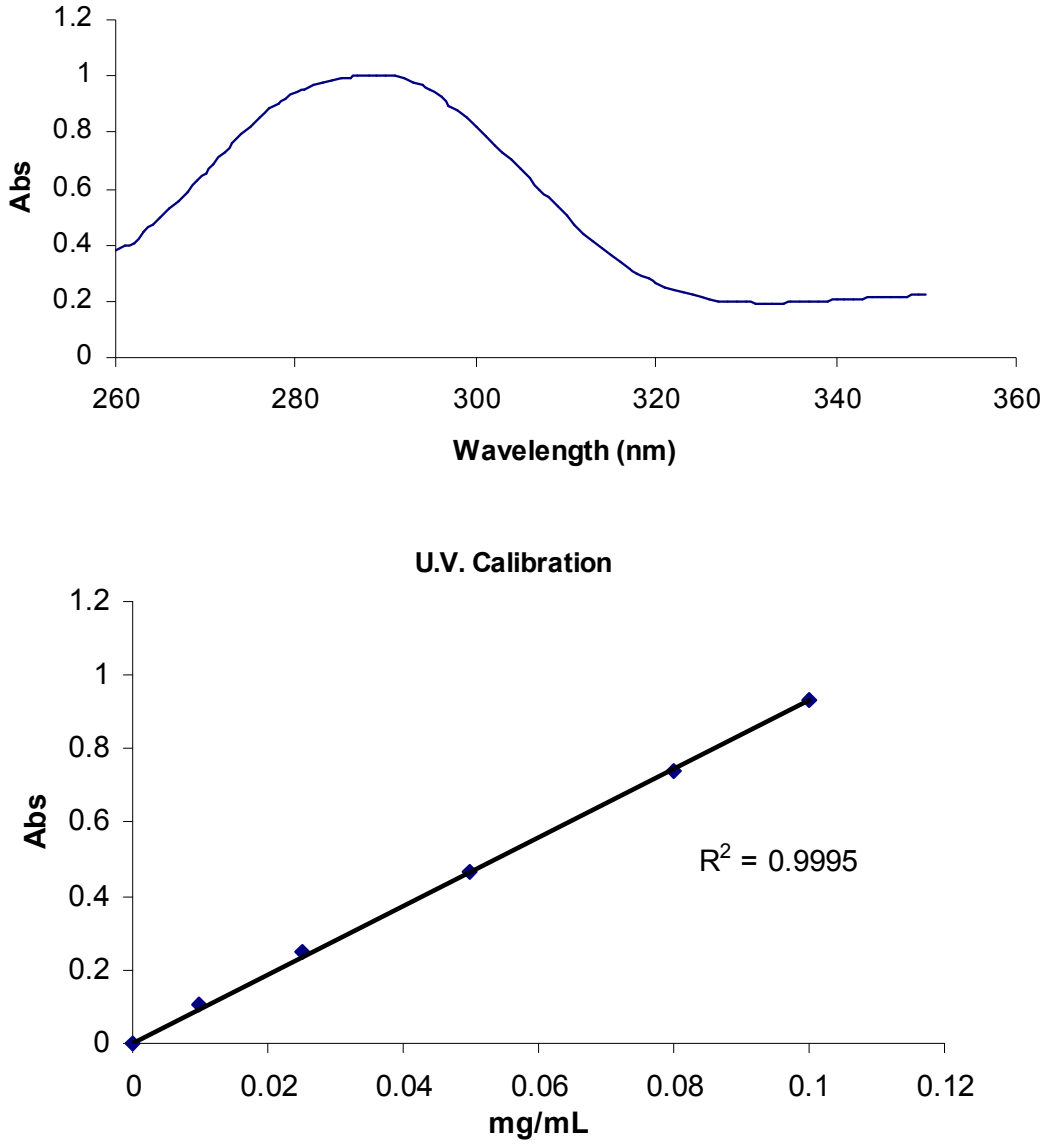

Figure 7.5 The U.V. profile of the linker (top) and the calibration curve (bottom) used for the quantification of the number of folate groups attached to the dendrimer.

Two sets of calibration standards were prepared initially in DMSO. The first set contained only the linker whilst the second set contained the linker along with the dendrimer, without being coupled, in order to determine what effect the dendrimer may have on the U.V. profile. The resulting profiles for both sets of standards were the same, indicating that the dendrimer does not affect the U.V. properties of the linker. Samples of all the dendrimer-folates were dissolved in DMSO to 10 mL and the U.V. absorbance recorded and used to determine the number of conjugated folic acid groups, Table 7.1.

Table 7.1: Quantification of bound folic acid linkers to the dendrimers.

Dendrimer	Number of folic acid groups
G3.5	4 ± 1
G4.5	5 ± 2
G5.5	8 ± 1
G6.5	8 ± 1

The results from the U.V. analysis provide further evidence to suggest the successful coupling of the linker to the dendrimer. A similar study by Ki Choi *et al*. conjugated folic acid to a G5 PAMAM-glutaric acid dendrimer via a ethylenediamine linker and they found that they could achieve eight folic acid groups per dendrimer structure which is similar to the results obtained for our work.[3] The folic acid targeted complex synthesised by Ki Choi *et al.* showed increased binding to cells which over express the folate receptor, compared to the non-targeted dendrimer complex, which suggests the number of folic acid linkers on our complex is sufficient to target the receptor.[3]

In order to determine if the introduction of the folate targeting group into the structure of the dendrimer-platinates increased their cytotoxicity; the $\{Pt(NH_3)_2\}^{2+}$ and $\{Pt(R,R\text{-dach})\}^{2+}$ dendrimer-complexes were incubated with the A2780 and A2780cis ovarian

cancer cell lines. In addition to their *in vitro* cytotoxicity the uptake of the drugs into the cells was measured by ICP-MS.

Studies by Brouwers *et al* have previously shown that it is possible to measure the retention of platinum within cells through ICP-MS.[4] The technique developed in this study can be applied to the dendrimer-platinates in order to determine if the folate targeting group is capable of increasing the platinum uptake of the cancer cells. The cells were therefore incubated overnight in RPMI at 37 ^{o}C and an atmosphere containing 10% CO_2 in air. The medium was then replaced with fresh medium or medium containing cisplatin, [Pt(*R,R*-dach)$(OH_2)_2$], non-targeted dendrimer-platinates or the folate targeted dendrimer-platinates. The cells were then incubated for a further 2 h or 4 h before the medium was removed and the cells washed with PBS and then lysed with nitric acid. The cells were then collected in a microfuge tube and incubated overnight at 65 ^{o}C. The digest was then diluted 100-fold with ultrapure water and analysed by ICP-MS to determine platinum content.

The analysis of the cisplatin dendrimer-platinates, Table 7.2, show that dendrimers decrease the uptake of cisplatin when compared to the free drug. In all cases the IC_{50} values for the dendrimer-platinates were higher than that of the free drug in both the sensitive and resistant cell lines and this supports the fact that less platinum is in cells. The observed decrease in uptake is possibly due to the different mechanisms of uptake as endocytosis as required with the dendrimer-platinates may be slower than passive diffusion of the free drug. This is supported by the decrease in cytotoxicity observed for these complexes, section 2.2.5.

Table 7.2: The cytotoxicity and platinum uptake of cisplatin, cisplatin dendrimer-platinates and folate targeted dendrimer-platinates.

Sample	Uptake (ppb)		IC_{50} (μmol)		
	2 hrs	**4 hrs**	**A2780**	**A2780cis**	**Rf**
cisplatin	0.571	1.34	0.501	7.8	15.6
G3.5[$Pt(NH_3)_2$]	0.019	0.128	>100	>100	
G4.5[$Pt(NH_3)_2$]	0.123	0.265	>100	>100	
G5.5[$Pt(NH_3)_2$]	0.113	0.213	>100	>100	
G6.5[$Pt(NH_3)_2$]	0.407	0.849	48	>100	
G3.5FA[$Pt(NH_3)_2$]	4.55	6.7	11.1	55	4.95
G4.5FA[$Pt(NH_3)_2$]	0.627	0.803	21.1	>100	
G5.5FA[$Pt(NH_3)_2$]	2.56	2.88	41.1	>100	
G6.5FA[$Pt(NH_3)_2$]	0.334	0.358	>100	>100	

The uptake of platinum increases between 2 h and 4 h, however the increase is less pronounced in folate targeted dendrimer-platinates, Table 7.2. The total uptake of platinum from the dendrimer-platinates is increased by the addition of the folate targeting group as this allows for receptor mediated endocytosis which may be more efficient in delivering the platinum into the cell. More efficient uptake of platinum is supported by the increase in cytotoxicity observed with the folate targeted G3.5 dendrimer-platinate. In the non-targeted dendrimers the higher generation complexes proved to be more cytotoxic than the smaller generations. In the higher generation, folate-targeted complexes decreased cytotoxicity was observed and this may be due to inefficient release of the drug from the endosome.

The $\{Pt(R,R\text{-dach})\}^{2+}$ dendrimer-platinates were also analysed in the same way, Table 7.3. In contrast to the results observed with the cisplatin dendrimer-platinates, all of the

{Pt(*R,R*-dach)}$^{2+}$ dendrimer-platinates are more cytotoxic than the free drug. This is supported by the increased platinum content found for all of the dendrimer-platinate complexes. The folate targeted dendrimer-platinates showed a decrease in uptake compared to the free dendrimer-platinates, possibly as a result of the folate group interfering with the aggregation of the dendrimer-platinates, Part 3.2.2. This decrease in cellular uptake results in a decrease in cytotoxicity of the targeted complexes compared to the free complexes.

Table 7.3: The *in vitro* cytotoxicity, and cellular uptake, of platinum from the {Pt(*R,R*-dach)}$^{2+}$ dendrimer-platinates.

Sample	Uptake		IC_{50} (μmol)		
	2 hrs	**4 hrs**	**A2780**	**A2780cis**	**Rf**
{Pt(*R,R*-dach) $(OH_2)_2$}	0.112	0.221	1.82	28	15.4
G3.5[Pt(*R,R*-dach)]	2.64	3.25	0.164	2.27	13.8
G4.5[Pt(*R,R*-dach)]	7.04	7.89	0.031	0.468	15.1
G5.5[Pt(*R,R*-dach)]	1.04	1.22	0.368	4.41	12.0
G6.5[Pt(*R,R*-dach)]	5.9	7.53	0.55	0.69	1.3
G3.5FA[Pt(*R,R*-dach)]	0.729	0.807	0.9	6.76	7.5
G4.5FA[Pt(*R,R*-dach)]	0.563	0.872	0.291	4.65	16.0
G5.5FA[Pt(*R,R*-dach)]	0.278	0.27	3.94	24.4	6.2
G6.5FA[Pt(*R,R*-dach)]	0.431	0.552	1.34	10.7	8.0

The observed uptake of platinum increases over time, however there is increased variability in the results for the {Pt(*R,R*-dach)}$^{2+}$ dendrimer-platinates compared to the equivalent {Pt$(NH_3)_2$}$^{2+}$ complexes. The aggregation of {Pt(*R,R*-dach)}$^{2+}$ dendrimer-platinates is likely to cause some of the drug to be trapped in dendrimer aggregation pockets and therefore not released into the cell efficiently. It is also possible that the {Pt(*R,R*-dach)}$^{2+}$ binds to the free carboxylate group of the folate targeting group thus disrupting the receptor mediated endocytosis of the complexes.

7.3 Conclusions

Folic acid was coupled to 1,6-diaminohexane to produce a method of targeting folate receptor over expressed in cancer cells in order to increase the selective delivery of the dendrimer-platinates synthesised in Part 1. This targeting group was successfully coupled to the dendrimer-platinates and the resulting complexes were found to contain 4 – 8 targeting moieties depending on dendrimer size. The folate targeted dendrimer-platinates were then assessed for *in vitro* cytotoxicity and cellular uptake. The folate targeting group was shown to increase the uptake of platinum from the $\{Pt(NH_3)_2\}^{2+}$ dendrimer-platinates but resulted in a decrease in the uptake of platinum from the $\{Pt(R,R\text{-dach})\}^{2+}$ dendrimer-platinates. The targeted cisplatin dendrimer-platinates were shown to be more cytotoxic than the non-targeted complexes, however, the inverse was observed for the $\{Pt(R,R\text{-dach})\}^{2+}$ complexes.

7.3 References

1. Wissmann, H.; Kleiner, H.-J. New Peptide Synthesis. *Angew. Chem. Int. Ed.* **1980,** 19, 133-134.

2. Zhang, Y.; Thomas, T. P.; Desai, A.; Zong, H.; Leroueil, P. R.; Majoros, I. J.; Baker, J. R. Targeted Dendrimeric Anticancer Prodrug: A Methotrexate-Folic Acid-Poly(amidoamine) Conjugate and a Novel, Rapid, "One Pot" Synthetic Approach. *Bioconjugate Chem.* 21, 489-495.

3. Ki Choi, S.; Thomas, T.; Li, M.-H.; Kotlyar, A.; Desai, A.; Baker, J. J. R. Light-controlled release of caged doxorubicin from folate receptor-targeting PAMAM dendrimer nanoconjugate. *Chem. Commun.* 46, 2632-2634.

4. Brouwers, E. E. M.; Tibben, M. M.; Rosing, H.; Hillebrand, M. J. X.; Joerger, M.; Schellens, J. H. M.; Beijnen, J. H. Sensitive inductively coupled plasma mass spectrometry assay for the determination of platinum originating from cisplatin, carboplatin, and oxaliplatin in human plasma ultrafiltrate. *Journal of Mass Spectrometry* **2006,** 41, 1186-1194.

Chapter 8: Experimental

8.1 Materials

Dendrimers were purchased from Dendritech or Sigma-Aldrich. Cisplatin, sodium nitrate, folic acid, DMSO (duterated and non-duterated), DMF, TEA, T3P, D_2O (99.9%), 1,6-diaminohexane were purchased from Sigma-Aldrich. All aqueous solutions were prepared using water filtered by a Millipore purification unit. Vivaspin™ columns used in centrifuge experiments were supplied by Sartorius Biolab or VWR.

8.2 Ultra Violet/Visible spectroscopy

U.V. spectra were obtained using a Cary 50 bio U.V. spectrophotometer measuring between 200 – 400 nm with a path length of 1 cm and scan speed of. Standards of 0.001 – 0.01 mg/mL folic acid linker were prepared in DMSO with and without dendrimer.

8.3 Synthesis of folic acid linker

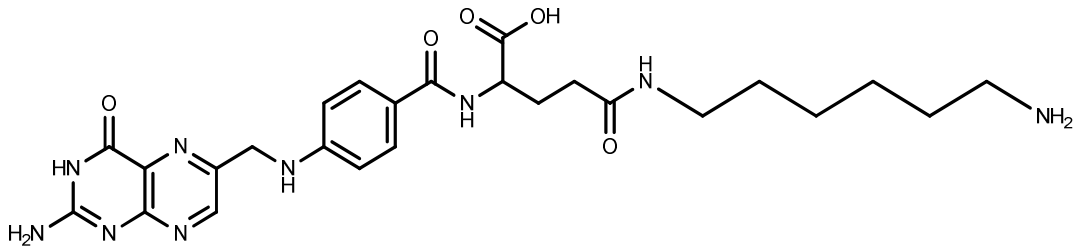

Folic acid (441.4 mg, 1 mmol) was dissolved, under nitrogen, in 100 mL anhydrous DMF and stirred with 1,6-diaminohexane (116.1 mg, 1 mmol) and TEA (2.5 mmol) at 0 ^oC for 1 h. Propylphosphonic anhydride (457 µL, 1.2 mmol) was then added dropwise to the solution which was then allowed to stir in an ice bath for a further 3 days. Water was then added to quench the reaction and precipitate the linker as an orange solid which was collected by filtration, washed with water (2 x 25 mL) and ether (2 x 25 mL) and then air dried. Yield: 484.5 mg, 90%.

8.4 Synthesis of dendrimer-folic acid conjugates

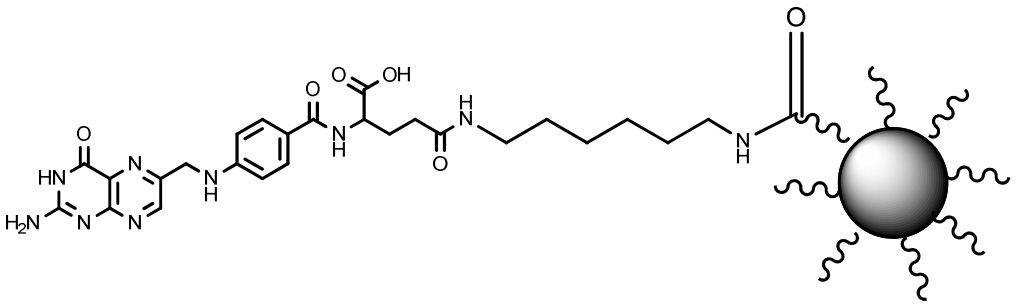

Lyophilised dendrimer (0.235 - 3.68 mM, 50 - 100 μL) was dissolved in anhydrous DMF (10 mL) and stirred with folic acid linker (10 mol equivalents) and TEA (64 – 512 mol equivalents) at 0 ^{o}C for 1 h under nitrogen. T3P (12 mol equivalents) was then added dropwise and the solution stirred for a further week at which point the solution was allowed to come to room temperature. The reaction was then quenched with water and the final volume completed to 300 mL with water, to ensure compatibility with the Vivaspin columns. The resulting solution was then centrifuged in Vivaspin™ columns with a 5 kDa molecular weight cut off membrane for 40 min at 3500 rpm. The dendrimer-folates were then centrifuged with 2 x 2 ml of D_2O The dendrimer-folate complexes were collected separately and retained in solution until needed.

8.5 Synthesis of dendrimer-folic acid-platinum conjugates

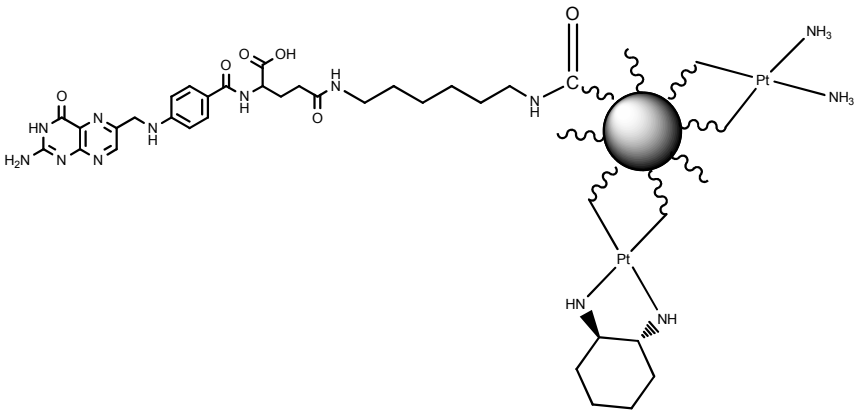

G3.5 - 6.5 dendrimer-folic acid conjugates were stirred for 5 h with TEA (256 – 2048 mol eq.) and aquated cisplatin or oxaliplatin (32 – 256 mol eq.). The solutions were then centrifuged in Viva spin columns and collected. The dendrimer-folic acid-platinum conjugates were retained in solution until required. The filtrate was collected and completed to 10 mL with 2% HNO_3 and then analysed for platinum content using ICP-MS.

8.6 *In vitro* growth inhibition assays

A2780, A2780cis and A2780cp ovarian cancer lines were grown in RPMI media containing 10% foetal calf serum, penicillin streptomycin and *L*-glutamate in a 5% CO_2 atmosphere. The cells were trypsinised, counted and adjusted to 500-1000 cells per well for the MTT stain assays and 2000 cells per well for the WST-1 stain assays (both in 96 well plates). Cisplatin, free dendrimer and drug-dendrimer complex stock solutions were diluted with RPMI to prepare a dilution series based on the total platinum concentration (0.1 – 100 μM cisplatin). 10 μL aliquots were taken from these solutions and added in triplicate to each well along with RPMI only. The plate was then cultured for 24, 48, 72 or 96 h and 50 μL of WST-1, followed by further incubation for 1 h. The absorbance of the WST-1 was measured using a plate reader at 450 nm, and the cells fixed with 4% paraformaldehyde with crystal violet used to stain the viable cells. The absorbance of the crystal violet stain was measured at 540 nm. For assays using the MTT stain: on the final day MTT (50 μL of a 5 mg/mL solution) was added to the 200 μL of medium in each well and the plates were incubated at 37 ^{o}C for 4 h in the dark. Medium and MTT was then removed and the MTT-formazan crystals dissolved in 200 μL DMSO. Glycine buffer (25 μL per well, 0.1 M, pH 10.5) was added and the absorbance measured at 570 nm in a multiwell plate reader.

8.7 Quantification of cellular uptake of platinum

Adherent cells (A2780 + A2780/cp70) were plated out at a density of 10^6 cells/well in 6 well plates and incubated overnight at 37°C in a humidified atmosphere of 10% CO_2 in air. The medium was then replaced with fresh medium alone or with medium containing cisplatin, oxaliplatin or experimental drug all at a concentration of 10□M and incubated for 2 or 4 hours. The medium was then removed and cells washed with ice cold PBS and the cells lysed by addition of 215□l of nitric acid (OPTIMA 68%, from Fisher Scientific) to each well. The cells were then collected into a microfuge tube and incubated overnight at 65°C in a heating block. Three further wells were used to estimate the number of cells per well. 50□l of the digest was then diluted 1/100 with ultrapure water containing Triton-X100 (0.1%). The platinum content of samples was determined by ICP-MS.

Chapter 9: General conclusions and Future work

9.1 General conclusions

The work detailed in this thesis describes the synthesis, characterisation and testing of PAMAM dendrimers conjugated to the active forms of both cisplatin and oxaliplatin with and without a folic acid based targeting group. The conjugation of platinum to carboxylate terminated dendrimers is readily achievable and the number of platinum groups which can be bound to the dendrimer increases with generation. The overall number of platinum moieties which can be bound, and the properties of the resulting complexes, are dependent on the nature of the platinum complex being used. The active component of cisplatin yielded and almost double the number of platinum groups bound to the dendrimer, compared to the equivalent oxaliplatin complex. It is possible that this is due to the steric bulk of the cyclohexane ring of oxaliplatin making it more difficult to bind to the amine sites within the branches. Despite the ease of synthesis of the complexes, it is difficult to achieve a consistent number of platinum groups on the dendrimer, making scale up to pharmaceutically relevant doses much more difficult.

The release of the platinum from the dendrimer was quantified in order to allow *in vitro* and *in vivo* experiments to be undertaken using relevant concentrations of platinum *i.e.* only the platinum which will be released from the dendrimer. The amount released from the dendrimer increases with generation, most likely as a result of increased steric crowding of the branches, decreasing the number of platinum molecules binding irreversibly to the amines in the branches. The irreversibly bound platinum represents increased manufacturing costs as sufficient platinum is used to achieve maximum drug loading, however not all this platinum delivers a therapeutic effect.

The *in vivo* studies carried out using the dendrimer-platinates demonstrated the necessity of selecting an appropriate staining agent. When the studies were carried out with WST-

1 the complexes were shown to be inactive, whereas studies carried out with the MTT assay showed a moderate degree of cytotoxicity, albeit lower than cisplatin. The smaller cisplatin dendrimer-platinate complexes, G3.5 and 4.5, exhibit a higher degree of cytotoxicity in the sensitive cell line but all complexes show significantly lower cytotoxicity in the resistant cell line, with the larger dendrimers showing less cross resistance between cell lines. The *in vivo* study of the G6.5 dendrimer-platinate, with the active component of cisplatin, showed the limitations of relying solely on the data obtained from *in vitro* cell work and highlighted the promise of the dendrimer-platinate complexes. The G6.5 complex proved to equally cytotoxic, at equimolar doses, to the maximum tolerated cisplatin dose, to mice carrying A2780 cell xenografts and was also able to slow tumour growth when given at higher doses. The dendrimer-platinates do however show similar levels of side effects to free cisplatin, as demonstrated by the similar degree of weight loss observed in the mice.

The folic acid linker conjugated to the dendrimer allowed for an active targeting complex to be synthesised however the low solubility of folic acid makes analysis difficult. The number of linker units bound to the dendrimers increases from G3.5-G5.5 with the G6.5 having approximately the same number as the G5.5. The effect of the targeting group on both cellular uptake and cytotoxicity can be measured and allows for comparison between the targeted and non-targeted complexes to be undertaken and also allows for correlations to be drawn with cellular uptake of platinum. The target cisplatin dendrimer-platinates showed higher platinum uptake than the free dendrimer-platinate which corresponds to the higher cytotoxicity also observed compared to the free dendrimer-platinate. Accumulation of platinum from the $\{Pt(R,R\text{-dach})\}^{2+}$ dendrimer-platinates decreased upon addition of the folate targeting group which corresponds to the decrease in cytotoxicity observed compared to the free dendrimer-platinate

In summary:

- Dendrimer-platinates can be readily synthesised, however consistent drug is difficult to achieve.
- Higher numbers of cisplatin moieties can be conjugated to the dendrimers than oxaliplatin moieties; possibly due to the steric bulk of the cyclohexane ring.
- The higher the dendrimer generation the greater the number of drug moieties that can be conjugated.
- The number of drug moieties released from the dendrimer increases with generation.
- The hydrodynamic radius of the cisplatin dendrimer-platinate complexes decreases on conjugation with the platinatium complexes due to limiting of hydrogen bonding with surrounding water molecules.
- The hydrodynamic radius of the oxaliplatin dendrimer-platinates increases on conjugation due to the likely aggregation resulting from the presence of cyclohexane rings.
- The cytotoxicity of the smaller (G3.5/4.5) dendrimer-platinate complexes is greater than the larger complexes in the sensitive cell line, however they exhibit a higher degree of cross resistance in the resistant cell line.
- When tested in vivo the G6.5 dendrimer-platinate exhibited similar activity to free cisplatin, however it could also be administered at higher doses than cisplatin which achieved a greater reduction in tumour growth.
- Folate targeting groups can be conjugated to the dendrimer-platinates, with a greater number able to be conjugated to the larger dendrimer-platinate complexes.
- Addition of the folate targeting group increases the cytoxicity of the cisplatin dendrimer-platinates but decreases the cytoxoxicity of the oxaliplatin dendrimer-platinate complexes.

9.2 Future work

9.2.1 Increase drug release from the dendrimer

The nature of the PAMAM dendrimer used in this work proved to be detrimental to the goal trying to be achieved, due to the presence of the amide and amine nitrogens in the branches binding irreversibly to the platinum. In order to increase the release efficiency of dendrimer-platinate complexes other types of dendrimers should be explored. The ideal dendrimer would retain the solubility of PAMAM dendrimers, whilst replacing the amide and amine groups in the branche;. however, as branch binding can occur it may be viable to use these sites as additional releasable binding sites when synthesising the dendrimer-platinate complex. The most commonly studied dendrimer after the PAMAM complexes is the polypropylene imine dendrimer, however, this is not suitable for binding to platinum complexes as this also has amine groups in the branches. One potential candidate is the polyglycerol-succinin-co-adipic acid dendrimer, originally synthesised by Grinstaff *et al.*, Figure 9.1.[1] The completed dendrimer structure is obtained by repeated esterification reactions and the branches are therefore composed of ester linkages and the synthesis can be terminated to have carboxylate surface groups suitable for binding to platinum complexes.[1] These complexes retain water solubility and a high degree of monodispersity, desirable for pharmaceutical formulations, and are also synthesised from biocompatible components.[1]

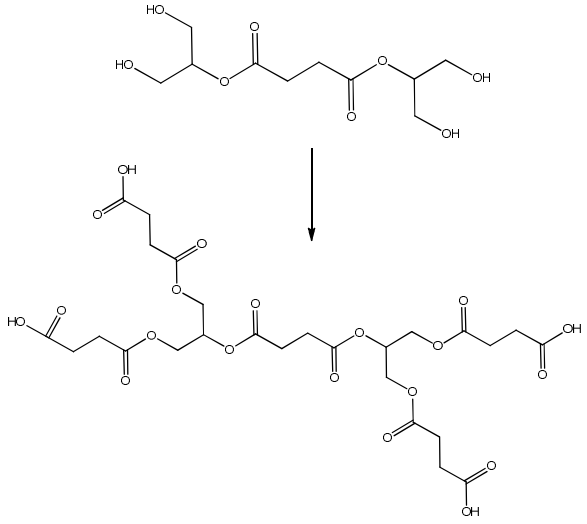

Figure 9.1 The dendrimer structure synthesised by Grinstaff *et al*.[1]

The branch binding which was evident with the PAMAM dendrimers is much less likely to occur between the oxygens, of the ester linkages, and the platinum complexes. In the event that binding does occur then the resulting interaction should be much weaker than between nitrogen and platinum, increasing the likelihood that the platinum can then be released. These favourable properties suggest that a similar study to that presented in this thesis should be carried out for these dendrimers to allow for a direct comparison to the PAMAM dendrimers.

9.2.2 Enhanced *in vivo* studies

The real measure of these types of drug delivery systems is the *in vivo* activity against their target. The *in vivo* study carried out with the cisplatin dendrimer complexes was rather short in timescale and narrow in scope. A more representative study using the same conditions but with an extended timescale could be used to monitor the tumour growth over a longer period of time to determine if the effect of the dendrimer-platinates is sustained. The studies should also be expanded to include all four of the different dendrimer size complexes, as well as the inclusion of mice carrying xenografts derived from platinum resistant cell lines. This enhanced investigation would deliver comparable activity data between the dendrimer-platinate complexes in addition to demonstrating if they are able to overcome resistance, a key marker in the development in new platinum drug entities.

In conjunction with the longer time course experiments, another study investigating the side effects from the dendrimer platinates should be carried out. Weight loss from mice in an *in vivo* study is a good indication of the systemic toxicity of the dendrimer-platinate complex but cannot be relied upon as a sole indicator of the adverse effects of a drug. Ideally a second study of the dendrimer-platinate complexes, either a specific sized dendrimer-platinate complex for initial screening or all of the complexes for a

comparative study, should be carried out to obtain data on the wide spectrum of side effects experienced with the platinum drugs. This kind of study would indicate if the dendrimer-platinate complexes are effective at targeting only tumour cells. This study could also be enhanced by coupling it with a whole organ platinum uptake pharmacokinetic study to look at uptake level of the dendrimer-platinate complexes.

9.2.3 Tumour penetration study

A problem that arises in the development of new drugs is inefficient penetration into the interior of the tumour. Poor diffusion of the drug away from the vasculature in the tumour results in the drug only reaching a small percentage of viable cells within the solid tumour. This means that the drug is able to act on the exterior cells whilst the interior cells, often the most aggressive, remain intact and allow the tumour to continue to grow. This can lead to the development of resistance. It is therefore necessary to determine how effective the dendrimer-platinate complexes are in penetrating tumours. One method of carrying out this type of study is to use tumour spheroids, as model of a tumour Figure 9.2.[2]

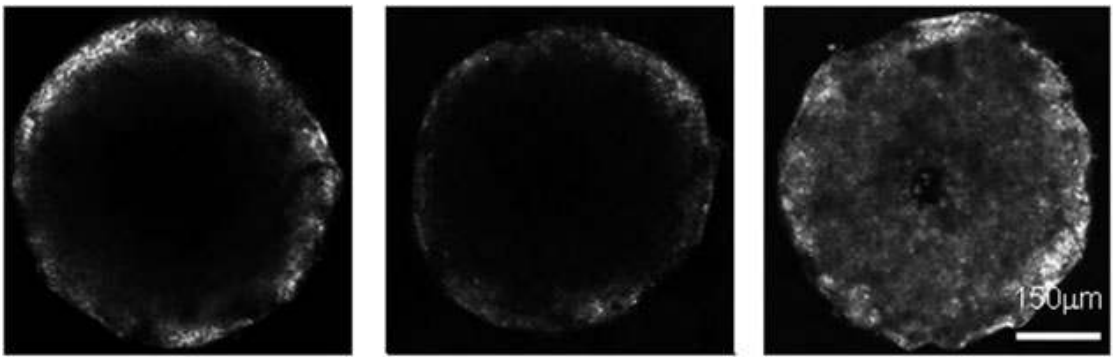

Figure 9.2 The fluoresence imaging of tumour spheroid.[2]

Tumour spheroids are three-dimensional spherical aggregates formed from permanent cell lines.[3] These aggregates allow the visualisation of both drug diffusion and cellular accumulation within a tumour.[2] Spheroids have already been used to analyse the

diffusion and cellular accumulation properties of anthraquinone and its platinum derivatives which further suggests that this may be a suitable approach to study the penetration of the dendrimer-platinate complexes into tumours.

9.2.4 Explore different drugs

The highly desirable properties of dendrimers, *i.e.* high solubility, monodispersity and ease of functionalisation, should make them ideal candidates for delivering most types of drugs and bioactive compounds. The work presented in this thesis should be expanded to encompass more than just the two platinum complexes studied. The other platinum complexes, should also be considered as well as the myriad of poor soluble drugs currently being used or developed. The platinum drug complex BBR3464 and its derivatives are candidates for further investigation as the overall +2 charge of these complexes allows for electrostatic interactions with the negatively dendrimer.

9.2.5 MTT and platinum

The results obtained from both the WST-1 and MTT stains during the *in vitro* cell studies indicate that the platinum influences the metabolism of these dyes. It is evident from this, and previous, studies that MTT is a more viable stain when using platinum anticancer drugs.[4] The reason for this preference is not know, however, it is possible that the platinum interferes with the metabolism of the WST-1 or MTT dyes. A side study should be carried out to determine the influence of platinum drugs to ensure that the most accurate results are being obtained.

9.2.6 Labelling studies of the dendrimer and platinum complexes

It is evident that the dendrimer-platinates are reaching the interior of the cell and delivering the desired anticancer effect. What is not known is the process by which this occurs and it is possible that through the use of labelling studies, where the dendrimer and platinum both have different labels, this may be determined. Fluoresence is commonly used to highlight the presence of material in cells. If fluoresence labels are

conjugated to the dendrimer and platinum it will allow visualisation of the route taken by the dendrimer-platinate to enter the cell. Incubation of the labelled complex with a suitable cell line and subsequent fluoresence imaging will show if both the dendrimer and platinum are taken into the cell, through a process such as endocytosis, or if the platinum is released from the dendrimer before being taken into the cell.

9.3 References

1. Carnahan, M. A.; Grinstaff, M. W. Synthesis of Generational Polyester Dendrimers Derived from Glycerol and Succinic or Adipic Acid. *Macromolecules* **2005,** 39, 609-616.

2. Bryce, N. S.; Zhang, J. Z.; Whan, R. M.; Yamamoto, N.; Hambley, T. W. Accumulation of an anthraquinone and its platinum complexes in cancer cell spheriods: The effect of charge on drug distribution in solid tumour models. *Chem. Commun.* **2009**, 2673-2675.

3. Kunz-Schughart, L. A.; Kreutz, M.; Knuechel, R. Multicellular spheroids: a three-dimensional in vitro culture system to study tumour biology. *Int. J. Exp. Pathol.* **1998,** 79, 1-23.

4. Wheate, N. J.; Abbott, G. M.; Tate, R. J.; Clements, C. J.; Edrada-Ebel, R.; Johnston, B. F. Side-on binding of p-sulphonatocalix[4]arene to the dinuclear platinum complex trans-[{PtCl(NH_3)$_2$)}$_2$u-dpzm]$^{2+}$ and its implications for anticancer drug delivery. *J. Inorg. Biochem.* **2009,** 103, 448-454.